A study on the low cost production methods of mesophase pitch based carbon fiber : Enhancement of the yield of mesophase pitch and shortening of the oxidation/stabilization time

島ノ江, 明生

https://doi.org/10.15017/4060196

出版情報：Kyushu University, 2019, 博士（工学）, 課程博士
バージョン：
権利関係：

A study on the low cost production methods of mesophase pitch based carbon fiber
−Enhancement of the yield of mesophase pitch and shortening of the oxidation-stabilization time−

Department of applied science for electronics and materials
interdisciplinary graduate school of engineering sciences
Kyushu university

Yoon・Miyawaki Lab

島ノ江　明生

Hiroki Shimanoe

February 2020

高性能ピッチ系炭素繊維の低価格化に関する研究
－前駆体ピッチの高収率化および不融化時間の短縮－

A study on the low cost production methods of mesophase pitch based carbon fiber
−Enhancement of the yield of mesophase pitch and shortening of the oxidation-stabilization time−

九州大学

総合理工学府

量子プロセス理工学専攻

2020 年 2 月

尹・宮脇研究室

島ノ江　明生

Hiroki Shimanoe

論文調査委員会

主査 九州大学　教授　　尹　聖昊

副査 九州大学　教授　　永長　久寛

副査 九州大学　准教授　宮脇　仁

Contents

Chapter 1. Introduction

1-1. Carbon fiber

Carbon fiber (CF) is a typical fibrous carbon which is composed of over 90 wt% of carbon atoms. At the end of the 19th century, Thomas Edison and Joseph Swan invented the incandescent bulb using carbonized cellulose (bamboo and cotton) as a filament because of excellent electrical conductivity and thermo-resistivity properties [1, 2]. This is considered to be the begin of CF. In 1959, Union Carbide Company started to produce the cellulose-based CFs, however, they showed low Tensile Strength (TS) and Young's Modulus (YM) due to their low graphitizable property after carbonization, therefore their application was very limited as an insulation material [3].

Polyacrylonitrile (PAN) and pitch-based CFs, which are now mainstream in the commercial CF productions, were first invented in the 1960s. In 1961, Shindo in Japan and Johnson and Morita in England have individually developed PAN-based CFs (PANCFs) with higher mechanical properties than those of cellulose-based CFs [4−6]. In 1963 and 1966, Ohtani has first developed both isotropic and mesophase pitch-based CFs (IPCFs & MPCFs) [7, 8].

Toray, Kureha, and Union Carbide companies stated to commercialize PANCFs, IPCFs and MPCFs in 1970s, respectively [9−12]. Nowadays, many companies produce PANCFs, IPCFs and MPCFs, and their main applications are fillers for composites in the areas of aerospace, military and sports [11−13].

CF reinforced plastics (CFRPs) have better specific TS and YM than those of steel, aluminum alloys and the other materials [14−17]. Therefore, CFRPs have been recognized as the main route to apply the CFs as important structural materials for aerospace, military and sports. In recent years, their main application has been expanded into the industries of energy-saving and environmental protection areas such as structural materials for electric vehicle (EV), windmill and construction [14−16]. The CF application to the car body is particularly expected due to its direct effect on reducing fossil fuel consumption through the EV weight lightening. Jim deVries

at Ford Motor Company proposed the required CF mechanical properties regarding TS, elongation ratio and YM of at least 1.7 GPa, 1.0% and 170 GPa, respectively, and he also required to lower the CF price to less than 10−12 $/kg for car body use [17].

1-2. Classification of CF

General CFs are classified into three types, PANCFs, IPCFs and MPCFs (**Fig. 1-1**). PAN and MPCFs are commercialized as high-performance CFs due to their high TS and YM [11, 13]. IPCF is commercialized as a general performance CF due to its low mechanical properties [12, 18−22].

1-2-1. *PANCFs*

PANCFs show higher TS (3.5–6.8 GPa), elongation ratio (0.6–2.4%), and YM (170–650 GPa) [11]. Toray Company commercialized many grade PANCFs such as T-300 (TS: 3.5 GPa, YM: 230 GPa), T-800 (TS: 5.4 GPa, YM: 300 GPa), T-1000 (TS: 7.4 GPa, YM: 300 GPa) and so on [11]. The fibrous PAN, a precursor of PANCF, is mainly prepared by the solution spinning of dissolution of PAN copolymer with solvents such as dimethylformamide (DMF) and dimethylsulfoxide (DMSO) [23]. After then, the PAN spun fiber is stabilized at 200–300°C in air or oxygen flows under tension to form pyridine ladder molecules [24]. Pyridine ladder molecules prevent a ring closure-dehydrogenation with exothermic reaction at carbonization and keep the fibrous form [24]. After stabilization, PANCFs are obtained by carbonization at 1500–3000°C to discharge nitrogen, oxygen and hydrogen elements as HCN, NH_3, N_2, CO_2 and NO_2, and develop the carbon hexagonal networks and graphitization at over 3000°C to form the graphitic structure for high mechanical properties [25]. Extension at carbonization and graphitization needs to increase a molecular orientation in the fiber axis direction and enhance TS of PANCFs [14]. PANCFs have high mechanical properties, but their

production cost is more than 20 $/kg mainly due to expensive PAN precursor fiber and its low carbonization yield. Thus, its application is usually limited to the advanced composite materials for the areas of aerospace and military.

1-2-2. *IPCFs*

Commercialized IPCFs exhibit a low TS (0.5–1.0 GPa) and YM (30–50 GPa), but they are manufactured with relatively low production cost due to the cheap raw material and high carbonization yield [12, 26]. Spinnable isotropic pitch (IP) is prepared by heat treatment such as distillation using coal tar pitch (CTP), ethylene bottom oil (EBO) and slurry oil (SO) as raw materials and is composed of polycyclic aromatic hydrocarbons [26, 27]. IPCF is obtained by melt-spinning, oxidation-stabilization at 200–350°C to form oxidative cross-linking among molecules of its spun fibers and carbonization, and mainly applied to insulation, a brake friction pad and so on due to its low thermal conductivity and high heat resistance (**Fig. 1-2**) [28]. IPCFs exhibit low mechanical properties, but recently, Kim *et al.* successfully developed an IP with a linear structure through a bromination-dehydrobromination reaction of EBO and CTP and prepared IPCFs with TS of 2.0–2.4 GPa [18]. However, this IPCF still suffers YM deficiency and the handling difficulties in the precursor pitch production. On the other hand, low cost CFs derived from lignin, liquefied wood, biotar and polyethylene were developed, but these CFs exhibit still low TS of 0.6–1.0 GPa and very low YM of 20–30 GPa [19–22].

1-2-3. *MPCFs*

Brooks and Talor first found a carbonaceous liquid crystal pitch (mesophase pitch; MP) at coal carbonization [29]. By the carbonization of an IP at over 400°C, the deposition, dehydrogenation and polycondensation enable to form special planar

polycyclic aromatic hydrocarbons, and in this phase mesophase spheres start to nucleate and grow to bulk mesophase through their agglomeration [30]. Mesophase spheres express, grow and coalesce during liquid-phase carbonization and finally change to 100% bulk MP. The size and morphology of anisotropic texture in MP are very dependent on the mobility of mesophase spheres (the fluidity of pitch matrix) during the growth and coalescence [30, 31]. If the viscosity is low, the arrangement of planar aromatic hydrocarbons can be easier to grow and coalescence and they are able to form the bulk flow domain type fusible MP. However, at the high viscosity, the fluidity of pitch decreases and MP becomes infusible with no flow domain.

So far spinnable mesophase pitch (SMP) has been considered to have both Lyotropic and Thermotropic liquid crystalline properties [32, 33]. Recently, our group has considered SMP should be only Lyotropic liquid crystal but Thermotropic one. SMP is usually composed of 2 kinds of molecular groups, that is, “solvent molecules” which show isotropic texture and “mesogen molecules” which do anisotropic one but almost infusible (**Fig. 1-3**) [32]. The size and morphology of the anisotropic texture of SMP depend on the ratio of solvent molecules and mesogen molecules [32]. This confirms the Lyotropic liquid crystalline property of SMP. If the concentration of mesogen molecules exceeds a certain value (the criteria of bulk mesophase expression), SMP can be obtained. **Fig. 1-4** shows the change of anisotropic texture by the ratio of benzene insoluble and soluble fractions of MP derived from naphthalene pitch [33]. Benzene insoluble is rich in mesogen molecules. The more the amount, the bigger the size of the anisotropic texture. Such size and shape of anisotropic texture depend on the temperature of heat treatment [33]. At high temperatures, the amount of anisotropic texture decreases because of the relatively low concentration of mesogen molecules, which must be due to the solvent-capability of solvent molecules [33]. This just looks a Thermotropic liquid crystal property. However, the amount of anisotropic texture

may decrease due to an increase in the solubility of mesogen molecules. Therefore, I can conclude that SMP must be a Lyotropic liquid crystal.

So far, SMP usually prepared from an IP by two processes of extraction of toluene insoluble and heat treatment, or heat treatment and centrifugation [34, 35]. Mochida *et al.* have proposed a very innovative preparation of SMP derived from naphthalene as a raw material by catalytic heat treatment using HF/BF_3 [36]. Furthermore, Hochgeschurtz *et al.* have proposed the preparation of SMP from the petroleum pitch by supercritical extraction [37]. Each of the above processes has advantages and disadvantages. For example, the two process methods have the advantage of cheaper equipment and operation costs, but the very low yield and very low spinnability of the SMP are still a problem. Mochida's and the supercritical extraction methods can produce relatively high yields of SMP, but the costly equipment and high process operation costs are problems to solve. In particular, SMP produced by the supercritical extraction shows a high yield compared to raw materials of 25 wt% or more, but it is known that the produced SMP has low spinnability.

Our group has recently proposed SMP can be prepared through the adequate hydrogenation, heat treatment and thin layer evaporation (TLE) of the aromatic hydrocarbons such as CTP and SO [38].

Here, hydrogenation usually lowers the carbon aromaticity of low materials of the highly polycyclic aromatic hydrocarbons and side alkyl chains of aliphatic groups [39]. Heat treatment of over 400°C with N_2 blowing can change such molecules to mesogen molecules which can be stacked in (002) direction. The amounts of solvent and mesogen molecules can be controlled by TLE for the removal of a little volatile matter.

1-3. Necessity of improvement of the yield of SMP

1-3-1. *Problems on preparation of SMP*

MPCF has high TS and YM and is expected as an effective filler for the applications to the car body, windmill frame and structural beam for construction. However, such applications of MPCFs have obviously limited because of the high price of MPCF, which must be due to the low yield of SMP and high costs of hydrogenation of raw materials and long-time energy consumable oxidation-stabilization of SMP fiber (**Fig. 1-5**) [40]. In general, severe hydrogenation of raw materials such as quinoline insoluble free CTP (QI free CTP) and SO is necessary for achieving the excellent spinnability of SMP. However, it results in the low preparation yield of SMP to less than 10 wt% for the raw materials of CTP and SO [38, 40]. For example, the yield of SMP derived from SO by hydrogenation using 1, 2, 3, 4-tetrahydroquinoline and heat treatment is 5.0–10.0 wt% [38]. Over 30 wt% as the yield of SMP is required to manufacture its CFs with a low production cost of 10–12 $/kg. The manufacturing processes, such as supercritical toluene extraction of SO and HF/BF_3-catalyzed preparation of naphthalene, have improved the production yield of SMP up to 20–45 wt% [36, 37]. However, as described previously, commercial production has been very limited due to costly equipment and its operation costs and the relatively low spinnability. For producing the low cost MPCFs, the first problem to be solved would be to produce SMP with high yield using a cheaper process with low operation costs. For this, a selection of cheap raw material and non-special high cost production process are very important. Without special production processes such as supercritical extraction or highly toxic catalytic process using HF/BF_3, a cheap raw material which exhibits high purity and has many aromatic hydrocarbons and usual production process (no or low degree hydrogenation, N_2 blowing heat treatment and TLE) needs to be used.

1-3-2. *Approach for improving SMP yield*

A coal direct extracted fraction (Hyper-coal: HPC) was tried to be an effective raw material to obtain high SMP. HPC is prepared by solvent extraction of coal at 350–400ºC under high pressure using mixed-methylnaphthalene and it shows various molecular properties dependent on the selected original coal and extraction conditions such as temperature and pressure (**Fig. 1-6**) [41–44]. HPC has a low price of 0.1 $/kg, a low impurity of less than 200 ppm and relatively high polycyclic aromatic hydrocarbons which are composed of 2–8 membered rings [41, 42]. The application of HPC has been still very limited to isotropic coke production, fuel for gasification, and additive to cheap binder pitches. In recent years, Yang *et al.* reported that spinnable IP was successfully developed by only mixed methyl naphthalene extraction and short-time TLE of HPC [43, 44]. Among aromatic ring compositions of 2–8 or more membered rings of HPC, relatively high polycyclic aromatic hydrocarbons are apt to convert into non-melted coke components under the same heat treatment condition [41]. However, HPC, which is prepared without high temperature heat treatment of over 800ºC like coal tar, contains some molecules with ethyl or longer alkyl side chain groups that interfere with the molecular stacking, which must be removed for obtaining mesogen molecules in the preparation of SMP [32]. For this reason, the hydrogenation reaction needs for leveling the aromatic structures and reducing the alkyl contents above ethyl [39].

Besides HPC, EBO is also a cheap source of polycyclic aromatic hydrocarbons, but it has aromatic hydrocarbons which are composed of 1–3 membered rings with a long-chain aliphatic group such as ethyl and propyl group [27]. EBO with low condensed aromatic rings with long-chain aliphatic groups is also very difficult to be converted into mesogen molecules because such molecular structures usually impede to produce the planar shaped molecules that must be a precondition to require the stacked structure

[32]. If the molecular structures EBO molecules can be optimized to accept to mesogen molecules by hydrogenation, the major components of EBO are decomposed into the lower polycyclic aromatic hydrocarbons and only very low yield of SMP can remain after N_2 blowing heat treatment. On the other hand, CTP and SO are relatively high polycyclic aromatic hydrocarbons [45, 46]. In particular, CTP is mainly composed of highly polycyclic aromatic hydrocarbons which are composed of 3–4 membered rings with only methyl group side chain [46]. Therefore, the molecular stacking probability of CTP and SO is higher than EBO. **Fig. 1-7** exhibits the average molecular structure of EBO, SO and CTP [27, 45, 46].

From the above reasons, I came up with the hybridization of EBO with CTP or SO. EBO is composed of aromatic hydrocarbons that have a role for solvent molecules and CTP and SO have aromatic hydrocarbons as mesogen molecules for the effective preparation of SMP with high yield. By adding CTP or SO into EBO, the mesophase growth and coalescence of EBO derived pitch can be improved. In the past, the binder pitch has been developed by the hybridization of CTP or SO with EBO [47, 48]. Through the hybridization of EBO with CTP or SO at an optimized balance, the novel approach for obtaining the high SMP yield without severe hydrogenation would become possible.

Commercialized SMP such as AR pitch has a 100% anisotropic texture and its derived MPCF usually exhibits high mechanical properties [36]. However, the spinnability of the AR pitch is still low, and its production cost is very high due to costly equipment and operation costs for the special heat treatment. For improving the spinnability and yield, I came up with that mesogen molecule extraction of AR-pitch and mixing its extract with separately prepared IPs for lowering the softening point (SP) of SMP. IP with a low SP is only composed of solvent molecules and can be prepared with high yield. If the obtained pitch exhibits sill the same anisotropic

textures even by adding some addition of IP, the SP of SMP can decrease with improving SMP yield.

1-4. Problem of long-time oxidation-stabilization and its solution

The manufacturing process of MPCFs consists of the multiple sub-processes of the SMP preparation, spinning, oxidation-stabilization, carbonization, graphitization and sizing. Though the reduction of SMP production cost is very important for manufacturing low price MPCF, it also needs to improve the production process for decreasing the production cost (**Fig. 1-5**). Especially, the sub-process of oxidation-stabilization is the most time and energy-consuming and costly process in CF manufacturing. Conventional oxidation-stabilization employs thermal oxidation using enough amount of atmospheric air flow at a temperature range of 150–300°C and a long duration of a few hours [49, 50]. Thus, it is one of the most important tasks to shorten the total stabilization time to reduce the cost of manufacturing CFs. However, shortening of the stabilization time, *i.e.* performing rapid oxidation at high temperatures, usually lower the mechanical properties through the formation of a heterogeneously oxidized state in the transverse section of pitch fibers [49]. Thus, stabilization should proceed slowly to confer optimal and homogeneous distribution of oxygen uptake on stabilized fibers across their transverse section, so a long stabilization time at a relatively low temperature is required (**Figs. 1-8** and **1-9**) [50].

The cause of a long stabilization time is usually due to the slow diffusion of oxygen molecules into the center part of pitch fiber. Yang *et al.* have estimated that the average radii of free volumes on various SMP derived MP fibers were in the ranges of 0.24–0.25 nm and 0.25–0.26 nm, respectively [51]. The average kinetic radii of oxygen and nitrogen are 0.17 and 0.19 nm, respectively, indicating that it is very difficult for the

effective air diffusion to occur for rapid oxidation reactions in MP fibers homogeneously in conventional atmospheric stabilization.

Cornec *et al.* and Fathollahi *et al.* reported that the oxidation-stabilization of MP fibers under a moderate oxygen pressure could be effective in raising the amount of oxygen uptake and increasing the stabilization depths significantly even at low temperature [52, 53]. Therefore, the stabilization-oxidation of MP fibers under high air pressure may enhance the slow diffusion rate of oxygen molecules and enable the homogeneous oxidation for a short time.

1-5. The objective and contents of this study

The objective of this study is the development of low price MPCFs by improvement of the SMP yield and shortening the oxidation-stabilization time.

In Chapter 1, the backgrounds, conception, approach and objective of this study were introduced.

In Chapter 2, preparation with a high yield of SMP using a coal direct extracted fraction and evaluation of its MPCF were performed. I adopted the very usual cheap production process of the three-step processes of hydrogenation, N_2 blowing heat treatment and TLE using HPC as the raw material for SMP with high yield. Hydrogenation was minimized to lower the molecular weight and high alkyl side chain groups to improve fluidity by low polycondensation [39]. N_2 blowing heat treatment also lowered high alkyl side chains to enhance the molecular stacking. TLE effectively removed volatile matters which were also the main reason for low spinnability. The obtained MPCFs were analyzed for the mechanical property according to standard methods.

In Chapter 3, I examined the effect on the growth and coalescence of anisotropic texture and developed SMP by the hybridization of EBO with CTP or SO. SMP was prepared by the hybridization of EBO with CTP or SO. Pressurized EBO, CTP and SO were hybridized by bromination-dehydrobromination to form intermolecular methylene bridge, to optimize the molecular structure, and to increase the average molecular weight and the compatibility, followed by the N_2 blowing heat treatment and TLE [18, 54]. The hybridization effect on the development of anisotropic textures was closely investigated.

In Chapter 4, the correlation between the anisotropic texture and the molecular stacking at various weight ratios of AR-THFI and AR-THFS was examined. I tried to decrease the SP of SMP using AR-THFI as mesogen fraction and CTP or SO derived IP with a low SP as solvent one. It was closely examined the correlation between the anisotropic texture and the molecular stacking at various weight ratios of mesogen molecules and solvent molecules, and tried to adjust the SP of SMP using IP with a low SP. By the tetrahydrofuran (THF) extraction of AR pitch which has 100 vol% of anisotropic texture was fractionated into THF insoluble fraction of AR pitch (AR-THFI) as mesogen molecules and THF soluble fraction (AR-THFS) as solvent molecules. After the mixing heat treatment at various weight ratios of AR-THFI as mesogen fraction and AR-THFS and IPs derived from CTP or SO with a SP of 140°C as solvent one, MP were re-prepared by low temperature annealing. The stacking height (Lc(002), interlayer spacing (d_{002}), anisotropic texture and softening points of the obtained pitches were examined for elucidating the Lyotropic liquid crystalline property of AR-pitch and lowering and improving its SP and yield, respectively.

In Chapter 5, I tried oxidation-stabilization under high pressure of air to reduce the total stabilization time without causing deterioration of the mechanical properties of MPCFs. The oxidative stabilization of MP fibers under various pressures was carried

out to examine the pressure effect on the oxidation reaction and mechanical properties. The oxygen uptake and distribution of AR pitch-based fiber stabilized under various pressure of air and the mechanical properties of its carbonized and graphitized fibers were examined.

In Chapter 6, the conclusions and future plans were summarized.

Reference

1. Edison TA. Electric lamp. US patent 223,898A;1880.
2. Edison TA. Manufacture of Filaments for Incandescent Electric Lamps. US patent 470,925;1892.
3. Bacon R. Filamentary graphite and method for producing the same. US patent 2,957,756;1959.
4. Shindo A, Fujii R, Sengoku S. Method for producing carbon products from an acrylonitrile-based synthetic polymer (in Japanese). Japan patent S37-4405;1959.
5. Johnson W, Watt W. Structure of high modulus carbon fibres. Nature 1967;215:384−6.
6. Morita K, Miyachi H, Hiramatsu T. Stabilization of acrylic fibers by sulfur atoms mechanism of stabilization. Carbon 1981; 19(1):11−8.
7. Ohtani S. On the carbon fiber from the molten pyrolysis products. Carbon 1965;3(1):31−4.
8. Ohtani S. Mechanism of the carbonization of MP carbon fiber at the low temperature range. Carbon 1967;5:219−25.
9. Singer LS. The mesophase and high modulus carbon fibers from pitch. Carbon 1978;16(6):409−15.
10. Takahashi R, Hosoi T, Aiba T, Konno T. Method for manufacturing petroleum pitch having high aromaticity. US patent 3,928,170;1975.
11. Toray Co Ltd. Technical data sheets. No. CFA-008, No. CFA-007, No. CFA-006, No. CFA-003, and No. CFA-002.
12. Nippon Graphite Fiber Co Ltd. Technical data sheets. YSH, YS and XN series.
13. Kureha Chemical Co Ltd. Product catalogue for carbon fiber. KRECA.
14. Newcomb BA. Processing, structure, and properties of carbon fibers. Compos Pt A Appl Sci Manuf 2016;91:262−82.

15. Liu Y, Kumar S. Recent progress in fabrication, structure, and properties of carbon fibers. Polym Rev 2012;52:234−58.
16. Soutis C. Fibre reinforced composites in aircraft construction. Prog Aero Sci 2005;41(2):143−51.
17. Yang KS, Kim BH, Yoon SH. Pitch based carbon fibers for automotive body and electrodes, Carbon Lett 2014;15:162−70.
18. Kim BJ, Eom Y, Kato O, Miyawaki J, Kim BC, Mochida I, et al. Preparation of carbon fibers with excellent mechanical properties from isotropic pitches. Carbon 2014;77:747−55.
19. Baker DA, Rials TG. Recent advances in low-cost carbon fiber manufacture from lignin. J Appl Polym Sci 2013;130(2):713−28.
20. Ma XJ, Zhao GJ. Structure and performance of fibers prepared from liquefied wood in phenol. Fibers Polym 2008;9:405−9.
21. Postema AR. De root H, Pennings AJ. Amorphous carbon fibres from linear low density polyethylene. J Mater Sci 1990;25:4216−22.
22. Prauchner MJ, Pasa VMD, Otani S, Otani C. Biopitch-based general purpose carbon fibers: Processing and properties. Carbon 2005;43(3):591−7.
23. Huang X. Fabrication and properties of carbon fibers. Materials 2009;2(4):2369−403.
24. Dalton S, Heatley F, Budd PM. Thermal stabilization of polyacrylonitrile fibres. Polymer 1999;40(20):5531−43.
25. Oberlin A. Carbonization and graphitization. Carbon 1984;22(6):521−41.
26. Alcañiz-Monge J, Cazorla-Amorós D, Linares-Solano A, Oya A, Sakamoto A, Hosm K. Preparation of general purpose carbon fibers from coal tar pitches with low softening point. Carbon 1997;35(8):1079−87.
27. Kim BJ, Kotegawa T, Eom Y, An J, Hong IP, Kato O, Nakabayashi K, Miyawaki J,

Yoon SH. Enhancing the tensile strength of isotropic pitch-based carbon fibers by improving the stabilization and carbonization properties of precursor pitch. Carbon 2016;99:649−57.

28. Edie DD. The effect of processing on the structure and properties of carbon fibers. Carbon 1998;36:345−62.
29. Brooks JD, Taylor GH. The formation of graphitizing carbons from the liquid phase. Carbon 1965;3(2):187−93.
30. Mochida I, Korai Y, Ku CH, Watanabe F, Sakai Y. Chemistry of synthesis, structure, preparation and application of aromatic-derived mesophase pitch. Carbon 2000;38(2):305−328.
31. Mochida I, Korai Y. The chemistry for the preparation of pitch based carbon fibers. Polymer 1986;35:456−9.
32. Korai Y, Mochida I. Preparation and properties of carbonaceous ,mesophase-i soluble mesophase produced from A240 and coal tar pitch. Carbon 1985;23(1):97−103.
33. Mochida I, Korai Y. Chemistry of mesophase pitch for its preparation and property design. J Fuel Soc Jpn 1985;64:796−808.
34. Diefendorfu RD, Riggs D. Manufacturing method of optically anisotropic deformable pitch, optically anisotropic pitch and pitch fiber. Japan patent S54-160427;1979.
35. Izumi T, Naito T, Nakamura T. Optically anisotropic carbonaceous pitch for carbon material, its nufacture, and manufacture of carbonaceous pitch fiber and carbon fiber. Japan patent S57-088016;1982.
36. Mochida I, Shimizu K, Korai Y, Otsuka H, Sakai Y, Fujiyama S. Preparation of mesophase pitch from aromatic hydrocarbons by the aid of HF/BF_3. Carbon 1990;28(2−3):311−9.

37. Hutchenson KW, Roebers JR, Thies MC. Fractionation of petroleum pitch by supercritical fluid extraction. Carbon 1991;29(2):215−23.
38. Kato O, Uemura S, Korai Y, Mochida I. Preparation of mesophase pitch and high performance carbon fiber from decant oil. J Jpn Petrol Inst 2004;47(2):100−6.
39. Otani S, Sanada Y. Foundation of carbonization engineering (in Japanese). Tokyo:Ohmsha;1980.
40. Mochida I, Sakai Y, Fujiyama S, Komatsu M. Development of process for manufacturing of mesophase pitch from aromatic hydrocarbons. Nippon Kagaku Kaishi 1997;1:1−10.
41. Hamaguchi M, Okuyama N. Manufacturing process and applications of the hyper-coal. Tanso 2013;257:149−56.
42. Okuyama N, Komatsu N, Shigehisa T, Kaneko T, Tsuruya S. Hyper-coal process to produce the ash-free coal. Fuel Process Technol 2004;85(8−10):947−67.
43. Yang J, Nakabayashi K, Miyawaki J, Yoon SH. Preparation of pitch based carbon fibers using hyper-coal as a raw material. Carbon 2016;106:28−36.
44. Yang J, Nakabayashi K, Miyawaki J, Yoon SH. Preparation of isotropic pitch-based carbon fiber using hyper coal through co-carbonation with ethylene bottom oil. J Ind Eng Chem 2016;34:397−404.
45. Zander M. On the composition of pitches. Fuel 1987;66(11):1536−39.
46. Mochida I, Oyama T, Korai Y. Formation scheme of needle coke from FCC-decant oil. Carbon 1988;26(1):49−55.
47. Bai BC, Kim JG, Kim JH, Lee CW, Lee YS, Im JS. Blending effect of pyrolyzed fuel oil and coal tar in pitch production for artificial graphite. Carbon Lett 2018;25:78−83.
48. Pérez M, Granda M, Santamaria R, Menéndez R. Preventing mesophase growth in petroleum pitches by the addition of coal-tar pitch. Carbon 2003;41(9):1854−7.

49. Matsumoto T, Mochida I. Oxygen distribution in oxidatively stabilized mesophase pitch fiber. Carbon 1993;31:143−7.
50. Yoon SH, Korai Y, Mochida I. Assessment and optimization of the stabilization process of mesophase pitch fibers by thermal analyses. Carbon 1994;32:281−7.
51. Yang H, Yoon SH, Korai Y, Mochida I, Kato O. Microvoids present in anisotropic mesophase pitch, their as-spun and annealed fibers. Chem Lett 2003;32:168−9.
52. Fathollahi B, Jones B, Chau PC, White JL. Injection and stabilization of mesophase pitch in the fabrication of carbon–carbon composites. Part III: Mesophase stabilization at low temperatures and elevated oxidation pressures. Carbon 2005;43:143−51.
53. Cornec LP, Rogers DK, Fain CC, Edie DD. A novel stabilization technique and its influence upon carbonization yield. Extended Abstracts, CARBON'92, Deutsche Keramische Gesellschaft, Essen, Germany 1992;710–2.
54. Ge C, Yang H, Miyawaki J, Mochida I, Yoon SH, Qiao W, Long D, Ling L. Synthesis and characterization of high-softening-point methylene-bridged pitches by visible light irradiation assisted free-radical bromination. Carbon 2015;95:780−8.

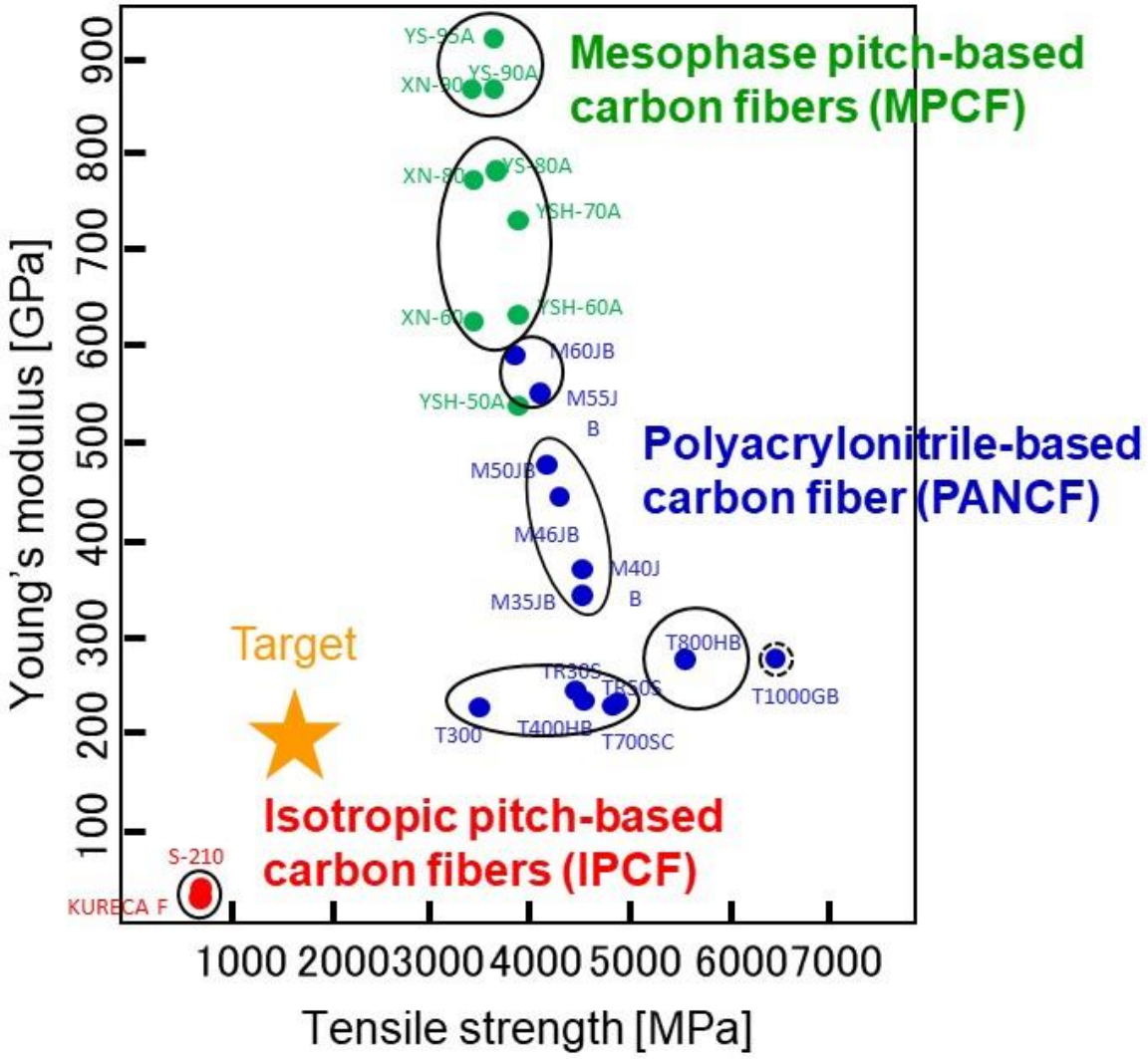

Fig. 1-1. The mechanical properties of CFs.

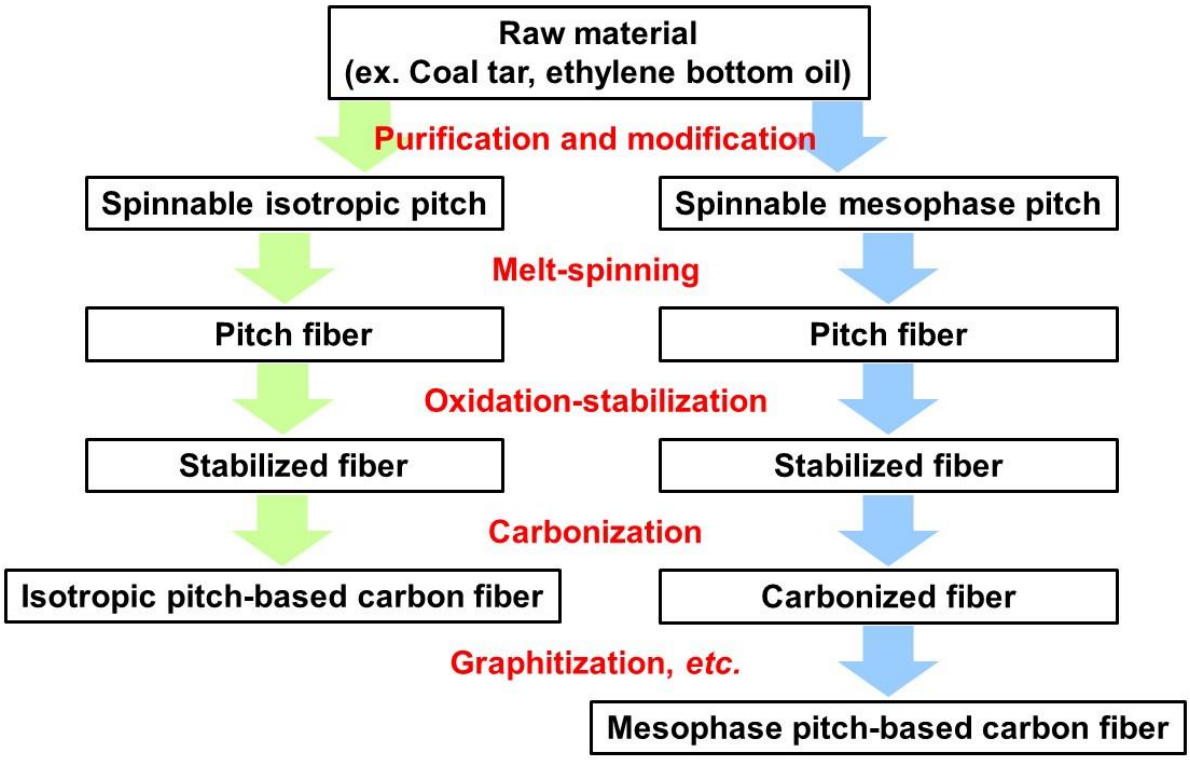

Fig. 1-2. Manufacturing process of pitch-based CFs.

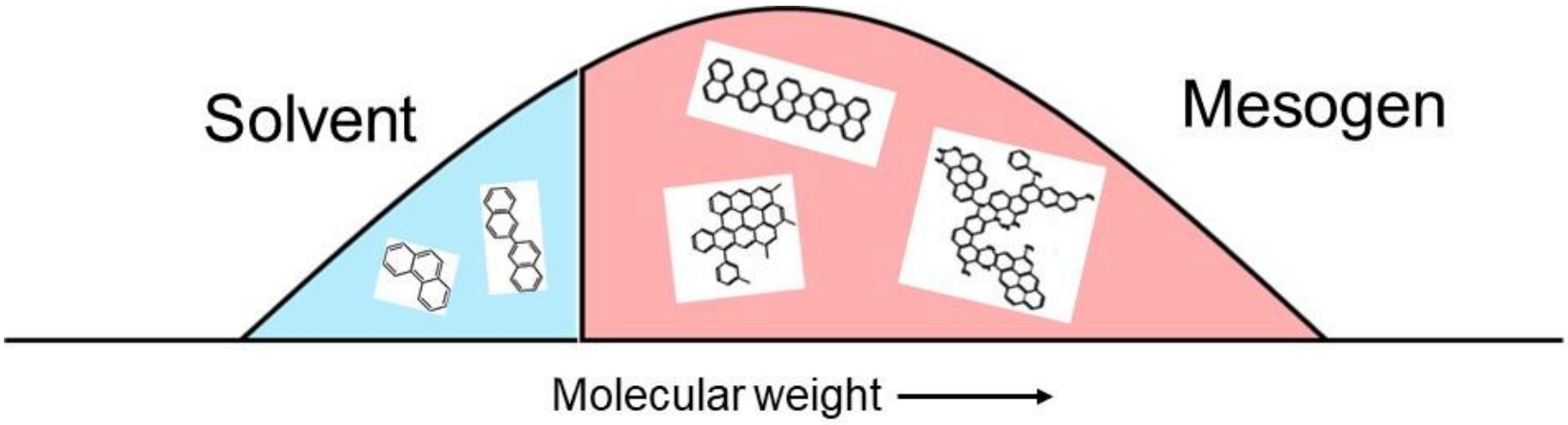

Fig. 1-3. The image of molecular weight distribution of MP's components.

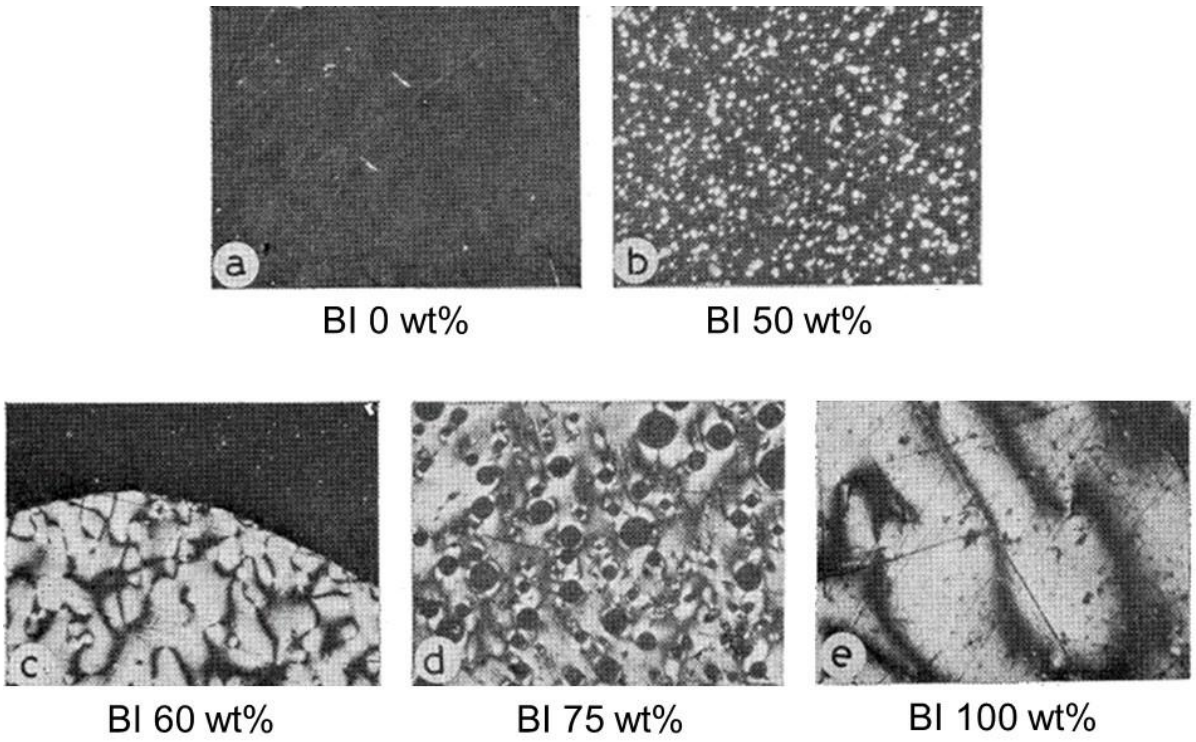

Fig. 1-4. The optical textures obtained by mixing benzene insoluble fraction (BI) and soluble fraction of MP derived from naphthalene pitch at various weight ratios and annealing.

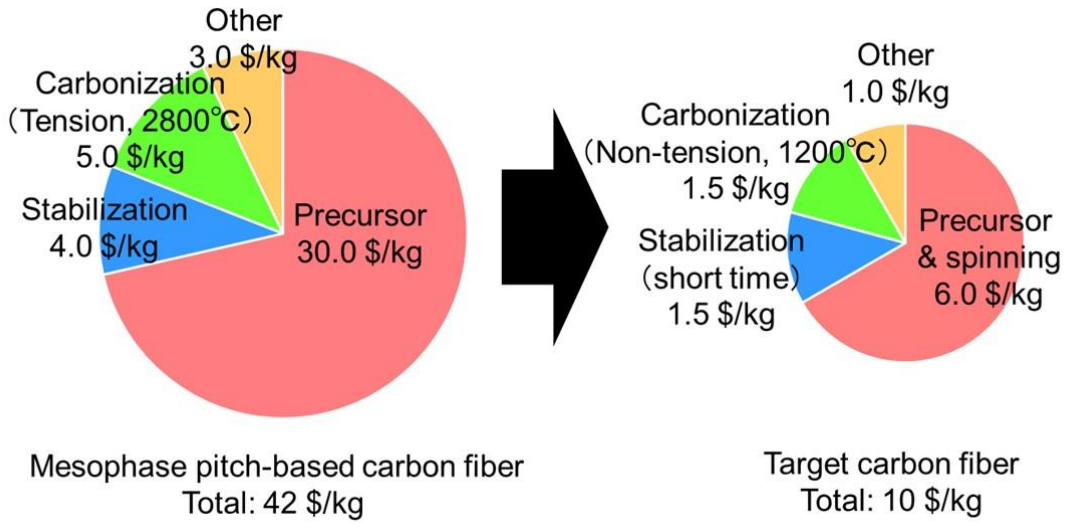

Fig. 1-5. The production costs of each manufacturing process of MP-based carbon fiber and target carbon fiber. based carbon fiber and target carbon fiber.

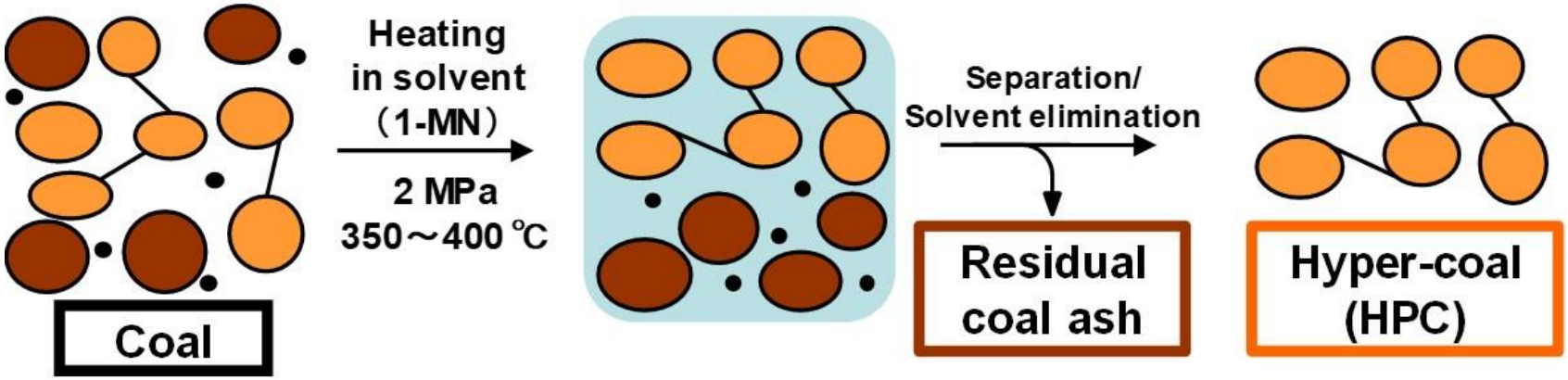

Fig. 1-6. Manufacturing process of Hyper-coal

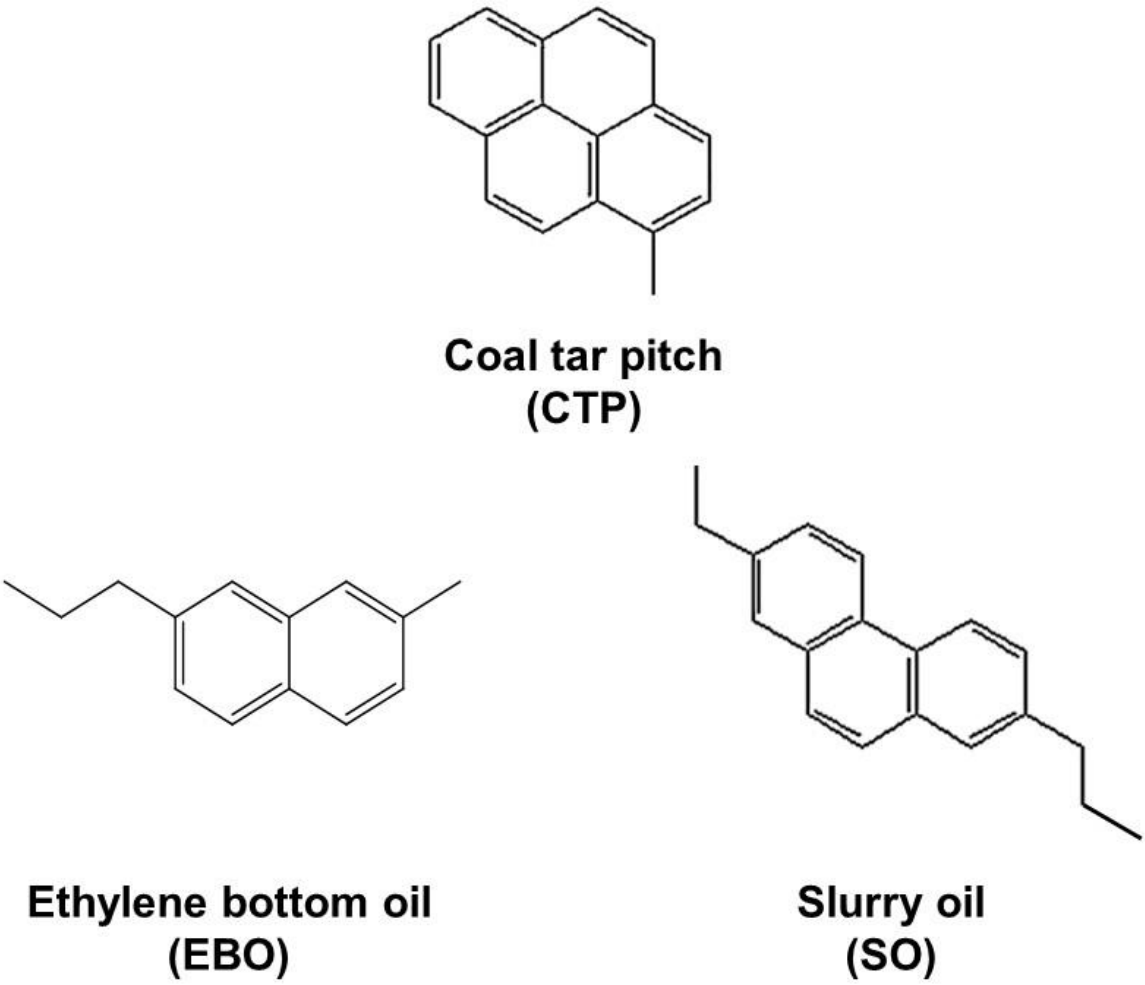

Fig. 1-7. Average molecular structure of CTP, EBO and SO.

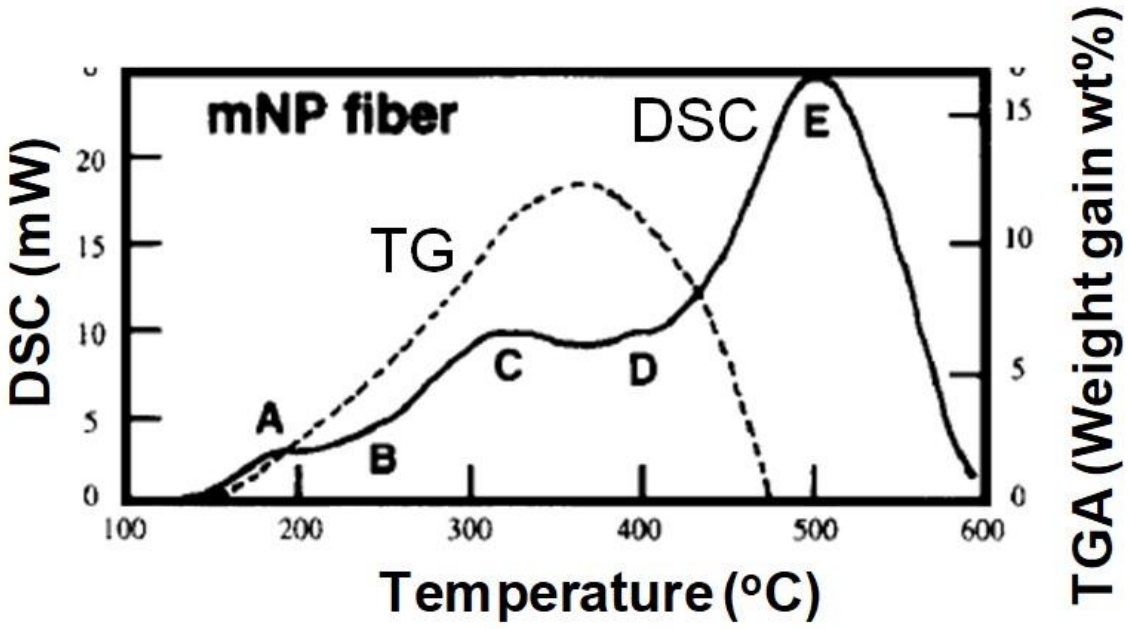

Fig. 1-8. DSC (solid line) and TGA (broken line) oxidation curves of a MP fiber (A: Oxidation of aliphatic groups on the surface of pitch fibers, B&C: Oxidation of aliphatic groups inside pitch fibers, D: Oxidation of aromatic carbons, E: Combustion).

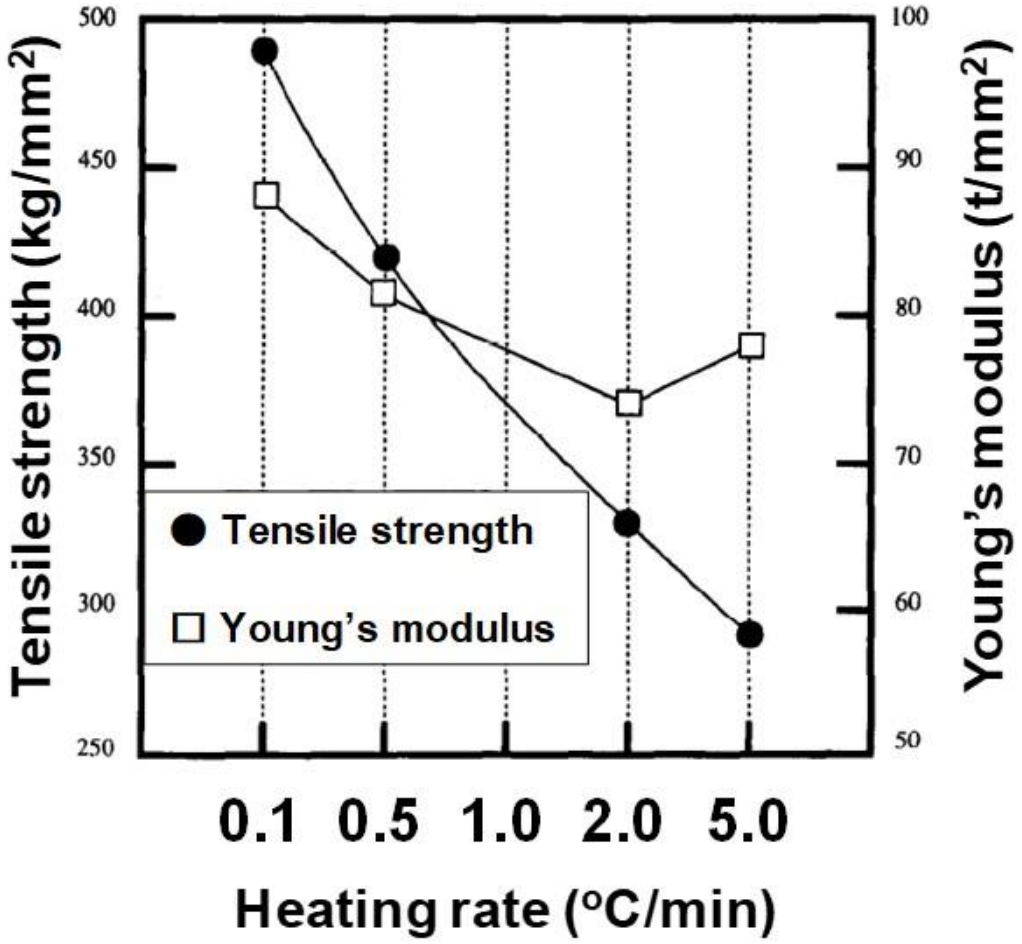

Fig. 1-9. TS and YM of CFs stabilized at various heating rates.

Chapter 2. Improvement of spinnable mesophase pitch yield using a coal direct extracted fraction

2-1. Introduction

Carbon fiber reinforced plastic (CFRP) which has lighter weight and higher strength than steel is considered as a suitable alternative as car-body material of automobiles [1−3]. Jim deVries of the Ford Motor Company recommended that the tensile strength (TS), elongation ratio and Young's modulus (YM) of CF for car frames should be at least 1.7 GPa, 1.0%, and 170 GPa, respectively, with a material price less than 10−12 $/kg [3]. Polyacrylonitrile-based carbon fibers (PANCFs) exhibit a higher TS, elongation ratio, and YM than the required mechanical properties [4]. However, its production cost is more than 20 $/kg due to expensive PAN precursor fiber and its low carbonization yield. On the other hand, isotropic pitch-based CFs (IPCFs) have low production costs owing to cheap raw material and a simple production process [5]. Nevertheless, IPCFs have not yet satisfied the required mechanical properties, exhibiting TS of 0.5–1.0 GPa and YM of 30–50 GPa [6]. The mechanical properties of IPCFs can be improved by designing novel molecular structures in the isotropic pitch (IP) precursor using biomass, polymers, and coal and petroleum by-products [7−9]. Kim *et al.* successfully developed IP with a linear structure through a bromination-dehydrobromination reaction of ethylene bottom oil and coal tar pitch and prepared IPCFs with TS of 2.0–2.4 GPa [9]. However, these fibers still suffer YM deficiency.

Mesophase pitch-based CFs (MPCFs) have high mechanical properties comparable to IPCFs [10]. TS, elongation ratio and YM of MPCFs are 2.2–3.5 GPa, 0.2–1.7%, and 140–820 GPa, respectively [11], but the applications of MPCFs are very limited because they have the high production cost due to low yield of spinnable mesophase pitch (SMP). For example, the yield of SMP derived from decant oil by hydrogenation using 1, 2, 3, 4-tetrahydroquinoline and heat treatment is 5.0–10.0 wt% [12]. We have

used direct coal extracted fraction (Hyper-coal: HPC) as an effective and inexpensive raw material for the development of functional carbon products [13]. HPC is a unique and cheap coal extracted material that can be obtained through direct solvent extraction of coal using 1-methylnaphthalene as a solvent at 350–400°C under high pressure, and it shows various molecular properties depending on the selected original coal and extraction conditions of temperature and pressure [13−15]. It has very interesting characteristics of low ash, high carbonization yield, and excellent thermoplastic properties [14−15]. However, the application of HPC has been still very limited to coke production, fuel for gasification, and additives for binder materials. Our group has reported a method for the simple preparation of spinnable IP using only solvent extraction and short-time thin layer evaporation (TLE) of HPC [13].

In this work, SMP with high pitch yield was developed through the usual three-step process of hydrogenation, N_2 blowing heat treatment, and short-time TLE using selected HPC as the raw material. Mesophase pitch (MP) with good spinnability was successfully fabricated at a yield of 50 wt% or more of raw HPC by optimizing each process. In addition, I prepared MP-based carbonized and graphitized fibers through melt spinning, stabilization, carbonization, and graphitization using the HPC-derived MP, and then, the mechanical properties of the obtained MPCFs were evaluated.

2-2. Experimental

2-2-1. *Preparation of SMP*

HPC was supplied by Kobe Steel Co. Ltd. and used as a raw material without further treatment. The used HPC was extracted using methyl naphthalene from the selected GR bitumen coal under the specific extraction conditions [16].

HPC and 1, 2, 3, 4-tetrahydronaphthalene (tetralin) were mixed at 1:1 or 1:2 ratios (w/w) and heat-treated at 400–450°C for 1–4 h under autogenous pressure using an

autoclave for hydrogenation. After removing tetralin from the hydrogenated HPC by vacuum distillation, the samples were successively heat-treated at 415°C for 3–4 h with N_2 blowing. The heating rate was 5°C/min and the flow rate of N_2 was 600 mL/min for 50 g of the hydrogenated HPC. After heat treatment with N_2 blowing heat treatment, light molecular volatile matters were removed by TLE at 390°C for 10 min under vacuum. The obtained pitches were abbreviated as HXNY and HXNY-TLE (HXNY denotes HPC hydrogenated at 450°C for X h at a 1:2 ratio of HPC:tetralin [w/w] followed by N_2 blowing heat treatment for Y h). **Fig. 2-1** shows schematic images of the SMP-manufacturing processes for N_2 blowing heat treatment and TLE.

2-2-2. *Melt-spinning, oxidation-stabilization, carbonization and graphitization*

The MP fibers were fabricated by a single-hole spinneret at 360–370°C with a homemade mono-hole melt-spinning apparatus, which has a stainless-steel die hole with diameter and length of 0.5 and 0.5 mm (L/D = 1), respectively [17]. **Fig. 2-2** shows schematic images of the monofilament spinning apparatus and spinneret. The MP fibers were stabilized at 270°C without a holding time under the air flow. The heating rate was 0.5 °C/min and the flow rate of air was 200 mL/min. The stabilized fibers were carbonized at 1000°C for 30 min with a heating rate of 20°C/min in a vacuum, and the carbonized fibers were also further graphitized at 2800°C for 10 min with a heating rate of 15 °C/min in an Ar atmosphere.

2-2-3. *Characterization*

The softening point (SP) and molten state of the prepared pitch were determined by thermal mechanical analysis (TMA) (TMA/SS6300; EXSTAR6300 SII; Seiko Co. Ltd., Tokyo, Japan) from room temperature to 400°C at a heating rate of 5°C/min under N_2 flow.

Elemental analyses were conducted to determine the carbon, hydrogen and nitrogen, contents, using an element analyzer (MT-5 CHN Corder; Yanako Co. Ltd., Tokyo, Japan). The oxygen content was calculated by weight using the following equation: $O_{diff.}$ [wt%] = (100–C–H–N).

Molecular weight distribution and the average molecular weights (AMWs) were estimated by time-of-flight mass spectrometry (TOF-MS) (JMS-S3000; JEOL Co. Ltd., Tokyo, Japan) after dissolving the pitch in tetrahydrofuran to a concentration of 1.0 wt%. The laser intensity was optimized to 55% with a delay time of 400 ns. Data more than 100 test points were collected for each sample.

^{13}C solid-state nuclear magnetic resonance spectroscopy (^{13}C-NMR) (ECA400; JEOL Co. Ltd.) was used to determine the molecular structure and aromaticity. Chemical shifts were normalized to the methyl carbon resonance of solid hexamethylbenzene at 17.4 ppm. Approximately 100 mg pulverized sample was added to a zirconia standard sample rotor (diameter: 3.2 mm). The acquisition time was 0.05 s with a pulse of 90° and a width of 15 kHz. The method of ^{13}C detection was DEPTH2 with magic-angle spinning (MAS) speed of 15 kHz.

Anisotropic textures of the obtained pitches were observed by polarization microscope (POM) (BX51-P; Olympus Co. Ltd., Tokyo, Japan).

Images of the structure of the transverse sections and the surface morphology of the graphitized fibers were obtained using a scanning electron microscope (JSM-6700F; JEOL Co. Ltd.). Micrographs were acquired with an accelerating voltage of 5 kV.

The mechanical properties of the carbonized and graphitized fibers were measured using a tensile tester (TENSILON/UTM-II-20; Orientec, Tokyo, Japan) in accordance with the JIS R 7606:2000 method.

2-3. Results and discussion

2-3-1. *Hydrogenation of HPC under various conditions*

Table 2-1 summarizes some of the physical and chemical properties of HPC hydrogenated under various conditions. **Fig. 2-3** shows the molecular weight distributions of as-received and hydrogenated HPCs under various conditions. **Fig. 2-4** shows the ^{13}C-NMR spectra of HPC hydrogenated under various conditions.

As shown in **Figs. 2-3** and **2-4**, it was clearly confirmed that as-received HPC already has a high AMW of 697 *m*/*z* and carbon aromaticity of 0.88, which were higher compared to typical IPs with high SP. This suggests that the as-received HPC, which was directly extracted from coal at a high temperature and high pressure with methylnaphthalene, already contains a large amount of high-molecular-weight and fully developed high polynuclear aromatic molecular compositions. To effectively manufacture a SMP using HPC as a raw material, it is necessary to induce the naphthenic for the flexible molecular structures of the prepared MP and effectively remove the alkyl components, except for the methyl group. In particular, it is essential to introduce an enough height of 002 type layered molecular stacking for the proper formation of flow domain texture of MP. Therefore, the hydrogenation of as-received HPC was carried out to simultaneously give the mesophase texture and flexible molecular structure for improved spinnability.

The TOF-MS and ^{13}C-NMR spectra confirmed that the heavy molecular components with *m*/*z* higher than 1000 were effectively converted into lighter molecular components by hydrogenation, and the high temperature treatment of hydrogenation easily caused a decomposition of heavy molecular components and changed methylene chains to short-chain alkyls such as methyl groups [13]. Therefore, the top peak molecular distribution and AMW of HPC hydrogenated at 450°C shifted to low molecular-weights. The longer the retention time of hydrogenation, the greater the

increase in light molecular components. However, two top peaks appeared after hydrogenation for 4 h. The results of elemental and ^{13}C-NMR analyses suggested that a coking reaction partially occurred because tetralin lost its hydrogen-donating property [18]. The exothermic coking reaction may cause excessive decomposition and increase specific molecules. The ^{13}C-NMR spectra of HPCs hydrogenated at 400°C and 430°C indicated an increase in the amount of methyl carbons (-CH_3, 17–23 ppm), methylene carbons inside aliphatic chains (-CH_2-, 23–34 ppm), and bridge/hydro-aromatic structures (Ar-CH_2-Ar, 34–50 ppm) [19]. However, those at 450°C indicated a decrease in the amount of -CH_3, -CH_2-, and Ar-CH_2-Ar. The longer the retention time of hydrogenation up to 3 h, the greater the increase in the amount of -CH_3. On the other hand, HPC hydrogenated at 450°C for 4 h exhibited a decrease in the amount of aliphatic carbons due to the coking reaction. Hydrogenation at high temperatures for long retention times caused the decomposition of methylene chains and heavy molecular components. Based on these results, the hydrogenation conditions of the as-received HPC were set to 450°C and 3 h.

2-3-2. *Formation of an anisotropic texture after hydrogenation and N_2 blowing heat treatment*

Table 2-2 summarizes some of the physical and chemical properties of the pitches obtained by hydrogenation, N_2 blowing heat treatment, and TLE. **Figs. 2-5** and **2-6** show the anisotropic textures and TMA profiles for determining the melting properties of the pitches obtained after N_2 blowing heat treatment, respectively.

N3, which was obtained by the N_2 blowing heat treatment of as-received HPC for 3 h, exhibited an anisotropic flow texture and pores, but could not be melted owing to coke production. The hydrogenation remarkably improved the melting behavior of resultant pitches. For example, H1N3 had the flow type anisotropic texture with

isotropic spheres and was completely melted at 370°C. However, upon melt-spinning, too high spinning temperatures caused decomposition and decreased its spinnability. H2N3 and H3N3 included many mesophase spheres and had SPs of 277°C and 258°C, respectively. Longer retention times of N_2 blowing heat treatment yielded more anisotropic textures with increasing SPs in the obtained pitches. H3N3, H3N3.5, and H3N4 showed high pitch yields of 55.7 wt%, 56.2 wt%, and 57.0 wt%, respectively. H4N3 included cokes and mesophase spheres and was not completely melted at 400°C. HPCs hydrogenated at 450°C for 3 h included many light molecular components with mesogens, and the obtained pitches featured many mesophase spheres with low SPs and high yield.

Figs. 2-7 and **2-8** show the anisotropic textures and melting properties of H3N3-TLE, H3N3.5-TLE, and H3N4-TLE. After a short TLE treatment, the mesophase textures of H3N3 and H3N3.5 were dramatically converted into bulk mesophase ones by slightly removing the light molecular components in the isotropic matrix. The obtained MPs of H3N3-TLE and H3N3.5-TLE showed many bulk flow textures with less than 20% isotropic spheres by volume. The MPs of H3N3-TLE and H3N3.5-TLE showed very high pitch yields of 54.9 wt% and 55.4 wt% and SPs of 267°C and 274°C, respectively. The SP and anisotropic texture of H3N4-TLE did not change, as enough light molecular components were already removed by N_2 blowing heat treatment. The SPs of H3N3-TLE and H3N3.5-TLE were lower than that of H3N4-TLE because the isotropic spheres may have had thermoplastic properties. HPC-derived MP was prepared at a high yield (>50 wt%) by hydrogenation and two-stage heat treatments.

In **Fig. 2-9**, the molecular weight distributions of the pitches obtained by N_2 blowing heat treatments are shown. The AMW values of the obtained pitches were slightly lower than those of the parent hydrogenated HPCs. This indicates that there may have been an increase in molecules with 400–800 m/z due to polycondensation. However,

AMW of H4N3 was higher than that of HPC hydrogenated at 450°C for 4 h. The exothermal reaction of coking caused excessive condensation and increased heavy molecular components. AMWs of H3N3-TLE and H3N3.5-TLE increased by removing the light molecular components by TLE. The obtained MPs included large quantities of mesogens with the *m*/*z* values of 400–800.

Fig. 2-10 shows ^{13}C-NMR spectra of the obtained pitches after the N_2 blowing heat treatment. The carbon aromaticity increased with increasing duration of the N_2 blowing heat treatment through polycondensation, and light molecular components, including non-mesogens, were removed. The more the amount of anisotropic structure increased, the more the amounts of -CH_2- and Ar-CH_2-Ar decreased [19]. The ^{13}C-NMR spectra of H3N4 indicated a decrease in the amount of -CH_2- and Ar-CH_2-Ar. The obtained MP included many aromatic carbons with methyl groups.

2-3-3. *Mechanical properties of HPC derived MPCFs*

Table 2-3 shows the evaluation results of the spinnability of H3N3-TLE and H3N3.5-TLE and the diameters of spun fibers. The spun fibers of H3N3-TLE and H3N3.5-TLE were successfully prepared by melt-spinning at winding speeds of 400 rpm and 600 rpm, respectively. However, a winding speed of 800 rpm was found to be too fast to wind the spun fiber. The obtained pitches had few heavy molecular components with *m*/*z* of 800–1000, which could impede a decrease in the viscosity of the obtained pitches at 360–370°C. The diameters of spun fibers of H3N3-TLE and H3N3.5-TLE at a winding speed of 600 rpm were 13.2 ± 0.5 μm and 13.4 ± 0.5 μm, respectively.

Fig. 2-11 shows the surface and cross-section structures of the graphitized fibers. The striation in the fiber axis direction was observed on the surface of the obtained fibers, and the radial-random structure was observed on the cross-section of the

obtained fibers. **Table 2-4** summarizes the mechanical properties of the carbonized and graphitized fibers of H3N3-TLE and H3N3.5-TLE. TS, elongation, and YM of the carbonized fibers of H3N3-TLE were 1.8 GPa, 1.4%, and 140 GPa, respectively, after carbonization at 1000°C for 30 min, and the values for H3N3-TLE were 1.8 GPa, 1.4%, and 130 GPa, respectively. TS of the carbonized fibers was high enough to meet the objective CFs for the car frame, however, the elongation properties and YM were still not satisfied. If the diameter of the carbonized fiber could be controlled to less than 10.0 μm through further improving the spinnability of the present MP, it must be fully expected to manufacture the MPCF which can be applied to the car frame.

2-4. Conclusion

SMP with high preparation yield of 54.9 wt% was successfully prepared through the three-step manufacturing process of hydrogenation, N_2 blowing heat treatment, and short TLE using HPC as an effective source of cheap raw material.

As-received HPC has many light and heavy molecular components including fully developed polynuclear aromatic components with methyl groups and methylene chains. The hydrogenation of HPC decreased the amount of methylene chains and heavy molecular components with high polynuclear aromatic compounds. The N_2 blowing heat treatment was necessary to reveal the mesophase texture but not to increase the molecular weight and mesogen contents, including aromatic carbons. The short TLE treatment was very effective to obtain the spinnable bulk texture of MP through the slight removal of non-mesogen light molecular components. H3N3-TLE and H3N3.5-TLE were very effectively converted into bulk MP with SPs increased by only less than 10°C.

The obtained SMPs had a high yield (>50 wt%), which was likely due to the high-molecular-weight and carbon aromaticity of the as-received HPC. HPC-derived

MPCFs showed high TS of 1.8 and 3.0 GPa and YM of 140 and 450 GPa after carbonization at 1000°C for 30 min and graphitization at 2800°C for 10 min, respectively.

We anticipate that the high-yield preparation of SMP from HPC as a raw material can decrease the production cost of MPCFs, which could provide the opportunity to apply CF to frames of popular cars.

Reference

1. Chand S. Carbon fibers for composites. J Mater Sci 2000;35(6):1303−13.
2. Huang X. Fabrication and properties of carbon fibers. Materials 2009;2(4):2369−403.
3. Yang KS, Kim BH, Yoon SH. Pitch based carbon fibers for automotive body and electrodes, Carbon Lett 2014;15:162−70.
4. Toray Co Ltd. Technical data sheets. No. CFA-008, No. CFA-007, No. CFA-006, No. CFA-003, and No. CFA-002.
5. Alcañiz-Monge J, Cazorla-Amorós D, Linares-Solano A, Oya A, Sakamoto A, Hosm K. Preparation of general purpose carbon fibers from coal tar pitches with low softening point. Carbon 1997;35(8):1079−87.
6. Kureha Chemical Co Ltd. Product catalogue for carbon fiber. KRECA.
7. Ma XJ, Zhao GJ. Structure and performance of fibers prepared from liquefied wood in phenol. Fibers Polym 2008;9:405−9.
8. Postema AR. De root H, Pennings AJ. Amorphous carbon fibres from linear low density polyethylene. J Mater Sci 1990;25:4216−22.
9. Kim BJ, Eom Y, Kato O, Miyawaki J, Kim BC, Mochida I, et al. Preparation of carbon fibers with excellent mechanical properties from isotropic pitches. Carbon 2014;77:747−55.
10. Edie DD. The effect of processing on the structure and properties of carbon fibers. Carbon 1998;36(4):345−62.
11. Mitsubishi Chemical Co Ltd. Product catalogue for carbon fibers.
12. Kato O, Uemura S, Korai Y, Mochida I. Preparation of mesophase pitch and high performance carbon fiber from decant oil. J Jpn Petrol Inst 2004;47(2):100−6.
13. Yang J, Nakabayashi K, Miyawaki J, Yoon SH. Preparation of pitch based carbon fibers using hyper-coal as a raw material. Carbon 2016;106:28−36.

14. Hamaguchi M, Okuyama N. Manufacturing process and applications of the hyper-coal. Tanso 2013;257:149−56.
15. Okuyama N, Komatsu N, Shigehisa T, Kaneko T, Tsuruya S. Hyper-coal process to produce the ash-free coal. Fuel Process Technol 2004;85(8−10):947−67.
16. Yang J, Nakabayashi K, Miyawaki J, Yoon SH. Preparation of isotropic pitch-based carbon fiber using hyper coal through co-carbonation with ethylene bottom oil. J Ind Eng Chem 2016;34:397−404.
17. Liu J, Shimanoe H, Nakabayashi K, Miyawaki J, Ko S, Jeon YP, et al. Preparation of isotropic pitch precursor for pitch-based carbon fiber through the co-carbonization of ethylene bottom oil and polyvinyl chloride. J Ind Eng Chem 2018;67:276−83.
18. Otani S, Sanada Y. Foundation of carbonization engineering (in Japanese). Tokyo: Ohmsha; 1980.
19. Diaz C, Blanco CG. NMR: A powerful tool in the characterization of coal tar pitch. Energy Fuels 2003;17(4):907−13.

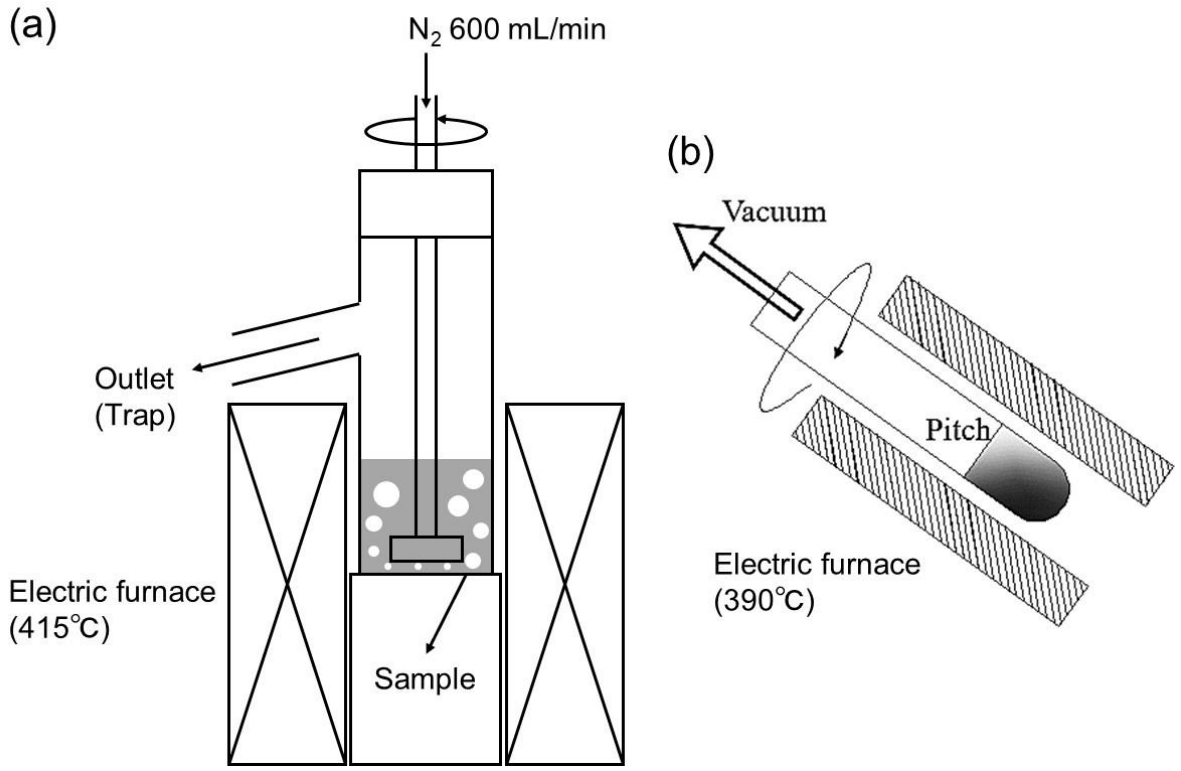

Fig. 2-1. Schematic picture of laboratory heat treatment apparatus: a) N_2 blowing heat treatment and b) TLE.

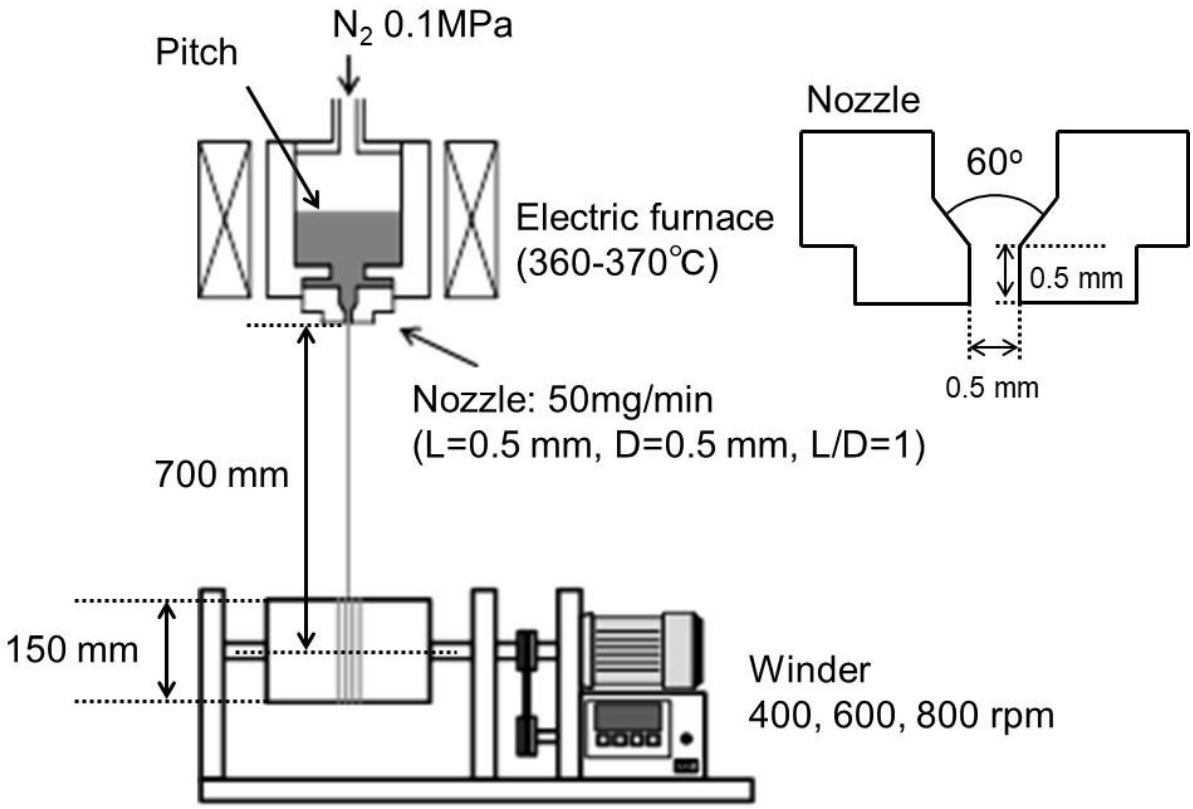

Fig. 2-2. Schematic picture of self-designed laboratory mono-hole melt-spinning apparatus.

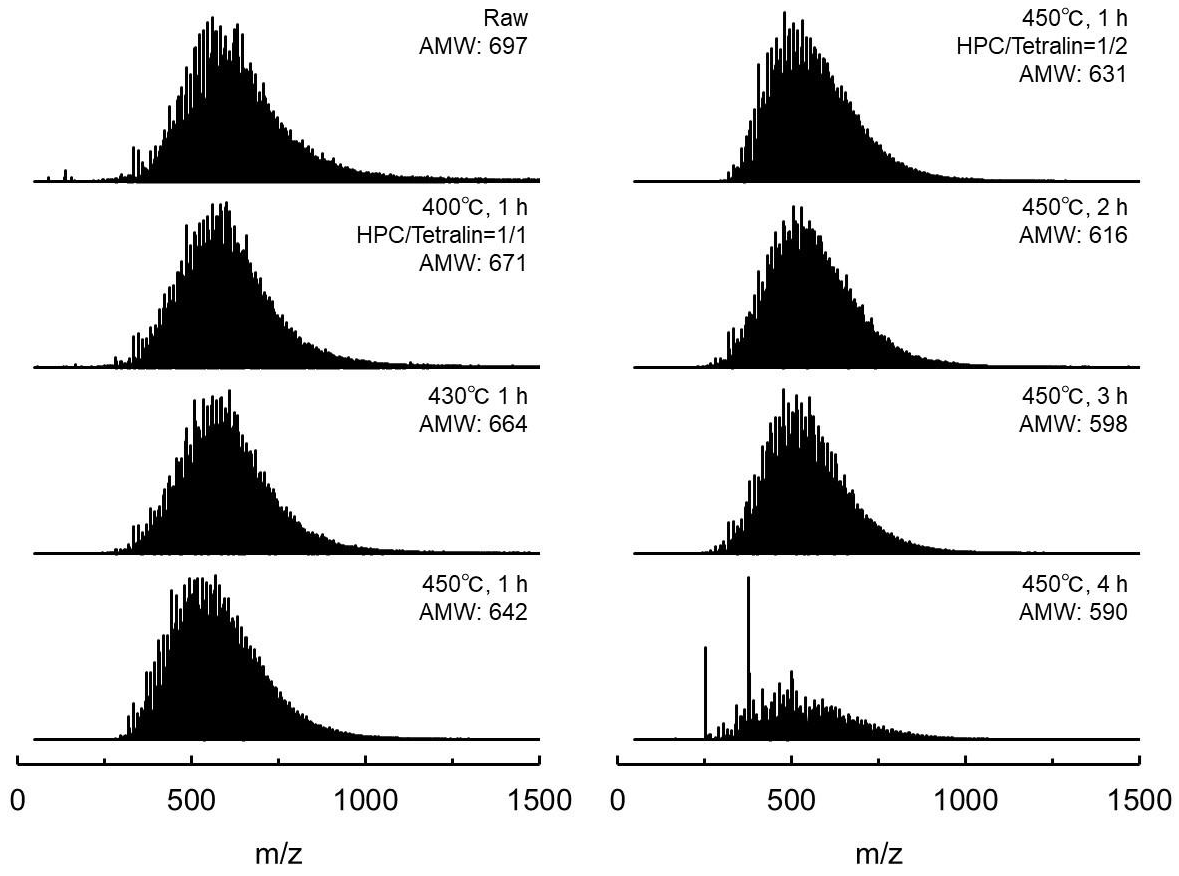

Fig. 2-3. The molecular weight distributions of HPC hydrogenated under various conditions.

.

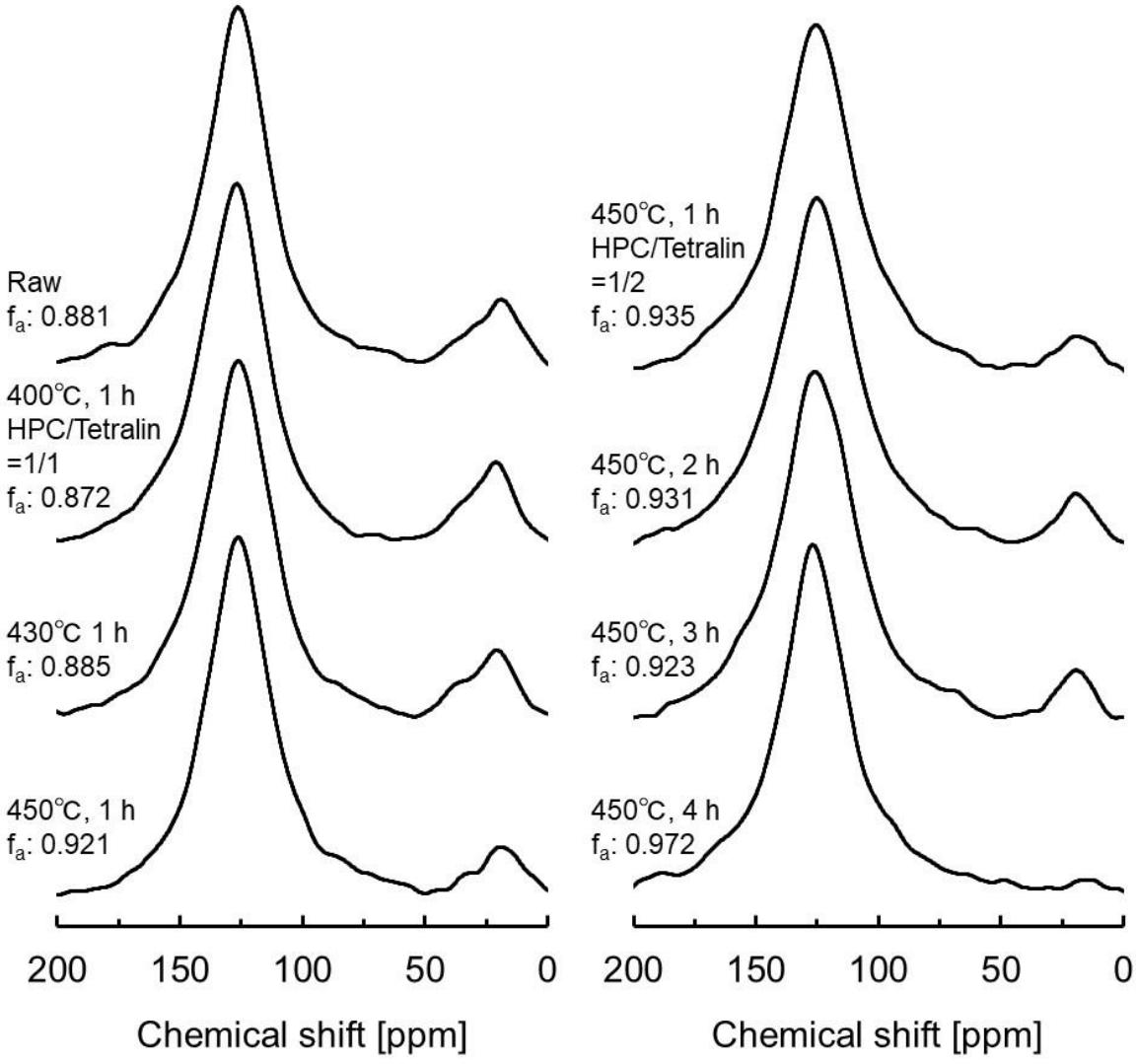

Fig. 2-4. ^{13}C-NMR spectra of HPC hydrogenated under various conditions.

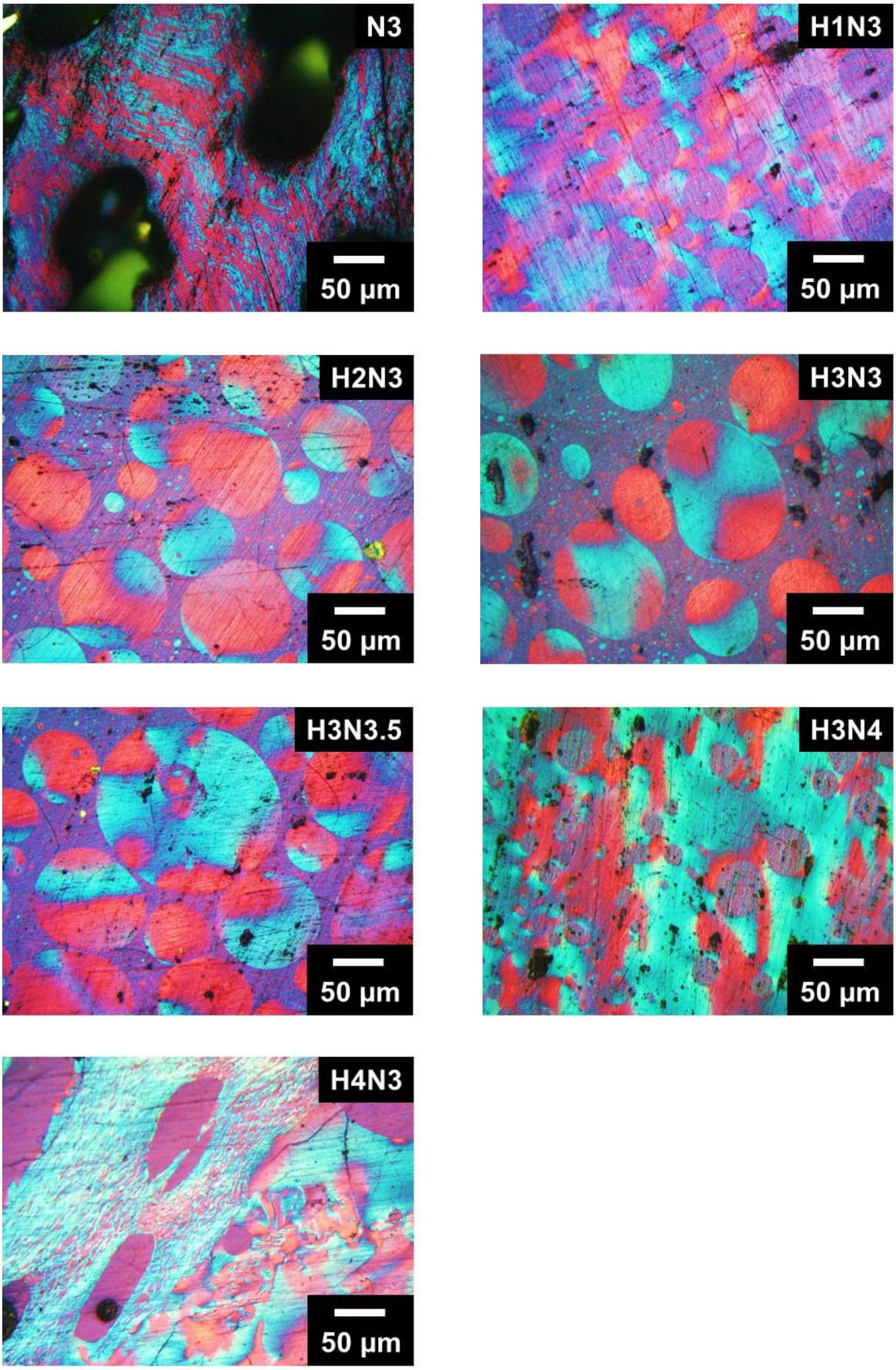

Fig. 2-5. POM images of the obtained pitches after N_2 blowing heat treatment.

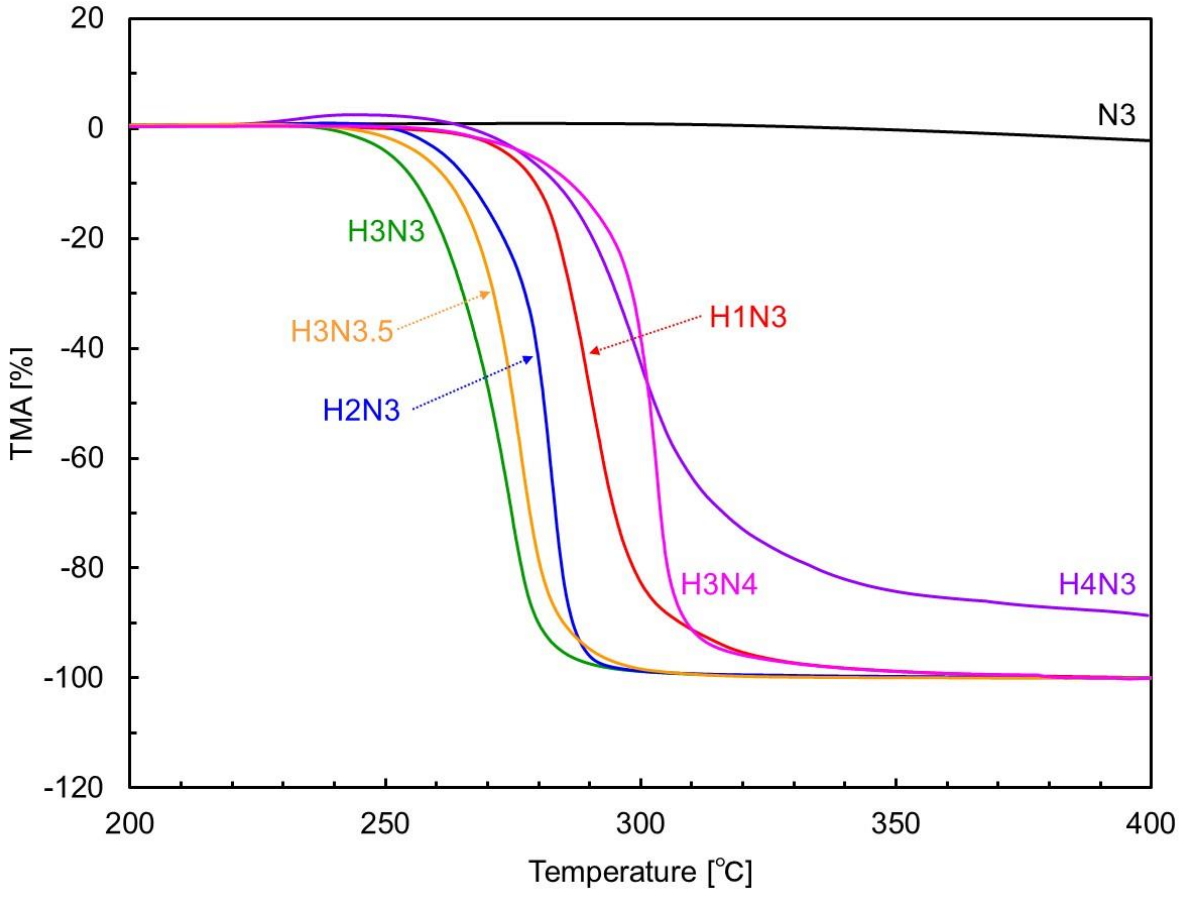

Fig. 2-6. TMA profiles of the obtained pitches after N_2 blowing heat treatment.

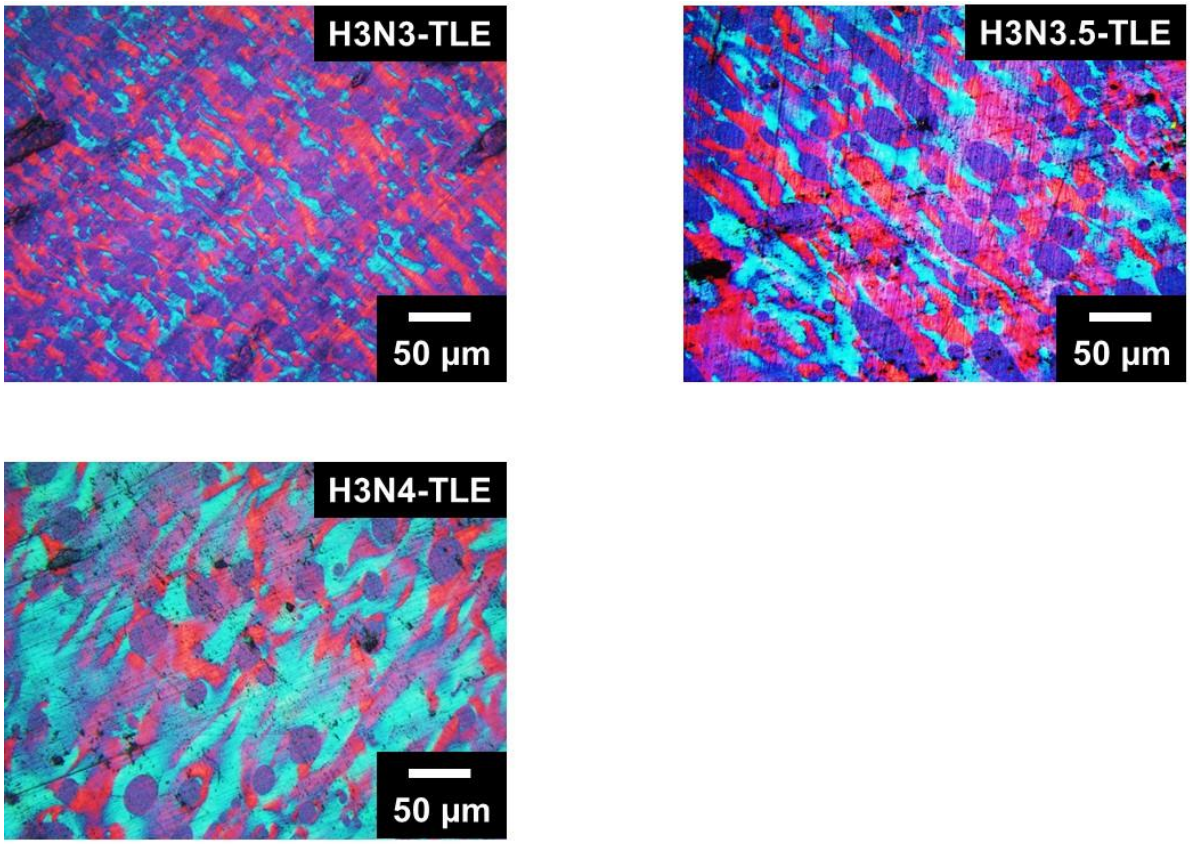

Fig. 2-7. POM images of the obtained pitches after N_2 blowing heat treatment and TLE.

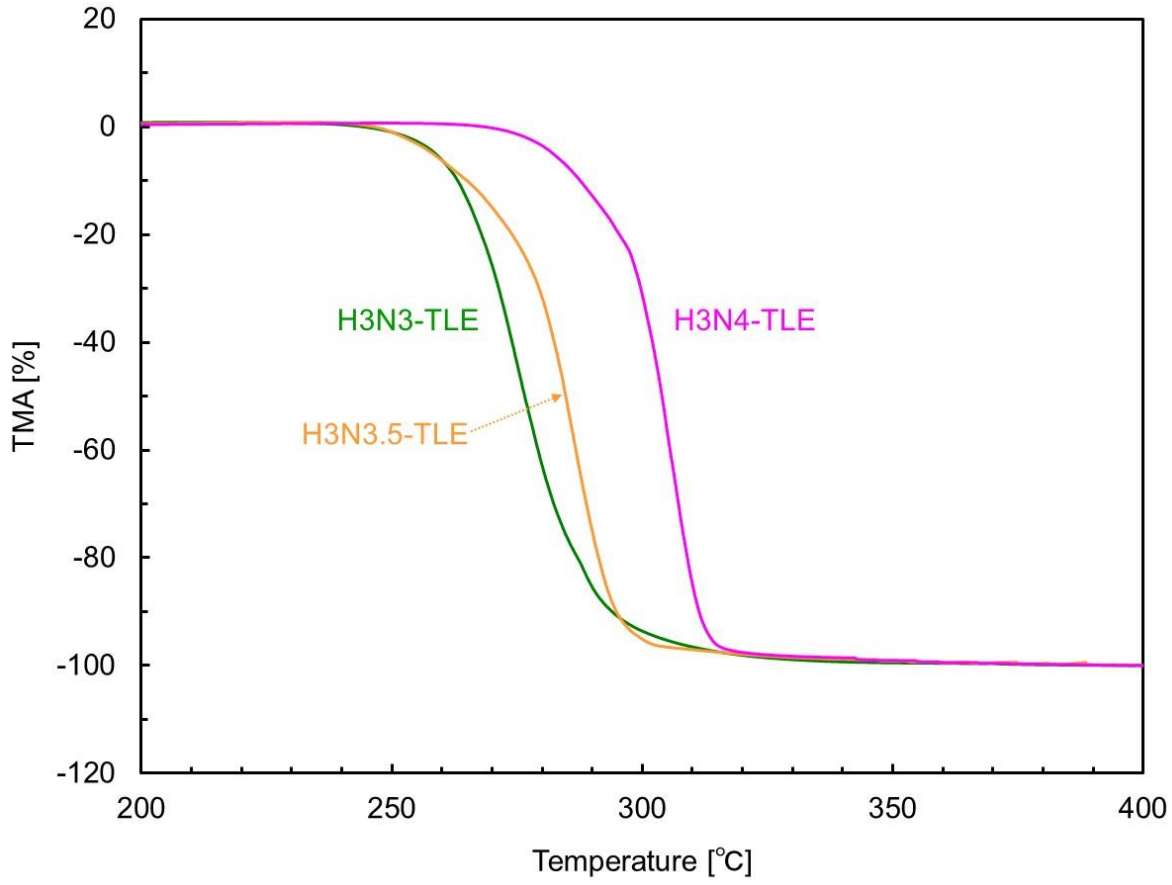

Fig. 2-8. TMA profiles of the obtained pitches after N_2 blowing heat treatment and TLE.

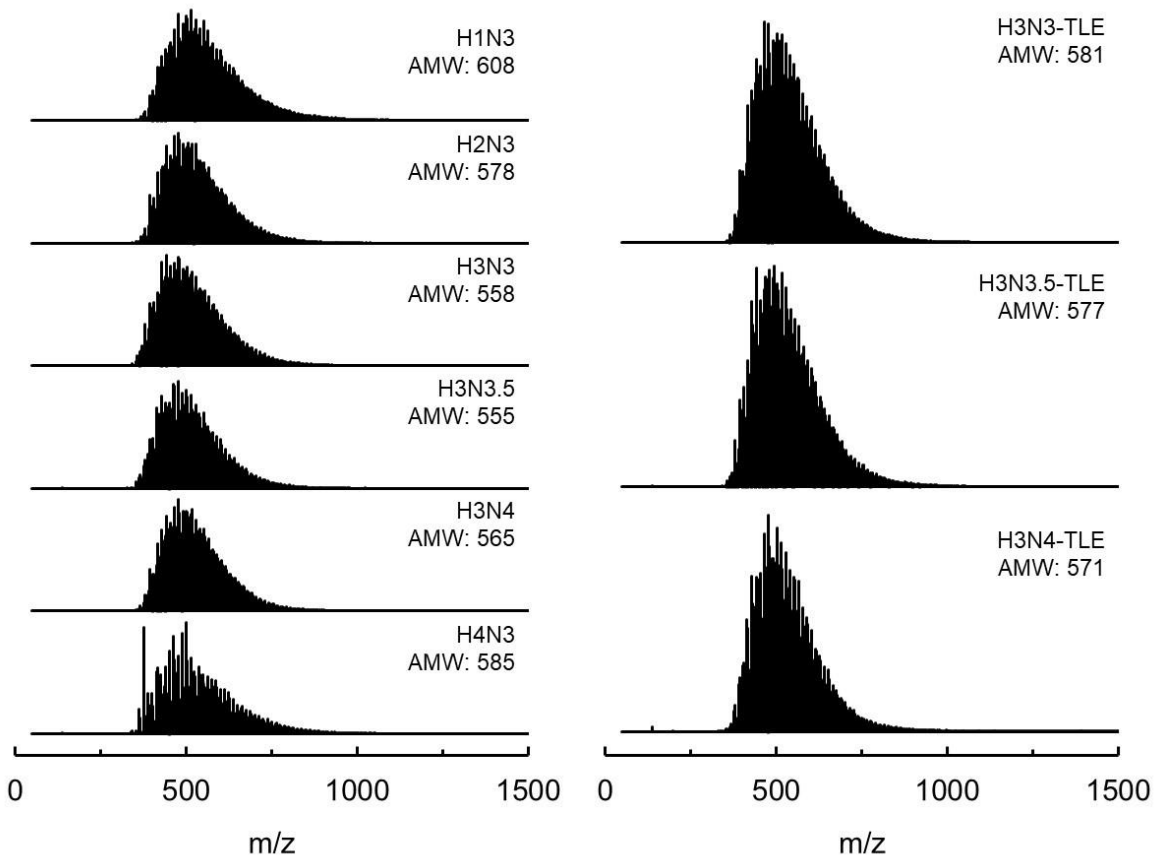

Fig. 2-9. The molecular weight distributions of the obtained pitches after N_2 blowing heat treatment and TLE.

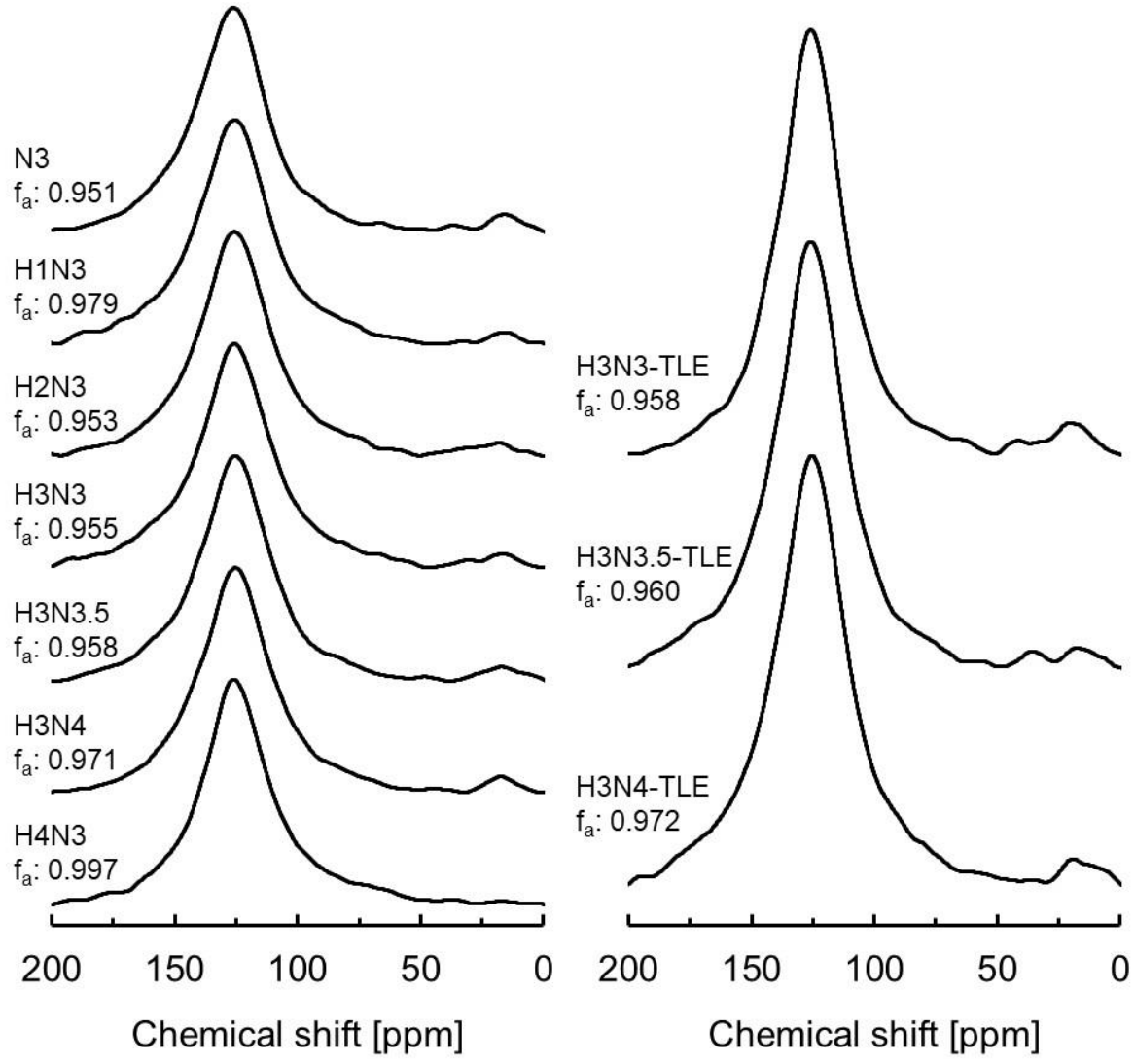

Fig. 2-10. ^{13}C-NMR spectra of the obtained pitches after N_2 blowing heat treatment and TLE.

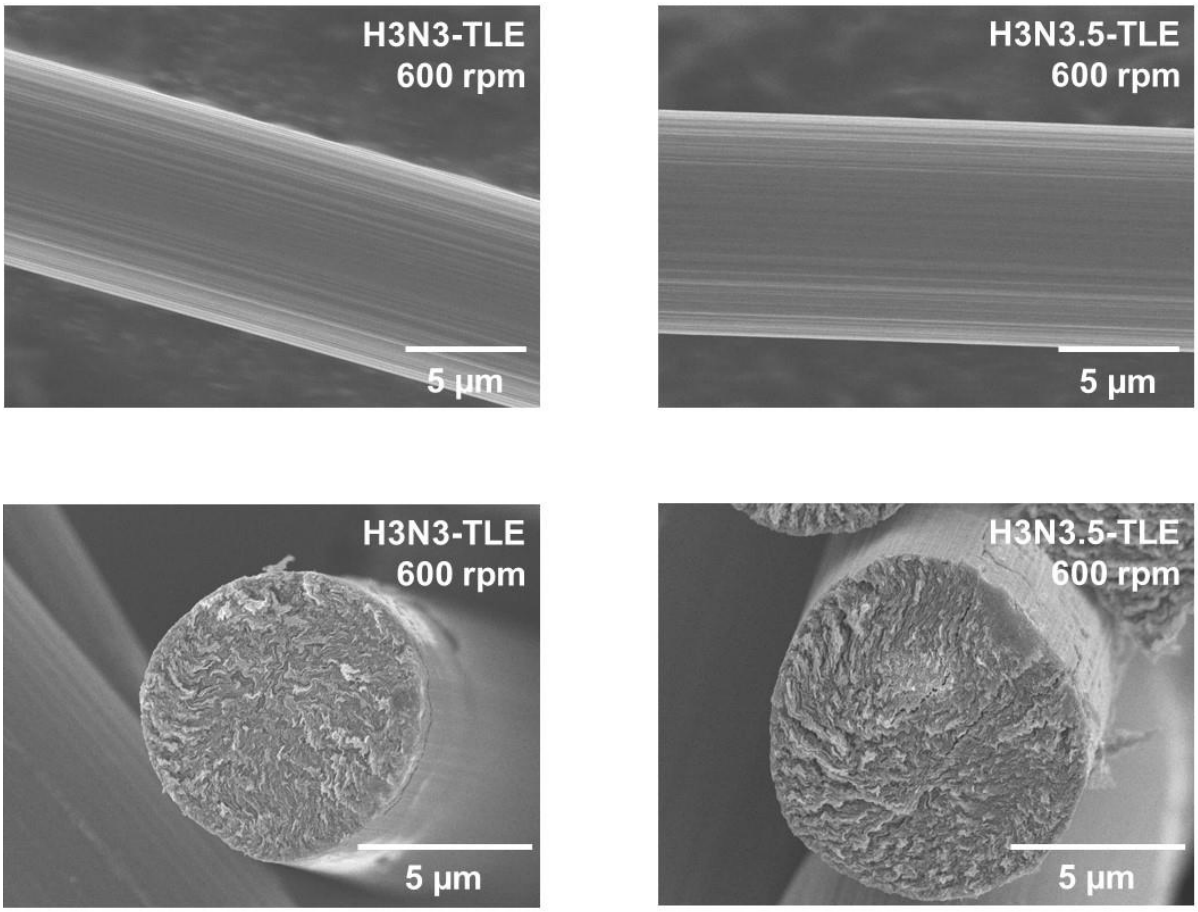

Fig. 2-11. SEM images of the surface structure and the cross-section of graphitized fibers of H3N3-TLE and H3N3.5-TLE.

Table 2-1 The physical and chemical properties of HPC hydrogenated under various conditions

HTT[a]	HPC/Tetralin	Holding time	Yield	Elemental analysis				TOF-MS	^{13}C-NMR
				C	H	N	$O_{diff.}$	AMW[b]	f_a[c]
[°C]	[w/w]	[h]	[wt%]	[wt%]	[wt%]	[wt%]	[wt%]	[−]	[−]
–	–	–	–	89.8	5.2	1.6	3.4	697	0.881
400			98.0	89.5	5.4	1.0	4.1	671	0.872
430	1/1	1	97.6	89.9	5.2	1.1	3.8	664	0.885
450			96.8	90.7	4.9	0.9	3.5	642	0.921
450	1/2	1	95.6	90.5	5.4	1.6	2.5	631	0.935
		2	95.1	90.9	5.4	1.6	2.1	616	0.931
		3	94.1	90.8	5.3	1.6	2.3	598	0.923
		4	93.5	93.4	4.6	0.8	1.2	590	0.972

[a] Heat treatment temperature

[b] Average molecular weight

[c] Carbon aromaticity

Table 2-2 The physical and chemical properties of the obtained pitches after N_2 blowing heat treatment and TLE

	Yield	TMA	Elemental analysis				TOF-MS	^{13}C-NMR
		SP[a]	C	H	N	$O_{diff.}$	AMW[b]	f_a[c]
	[wt%]	[°C]	[wt%]	[wt%]	[wt%]	[wt%]	[−]	[−]
N3	88.3	−	89.9	4.8	0.8	4.5	−	0.951
H1N3	69.4	281	91.4	4.5	0.9	3.2	608	0.979
H2N3	62.0	277	91.4	4.6	0.9	3.1	578	0.953
H3N3	55.7	258	91.4	4.5	0.8	3.3	558	0.955
H3N3.5	56.2	264	91.6	4.4	0.8	3.2	555	0.958
H3N4	57.0	296	91.4	4.4	0.7	3.5	565	0.971
H4N3	54.6	286	93.8	3.8	0.4	2.0	585	0.997
H3N3-TLE	54.9	267	91.5	4.5	0.7	3.3	581	0.958
H3N3.5-TLE	55.4	274	91.7	4.4	1.0	2.9	577	0.960
H3N4-TLE	57.0	296	91.7	4.3	0.8	3.2	571	0.972

[a] Softening point

[b] Average molecular weight

[c] Carbon aromaticity

Table 2-3 The spinnability of H3N3-TLE and H3N3.5-TLE using self-designed laboratory mono-hole melt-spinning apparatus and the average diameter of spun fibers

	Breakage number			Diameter		
	400 rpm [/3 min]	600 rpm [/3 min]	800 rpm [/3min]	400 rpm [μm]	600 rpm [μm]	800 rpm [μm]
H3N3-TLE	3	8	−	16.5±0.5	13.2±0.5	−
H3N3.5-TLE	4	9	−	16.5±0.5	13.4±0.5	−

Table 2-4 The yields and mechanical properties of carbonized and graphitized fibers (Spun fibers at winding speeds of 600 rpm)

	Stabilization	Carbonization					Graphitization				
	Yield	Yield	Diameter	TS[a]	YM[b]	E[c]	Yield	Diameter	TS[a]	YM[b]	E[c]
	[%]	[%]	[μm]	[GPa]	[GPa]	[%]	[%]	[μm]	[GPa]	[GPa]	[%]
H3N3-TLE	109.0	84.7	10.2±0.5	1.8±0.4	140±20	1.4±0.3	83.8	9.3±0.4	3.0±0.4	450±60	0.7±0.1
H3N3.5-TLE	108.5	83.9	10.5±0.5	1.8±0.5	130±20	1.4±0.2	83.2	9.8±0.3	2.4±0.4	370±50	0.7±0.1

[a] Average tensile strength

[b] Average Young's modulus

[c] Average elongation

Chapter 3. Preparation of spinnable mesophase pitch by hybridization of raw materials

3-1. Introduction

Spinnable mesophase pitch (SMP) is used as an effective precursor for high-performance mesophase pitch-based carbon fiber (MPCF) [1, 2]. As an effective MPCF precursor, its high price has been considered as the main obstacle to broaden the MPCF application areas. SMP is commercially produced from the petroleum and coal residues (slurry oil (SO) and coal tar pitch (CTP)) through the complicated manufacturing processes of purification, hydrogenation, mesofication in liquid phase carbonization and other subside treatments such as volatile matter removal process with less than 10 wt% of final pitch yield to its raw material [3, 4].

Purification removes impurities such as inorganic materials and is costly. Hydrogenation can lower the softening point (SP) of obtained SMP by introducing naphthenic structure and reducing long-chain alkyl side groups, and coincidentally decreasing excess carbon-aromaticity which is difficult to solve [5]. However, the hydrogenation of raw materials is considered as a main reason for decreasing the pitch yield and increasing the production cost. Therefore, the development of SMP without hydrogenation has been a long-time requirement for manufacturing the low price MPCF. Furthermore, the manufacturing processes, such as supercritical toluene extraction of SO and HF/BF_3-catalyzed preparation of AR-mesophase pitch, have improved the production yield of mesophase pitch (MP) up to over 20 wt% [6, 7]. However, commercial production has been very limited due to the costly equipment and their operation costs, difficulty of operation, and relatively low spinnability. Thus, the usual inexpensive production process (*e.g.* N_2 blowing heat treatment and thin layer evaporation (TLE)) needs to be used.

In this study, I tried to prepare SMP and examine the effects on the growth and coalescence of anisotropic textures through the hybridization of ethylene bottom oil (EBO) with CTP or SO. SMP is composed of solvent molecules that have hydrogen donation property and mesogen molecules such as planar polycyclic aromatic hydrocarbons with short-chain aliphatic side groups [8]. EBO is composed of aromatic hydrocarbons which have a role for a solvent for mesogen molecules, and CTP and SO have aromatic hydrocarbons as mesogen molecules [9−11]. Adding CTP or SO into EBO, the mesophase expression, growth and coalescence of EBO derived pitch can be improved. By hybridizing EBO, CTP and SO with optimized balance, SMP may be prepared without excess hydrogenation. Hybridized EBO with CTP or SO was reacted by bromination-dehydrobromination to form intermolecular methylene bridge, optimize the molecular structure and increase the average molecular weight and the compatibility, followed by the N_2 blowing heat treatment and TLE [12, 13].

3-2. Experimental

3-2-1. *Pretreatment of raw materials*

Tetrahydrofuran soluble fractions of EBO, CTP and SO were used as raw materials for SMP. EBO was pretreated by pressurized heat treatment at 370°C for 3 h under autogenous pressure to increase molecular weight (EBOp). EBOp was continuously heat treated by bromination at 110°C for 2 h under Ar atmospheres using 0, 5 or 10 wt% of Br_2 and dehydrobromination at 370°C for 3 h under Ar atmospheres. EBOp and CTP or SO were mixed at the weight ratio of 3:7, 5:5 and 7:3, and the mixture was treated by bromination-dehydrobromination under the same conditions (EBOp/CTP, EBOp/SO and CTP/SO). **Table 3-1** exhibits the average molecular weight and carbon aromaticity of raw materials.

3-2-2. *Preparation of SMP*

SMPs were obtained by heat treatment at 425°C for 3−4 h with N_2 blowing heat treatment. The heating rate was 5°C/min and the flow rate of N_2 was 600 mL/min for 50 g of sample. After the heat treatment with N_2 blowing, light molecular components were removed by TLE at 390−410°C for 0−10 min under vacuum. **Fig. 3-1** shows the schematic images of the MP-manufacturing processes for N_2 blowing heat treatment and TLE.

3-2-3. *Characterization*

SPs of the prepared pitch were determined by thermal mechanical analysis (TMA) (TMA/SS6300; EXSTAR6300 SII; Seiko Co. Ltd., Tokyo, Japan) from room temperature to 400°C at a heating rate of 5°C/min under N_2 flow.

Anisotropic textures of the obtained pitches were observed by polarization microscopy (POM) (BX51-P; Olympus Co. Ltd., Tokyo, Japan).

3-3. Results and discussion

3-3-1. *Effect of raw material hybridization on the expression of anisotropic texture*

Table 3-2 shows the yield and SP of the obtained pitches after the N_2 blowing heat treatment. **Fig. 3-2** shows the anisotropic textures of the obtained pitches after the N_2 blowing heat treatment. The obtained pitch derived from EBOp brominated using 0, 5 and 10 wt% of Br_2 exhibited high yields of 20.4, 21.7, 22.9 wt%, respectively. However, these samples brominated using 0 and 5 wt% of Br_2 had very high SPs of 320 and 324°C, respectively. Especially, at 10 wt% of B_2, the obtained pitch was not able to be melted and might change to a coke. The melt-spinning of the MPs derived from EBOp only was failed because the decomposition of the prepared pitches occurred at spinning temperature. In **Fig. 3-2**, MP derived from EBOp brominated at 5 wt% showed a mosaic

texture. If the fluidity of the pitch is good, the pitch shows the rapid growth of mesophase spheres and good coalescence property during liquid phase carbonization and the MP with flow domain anisotropic texture is possible to obtain [14]. Therefore, much small mesophase spheres of the pitch derived from EBOp only might confirm that the agglomeration and coalescence of the finely nucleated mesophase spheres were difficult due to the high viscosity.

EBOp/CTP derived pitch showed a higher pitch yield of 27.0 wt% than EBOp/SO and CTP/SO derived pitches (19.8 and 21.5 wt%, respectively). EBOp/CTP, EBOp/SO and CTP/SO derived pitches exhibited SPs of 256, 285 and 236°C, respectively. As shown in **Table 3-1** and **Fig. 3-2**, the EBOp derived pitch had mosaic anisotropic texture because EBOp is composed of aromatic hydrocarbons which include low condensed aromatic rings and long side chains of aliphatic groups which impede the molecular stacking. On the other hand, the EBOp/CTP derived pitch had mesophase spheres (Anisotropy: 50 vol%) because CTP has polycyclic aromatic hydrocarbons with short side chains of aliphatic groups such as methyl group and shows high molecular stacking property [4, 9, 10]. Thus, the growth and coalescence of mesophase spheres were improved by the addition of CTP into EBOp.

The EBOp/SO derived pitch showed the same volume of anisotropic texture with EBOp/CTP derived pitch, but the size of mesophase spheres was smaller and the agglomerated anisotropic textures appeared more distorted than EBOp/CTP derived one. SO was composed of aromatic hydrocarbons with higher condensed aromatic rings than EBOp, so the growth of mesophase spheres was a little improved by the addition of SO [11]. However, the coalescence of mesophase spheres derived from EBOp/SO was low because SO includes many long side-chained aliphatic groups.

CTP/SO derived pitch was more volume and size of anisotropic texture than other pitches due to high molecular stacking properties. From the yield, SP and anisotropic

texture of the obtained pitches, the pitch including much mesophase spheres with low SP can be obtained by the hybridization of EBOp and CTP.

3-3-2. *Optimization of the hybridization ratio of EBOp and CTP*

Table 3-2 and **Fig. 3-3** show pitch yield, SP and anisotropic texture of the obtained pitches after treatments of bromination-dehydrobromination and N_2 blowing heat treatment of EBOp and CTP with the hybridization ratios (w/w) of 3:7, 5:5 and 7:3. With increasing the addition amount of CTP to EBOp, the growth and coalescence of mesophase spheres were much improved, and SP decreased. After TLE of the EBOp/CTP derived pitch brominated at a weight ratio of 3:7, the MP including the anisotropic texture of 80 vol%, SP of 285°C and pitch yield of 23.1 wt% was obtained (**Fig. 3-4**). MP derived from CTP without hydrogenation generally showed a high SP of over 300°C due to highly condensed aromatic molecules [15]. The lower SP and good fluidity of the obtained MP using the hybridized EBOp/CTP (3/7) might confirm that the hybridization of EBO and CTP is an effective method to prepare the SMP without severe hydrogenation of raw materials.

3-4. Conclusion

SMP with a high yield of 23.1 wt% was successfully prepared using hybridized EBOp and CTP through bromination-dehydrobromination, N_2 blowing heat treatment and short-time TLE. From the results, it can be concluded that the raw material hybridization method reflecting the molecular structural characteristics on mesophase formation of each raw material is very effective for SMP manufacturing with low SP and high yield without hydrogenation. The MP derived from EBOp/CTP with the hybridization ratios of 3:7 (w/w) showed the anisotropic texture of 80 vol%, SP of 285°C and pitch yield of 23.1 wt% with relatively good fluidity.

Reference

1. Edie DD. The effect of processing on the structure and properties of carbon fibers. Carbon 1998;36(4):345−62.
2. Mochida I, Korai Y, Ku CH, Watanabe F, Sakai Y. Chemistry of synthesis, structure, preparation and application of aromatic-derived mesophase pitch. Carbon 2000;38(2):305−328.
3. Kato O, Uemura S, Korai Y, Mochida I. Preparation of mesophase pitch and high performance carbon fiber from decant oil. J Jpn Petrol Inst 2004;47(2):100−6.
4. Mochida I, Sakai Y, Fujiyama S, Komatsu M. Development of process for manufacturing of mesophase pitch from aromatic hydrocarbons. Nippon Kagaku Kaishi 1997;1:1−10.
5. Otani S, Sanada Y. Foundation of carbonization engineering (in Japanese). Tokyo: Ohmsha; 1980.
6. Zhuang MS, Gast K, Thies MC. Stagewise fractionation of petroleum pitches with supercritical toluene. Ind. Eng. Chem. Res. 2002;41(1):78−84.
7. Mochida I, Shimizu K, Korai Y, Otsuka H, Sakai Y, Fujiyama S. Preparation of mesophase pitch from aromatic hydrocarbons by the aid of HF/BF_3. Carbon 1990;28(2−3):311−9.
8. Korai Y, Mochida I. Preparation and properties of carbonaceous ,mesophase-i soluble mesophase produced from A240 and coal tar pitch. Carbon 1985;23(1):97−103.
9. Kim BJ, Kotegawa T, Eom Y, An J, Hong IP, Kato O, Nakabayashi K, Miyawaki J, Yoon SH. Enhancing the tensile strength of isotropic pitch-based carbon fibers by improving the stabilization and carbonization properties of precursor pitch. Carbon 2016;99:649−57.
10. Zander M. On the composition of pitches. Fuel 1987;66(11):1536−39.

11. Mochida I, Oyama T, Korai Y. Formation scheme of needle coke from FCC-decant oil. Carbon 1988;26(1):49−55.
12. Ge C, Yang H, Miyawaki J, Mochida I, Yoon SH, Qiao W, Long D, Ling L. Synthesis and characterization of high-softening-point methylenebridged pitches by visible light irradiation assisted free-radical bromination. Carbon 2015;95:780−8.
13. Kim BJ, Eom Y, Kato O, Miyawaki J, Kim BC, Mochida I, et al. Preparation of carbon fibers with excellent mechanical properties from isotropic pitches. Carbon 2014;77:747−55.
14. Mochida I, Korai Y. The chemistry for the preparation of pitch based carbon fibers. Polymer 1986;35:456−9.
15. Arai Y. Pitch-based carbon fiber. Tanso 2010;241:15−20.

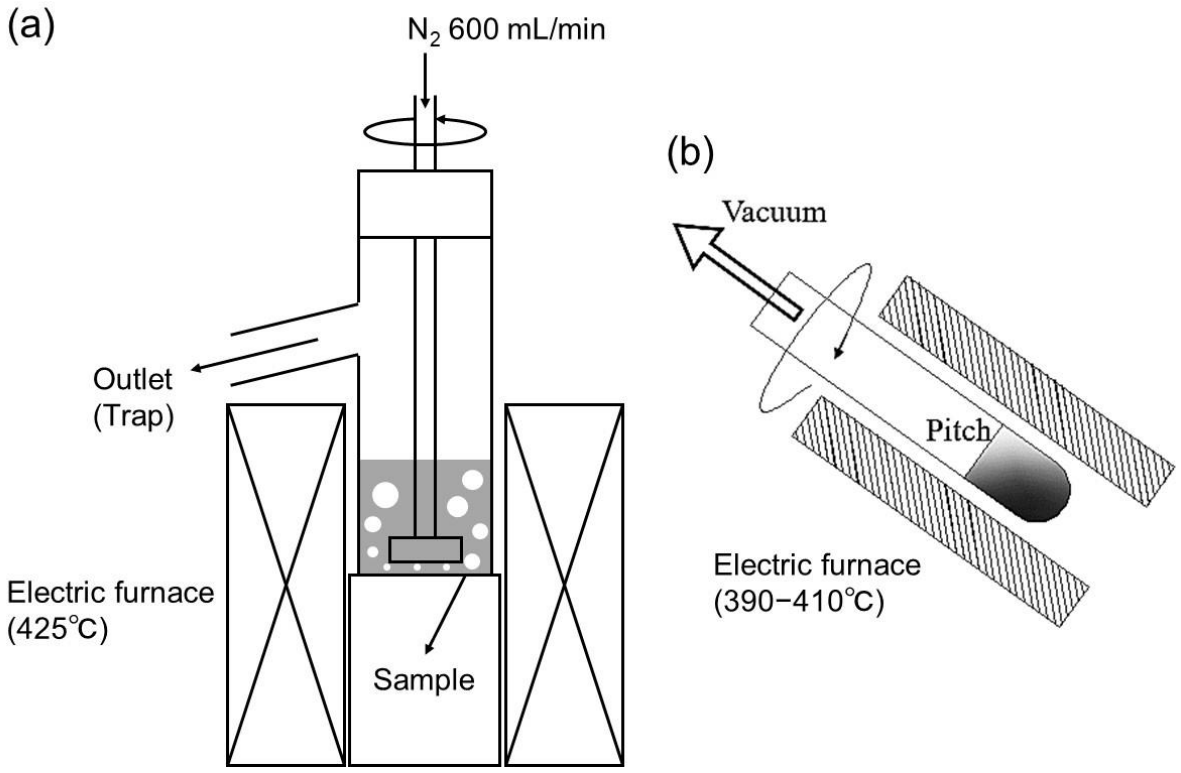

Fig. 3-1. Schematic picture of laboratory heat treatment apparatus: a) N_2 blowing heat treatment and b) TLE.

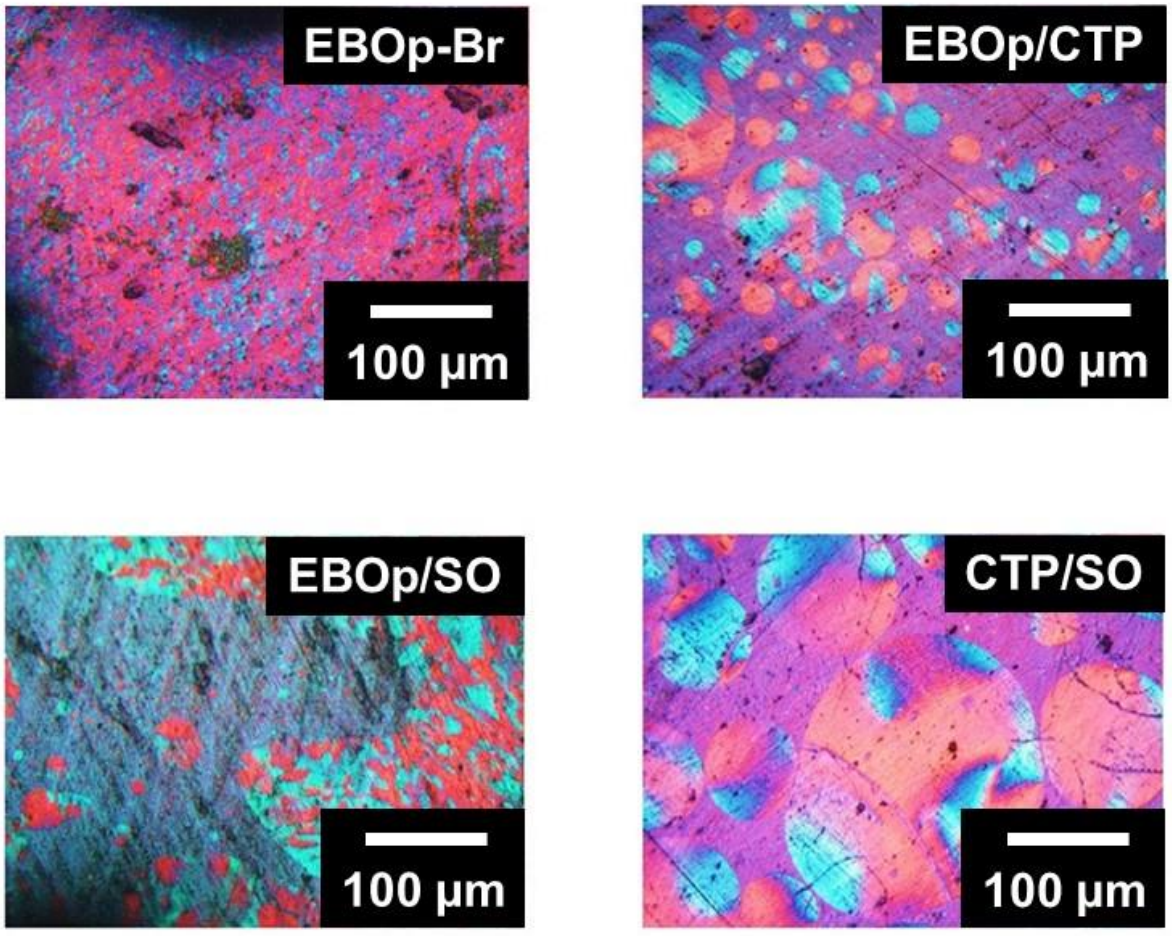

Fig. 3-2. The anisotropic textures of the pitches derived from various raw materials after N_2 blowing heat treatment (Br_2: 5 wt%).

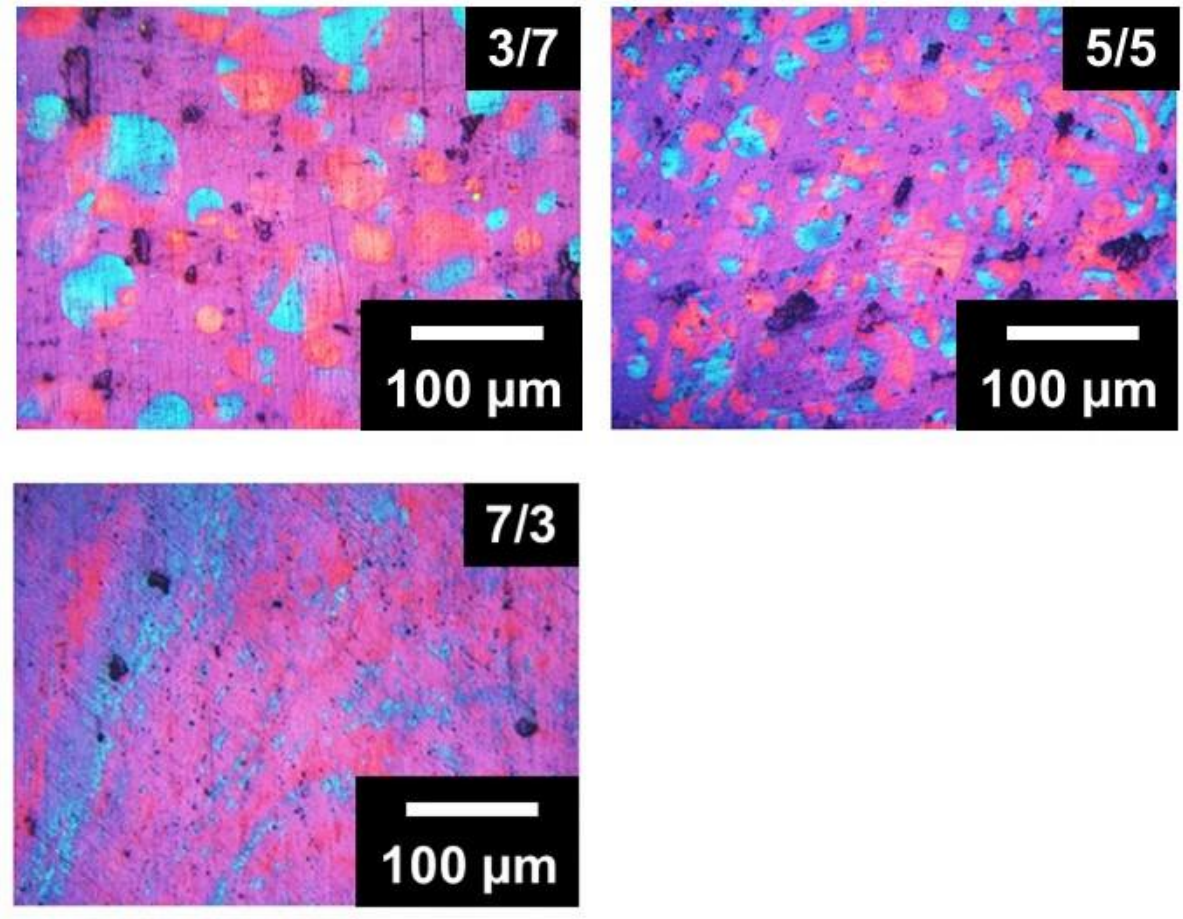

Fig. 3-3. The anisotropic textures of the pitches derived from EBOp/CTP at various weight ratios after N_2 blowing heat treatment (Br_2: 5 wt%).

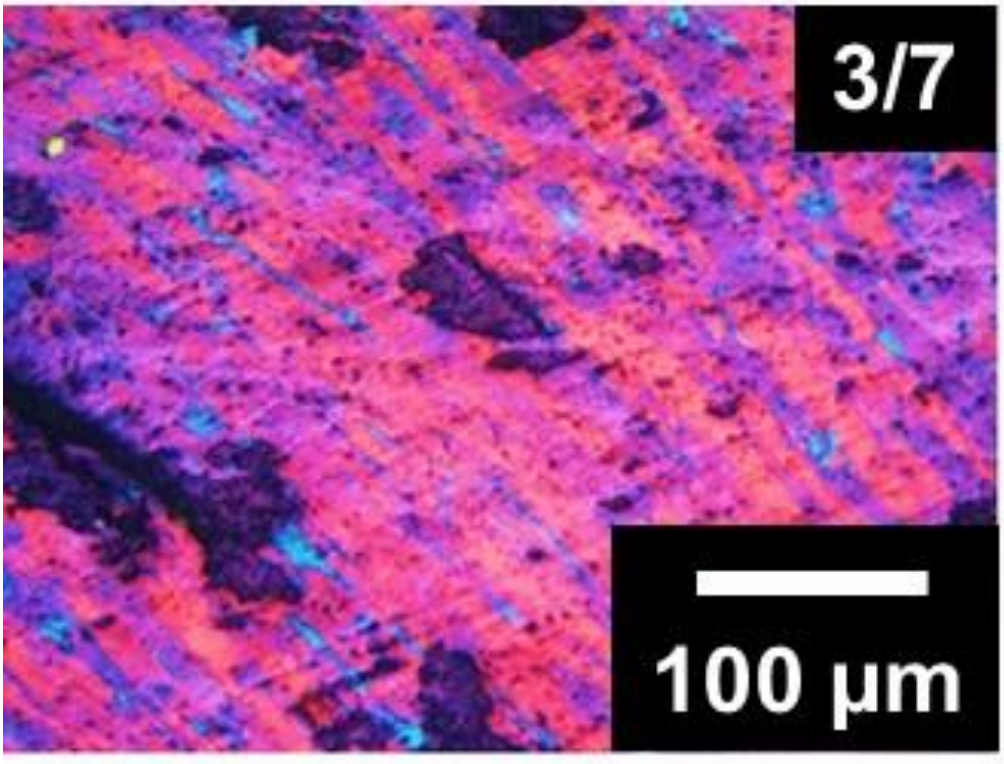

Fig. 3-4. The anisotropic textures of the pitches derived from EBOp/CTP at weight ratio of 3/7 after N_2 blowing heat treatment and TLE (Br_2: 5 wt%).

Table 3-1 The aromaticity and average molecular weight of raw materials

	^{13}C-NMR	TOF-MS
	f_a*	AMW**
	[−]	[−]
EBO	0.748	202
EBOp	0.735	318
CTP	0.966	321
SO	0.701	264

* Carbon aromaticity

** Average molecular weight

Table 3-2 The yield and softening points of the pitches obtained by bromination-dehydrobromination and N_2 blowing heat treatment

	Bromination-dehydrobromination			N_2 blowing heat treatment			
	Weight ratio	Br_2 amount	Yield	Soaking time	Yield	Softening point	Anisotropy
	[w/w]	[wt%]	[wt%]	[h]	[wt%]	[℃]	[vol%]
EBOp	−	0	66.6	3	20.4	320	100
		5	65.8		21.7	324	100
		10	55.9		22.9	−	−
EBOp/CTP	5/5	5	82.2	3	27.0	256	50
EBOp/SO			80.8		19.8	285	50
CTP/SO			82.2		21.5	236	60
EBOp/CTP	3/7	5	70.9	4	24.7	254	50
	5/5		82.2		25.5	279	60
	7/3		85.9		29.1	313	−

Chapter 4. Elucidation of Lyotropic liquid crystalline characteristics of mesophase pitch and modifying its property and yield

4-1. Introduction

Spinnable mesophase pitch (SMP), which is one of the important precursors for high performance carbon fiber, is usually produced through heat treatment of petroleum and coal residues such as slurry oil (SO) and coal tar pitch (CTP) and other aromatic hydrocarbons. SMP is formed by the liquid phase carbonization of such raw materials at 350−500ºC through volatilizing low molecular weight and stacking planar condensed polycyclic aromatic hydrocarbons in a certain direction [1, 2].

SMP was known to have Lyotropic liquid crystal property [3, 4]. In general, Lyotropic liquid crystal can show the specific liquid crystalline phase if its concentration to a specific solvent is over the critical value. However, SMP has a different molecular composition from typical Lyotropic liquid crystalline materials. Lyotropic liquid crystal usually consists of mesogen molecules themselves, however, SMP is composed of both of mesogen molecules and solvent ones. Mesogen and solvent molecules of SMP have a similar molecular structure but mesogen ones show larger molecular weight [4]. The expression and shape of the anisotropic texture of SMP should depend on the ratio of the solvent component and mesogen one in SMP [4]. Soap, one of the typical Lyotropic liquid crystals, is composed of specific molecules that have two different functions of hydrophilic and lyophilic in one molecule. Such soap molecules form a very special molecular assembly of micelle above the critical micelle concentration (CMC). SMP does not have different two functions in one molecule, but it is composed of relatively highly planar molecules which can be easily stacked in the direction of (002). Korai *et al.* have reported that the molecular stacking height (Lc) of the mesophase pitch (MP) is larger than that of the isotropic pitch in both solid and melt states [5], which means that SMP shows very

specific molecular assembly similar with soap molecules instead of the micelle. Kim *et al.* have reported that a number of carbon hexagonal sheets in cluster effected on microdomain structure and showed different graphitizability [6]. So far, however, the correlation between the molecular stacking and optical anisotropy is not yet accurately understood.

AR pitch, which was commercialized by Mitsubishi Gas Chemical Co. Ltd., has an anisotropic texture of 100 vol% and its carbon fiber exhibits high mechanical properties [7]. In this study, we tried to examine the Lyotropic property of SMP using the mesogen molecules of AR pitch and also investigate the correlation between the molecular stacking and optical anisotropy.

In order to extract mesogen fraction from SMP, we carried out solvent extraction of AR pitch with tetrahydrofuran (THF), and assumed THF insoluble component (THFI) of AR pitch as mesogen fraction and THF soluble component (THFS) as a solvent fraction. Since the solubility of the mesogen fraction varies depending on the molecular structure of the solvent. As solvent fractions, two isotropic pitches having the same softening point (SP) with THFS of AR pitch were prepared from CTP and SO.

In order to examine the effect of the concentration of mesogen fraction on the anisotropic texture and Lc of SMP, various ratios of mesogen fraction /isotropic pitch were prepared and annealed at 350°C for 30 min. Finally, the correlation of anisotropic contents and molecular stacking property was examined based on the measured values of the anisotropic contents and Lc. SP of the re-prepared pitch was also measured for investigation the SP decreasing effect with increasing the mixing fraction of various solvent fractions.

4-2. Experimental

4-2-1. *Materials and preparation*

AR pitch was supplied from Mitsubishi Gas Chemical Co. Ltd. After the pulverizing, AR pitch THF insoluble fraction (AR-THFI) and its THF soluble fraction (AR-THFS) were obtained by solvent fractionation using THF at 50°C. The yields of AR-THFI and AR-THFS were 70 and 30 wt%, respectively. AR-THFI and AR-THFS were mixed at weight ratios of 7:3, 6:4, 5:5, 4:6, 3:7, 2:8 and 1:9 (w/w) and heat-treated at 350°C for 30 min under N_2 atmospheres. The heating rate was 5°C/min.

Isotropic pitches derived from CTP (CTP140) and SO (SO140) were used as solvent molecules. SPs of CTP140 and SO140 were carefully controlled to 140°C by TLE because that of AR-THFS was 140°C. Mesogen fraction (AR-THFI) and solvent one (CTP140 or SO140) were mixed at weight ratios of 7:3, 6:4, 5:5, 4:6 and 3:7 (w/w) and annealed at 350°C for 30 min under the same conditions (AR-THFI/CTP140 and AR-THFI/SO140).

4-2-2. *Characterization*

The stacking structure was examined by X-ray diffractometer (XRD, RINT-Ultima Ⅲ, Rigaku Co., Tokyo, Japan) with CuK α radiation of 30 kV and 40 mA. Scanning 2θ range was 0–60° at the scan speed of 0.05°/min. The interlayer spacing (d_{002}), the stacking height (Lc(002)) and the number of stacking sheets were calculated by Brag (Eq. 1), Scherrer (Eq. 2) equations and equation (Eq. 3), respectively [8, 9].

$$n\lambda = 2d\sin\theta \quad (1)$$

$$Lc = K\lambda / \beta\cos\theta \quad (2)$$

$$\text{Number of sheets} = Lc/d+1 \quad (3)$$

where, θ is the scattering angle, λ is the wavelength of the X-rays used, and β is the half-maximum line width in radian. The form factor K is 0.9 for Lc according to Jeffrey *et al.* [10]. The values of d_{002} and Lc of samples were evaluated at 25–300ºC.

SP of the prepared pitch were determined by thermal mechanical analysis (TMA) (TMA/SS6300; EXSTAR6300 SII; Seiko Co. Ltd., Tokyo, Japan) from room temperature to 400°C at a heating rate of 5°C/min under N_2 flow.

Anisotropic textures of the obtained pitches were observed by polarization microscope (POM) (BX51-P; Olympus Co. Ltd., Tokyo, Japan) using a heating stage at 25, 100, 200, 250 and 300°C.

4-3. Results and discussion

4-3-1. *The correlation between the molecular stacking and anisotropic texture*

Fig. 4-1 shows POM images of the sample pitches obtained using mixtures of various ratios of AR-THFI and AR-THFS. AR-THFS was fully isotropic, so it could be considered that AR-THFS does not include mesogen molecules. At weight ratios of 7:3, 6:4 and 5:5 of AR-THFI and AR-THFS, the obtained pitches showed 100 vol% anisotropic texture. At weight ratios of 4:6 of AR-THFI and AR-THFS, the obtained pitch showed bulk anisotropic textures with isotropic spheres. As further increasing the amount of AR-THFS, the isotropic matrix appeared with very small mesophase spheres (3:7, 2:8 and 1:9). **Fig. 4-2** and **Table 4-1** shows the molecular stacking parameters of AR-THFI/AR-THFS mixtures with various mixing ratios. At weight ratios of 3:7, 2:8 and 1:9, the values of d_{002} and Lc(002) of obtained pitches, in which isotropic matrix appeared, were larger and smaller than those of obtained pitches which includes much anisotropic textures, respectively. Therefore, the number of stacked sheets decreased in the conversion of a matrix from anisotropic to isotropic (**Fig. 4-3**). From these results, it was found that the pitches which had the stacking sheets of over

10 indicated anisotropic textures but the pitches having the stacking sheets of about 7 showed the conversion of a matrix from anisotropic to isotropic.

Figs. 4-4 and **4-5** exhibit the stacking parameters and anisotropic textures of the obtained pitches according to mixing ratio and XRD measuring temperature. Increasing the measuring temperature, d_{002} increased and Lc decreased. Therefore, the number of stacking sheets decreased with increasing the measuring temperature. However, the number of stacking sheets of the obtained pitches which had anisotropic textures of 100 vol% at high temperature was larger than those of the obtained pitches showing much isotropic matrix at room temperature. Thus, it could be suggested that SMP shows its Lyotropic liquid crystalline characteristics with the formation of the specific molecular assembly of molecular stacking at both room and high temperature.

4-3-2. *Reduction of SP of MP using isotropic pitch*

Figs. 4-6 and **4-7** and **Table 4-2** show textures and SP of AR-THFI/CTP140 and AR-THFI/SO140. At the mixing ratios of 7:3 and 6:4, AR-THFI/CTP140 exhibited 100 vol% anisotropic textures. As further increasing the amount of CTP140, isotropic spheres started to appear in the bulk anisotropic texture and finally the matrix texture was converted from anisotropic to isotropic. At the weight ratios of 6:4 and 5:5 of AR-THFI/CTP140, SPs were 235 and 223°C, respectively, which were lower than that of the pristine AR pitch (240°C). AR-THFI/SO140 showed the structure separated anisotropy and isotropy phases at all weight ratios. Thus, the difference of physical properties such as the structure and molecular weight of solvent fractions might be effect on the compatibility of anisotropy and isotropy phases.

Figs. 4-8 and **4-9** and **Table 4-3** show the stacking parameters of AR-THFI/CTP140 at various weight ratios. The obtained pitches with bulk anisotropic texture showed small d_{002} and large Lc values, giving rise to a large number of stacking sheets. After

converting the texture from anisotropic to isotropic, the values of d_{002} increased and Lc and the number of stacking sheets greatly decreased. From a comparison between **Figs. 4-3** and **4-9**, the number of stacking sheets of AR-THFI/CTP140 derived MP appeared larger than that of AR pitch. A solvent fraction of CTP140 contributed to increasing the molecular stacking because the molecular stacking property of CTP derived pitch usually shows the higher stacking property than the pitches derived from naphthalene and other petroleum residues [11, 12].

4-4. Conclusion

In this study, we examined Lyotropic characteristics of MP using AR-pitch as a sample. From the results, we newly understood the followings.

① SMP is surely a Lyotropic liquid crystal.

② Because SMP is composed of planar molecules, if the concentration of the mesogen fraction goes to be above the critical value, the different higher molecular stacking structure forms as a special molecular assembly and the texture is converted to be bulk anisotropic.

③ AR pitch, which represents 100 vol% of anisotropic texture, is originally composed of 7:3 ratios of mesogen and solvent fractions, but the same 100 vol% anisotropic texture was also observed even at the ratios of 6:4 and 5:5, and the molecular stacking property was rather higher at the ratio of 6:4 than that of the original AR pitch, which might indicate that the ratio of 6:4 is the optimal mixing balance of mesogen and solvent fractions.

④ The alternative solvent fractions of the CTP and SO derived isotropic pitches, which have the same SP with isotropic texture same with THFS of AR pitch, have lower solvent properties than AR-THFS. Among them, the CTP derived isotropic pitch has higher solvent ability than the SO derived isotropic one. When CTP

derived isotropic pitch was used as a solvent, it showed 100 vol% of anisotropic texture up to 6:4, and the MP obtained at 6:4 had a lower SP than the pristine AR pitch, and pitch yield might be improved by higher than 10 wt%. Therefore, using this method, we can expect that the pitch yield and spinnability can be improved.

The future improvement and complementary points of this study are as follows;

① Accurate definition and specification of mesogen fraction in SMP.

② Better understanding of the differences of mesogen fractions from various resources such as CTP and petroleum and the preparation of more effective mesogen fraction.

③ Identifying the solution mechanism of mesogen fraction with solvent one and finding out the decisive solution factor.

④ Preparation low price SMP using this characteristics.

Reference

1. Mochida I, Korai Y, Ku CH, Watanabe F, Sakai Y. Chemistry of synthesis, structure, preparation and application of aromatic-derived mesophase pitch. Carbon 2000;38(2):305−328.
2. Mochida I, Korai Y. The chemistry for the preparation of pitch based carbon fibers. Polymer 1986;35:456−9.
3. Korai Y, Mochida I. Preparation and properties of carbonaceous ,mesophase-i soluble mesophase produced from A240 and coal tar pitch. Carbon 1985;23(1):97−103.
4. Mochida I, Korai Y. Chemistry of mesophase pitch for its preparation and property design. J Fuel Soc Jpn 1985;64:796−808.
5. Korai Y, Mochida I. Molecular assembly of mesophase and isotropic pitches at their fused states. Carbon 1992;30(7):1019−24.
6. Kim DW, Kil HS, Kim J, Mochida I, Nakabayashi K, Rhee CK, Miyawaki J, Yoon SH. Highly graphitized carbon from non-graphitizable raw material and its formation mechanism based on domain theory. Carbon 2017;121:301−8.
7. Mochida I, Shimizu K, Korai Y, Otsuka H, Sakai Y, Fujiyama S. Preparation of mesophase pitch from aromatic hydrocarbons by the aid of HF/BF3. Carbon 1990;28(2−3):311−9.
8. Endo M, Kim C, Karaki T, Kasai T, Matthews MJ, Brown SDM, Dresselhaus MS, Tamaki T, Nishimura Y. Structural characterization of milled mesophase pitch-based carbon fibers. Carbon 1998;36(11):1633−41.
9. Short MA, Walker Jr. PL. Measurement of interlayer spacings and crystal sizes in turbostratic carbons. Carbon 1963;1(1):3−9.
10. Jeffery JW. Methods in X-ray crystallography. Academic Press 1971:83.
11. Korai Y, Mochida I. Preparation and properties of carbonaceous ,mesophase-i soluble mesophase produced from A240 and coal tar pitch. Carbon 1985;23(1):97−103.
12. Zander M. On the composition of pitches. Fuel 1987;66(11):1536−39.

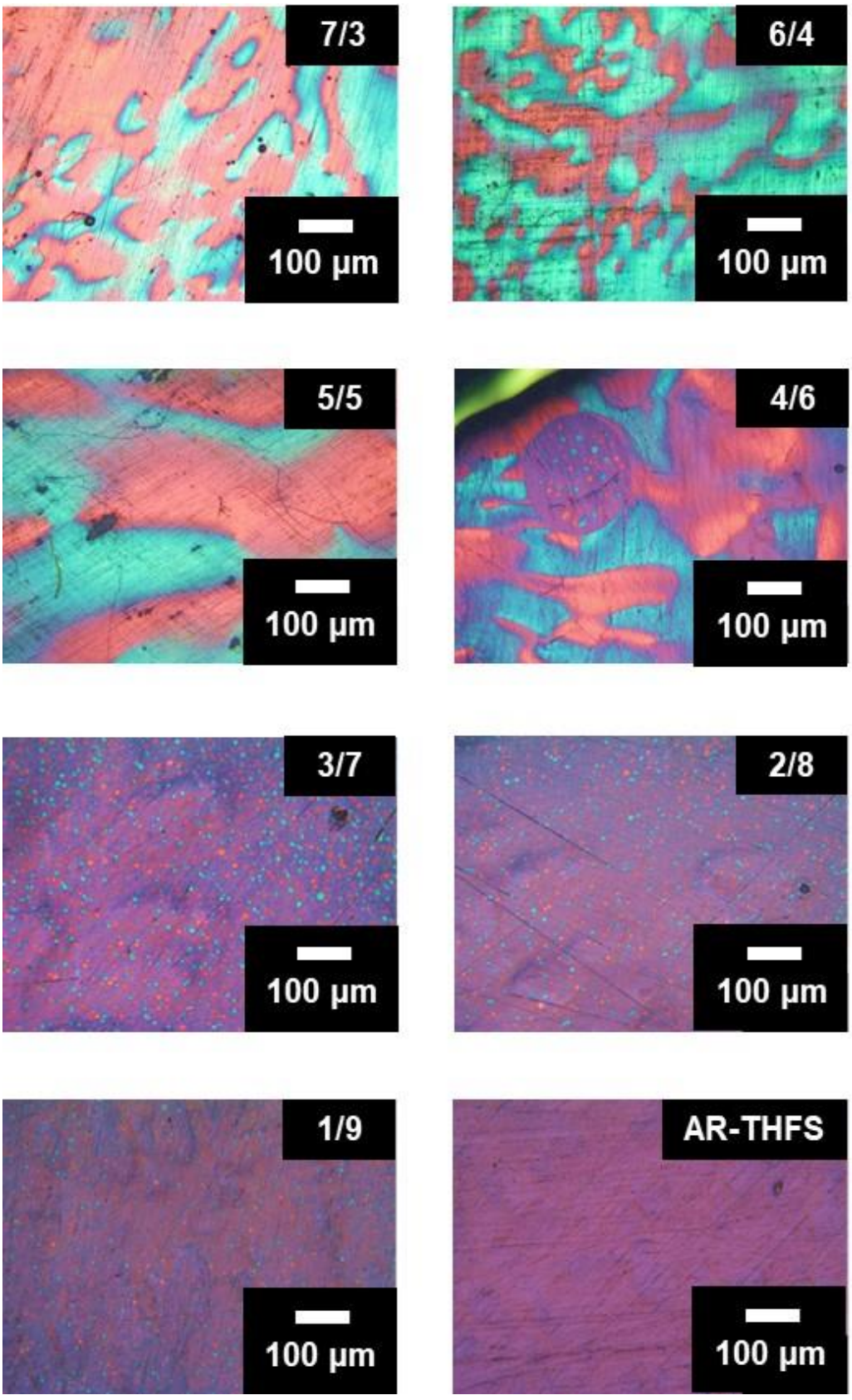

Fig. 4-1. The anisotropic textures of the pitches derived from AR-THFI/AR-THFS at various weight ratios.

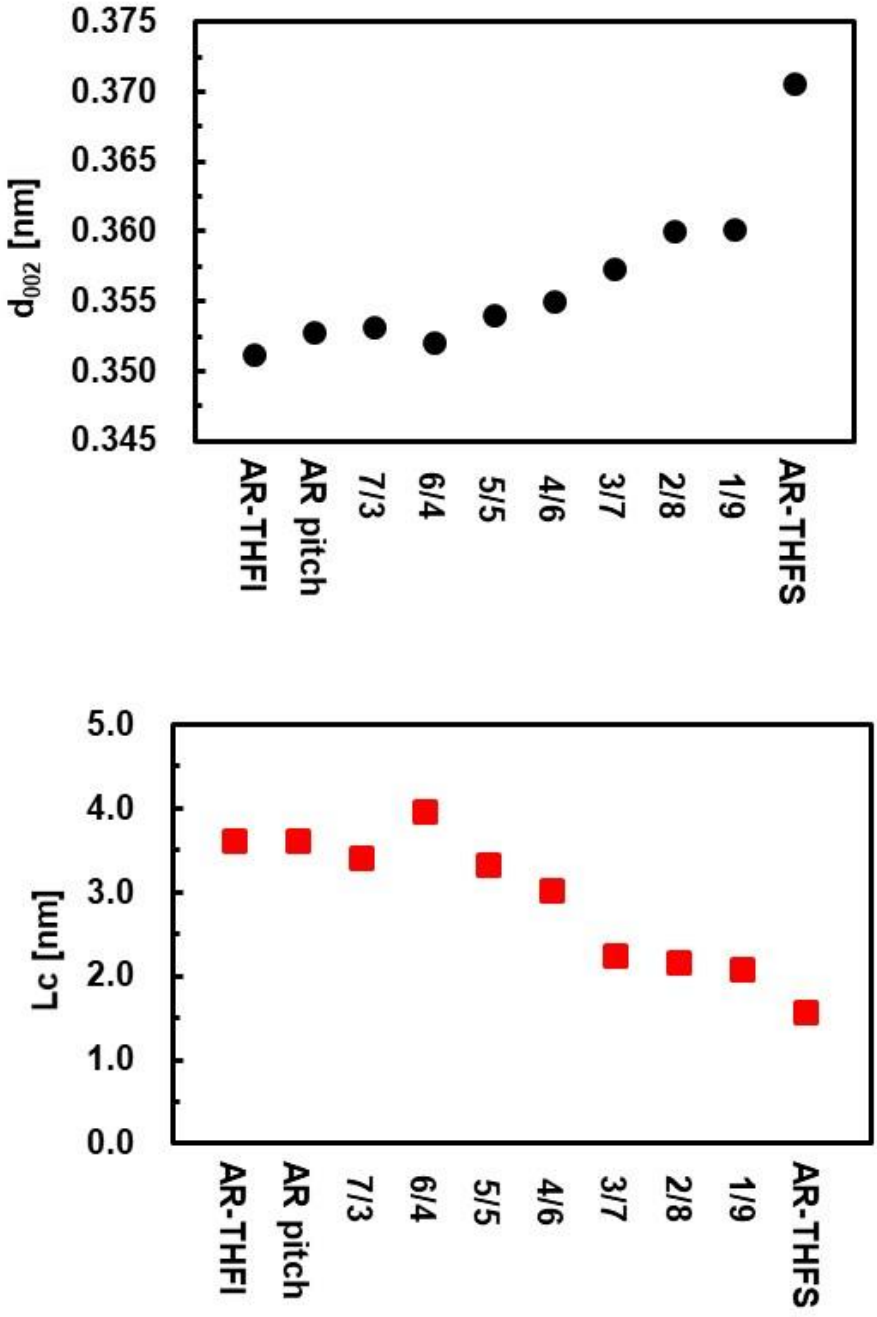

Fig. 4-2. The stacking parameters of the pitches derived from AR-THFI/AR-THFS at various weight ratios.

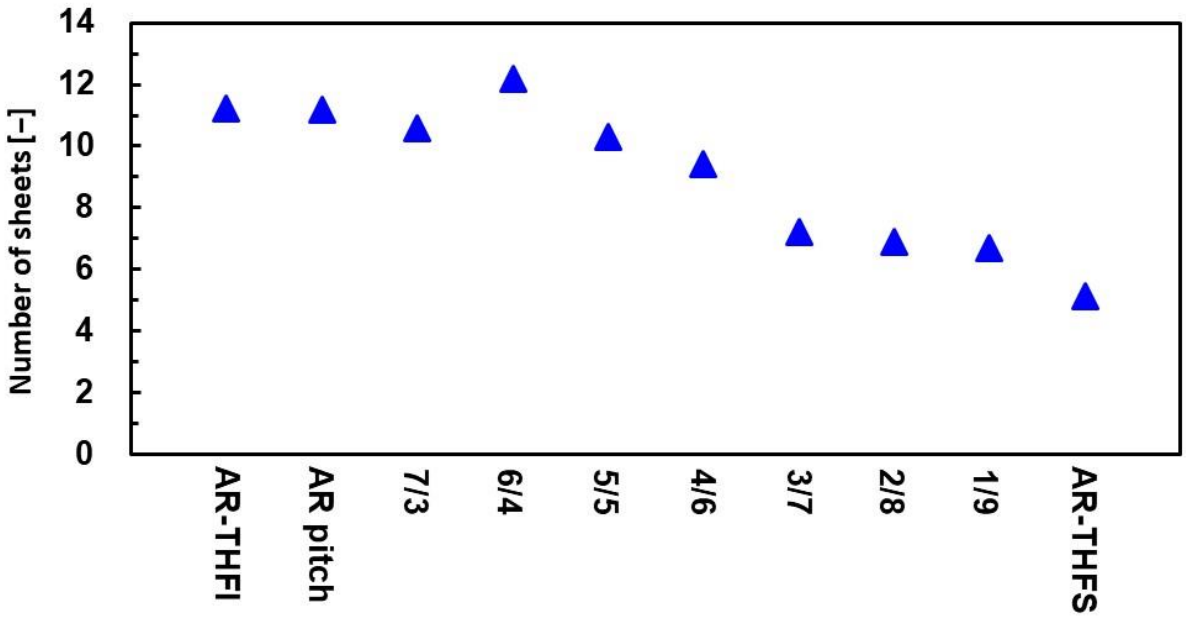

Fig. 4-3. The number of stacking sheets of the pitches derived from AR-THFI/AR-THFS at various weight ratios.

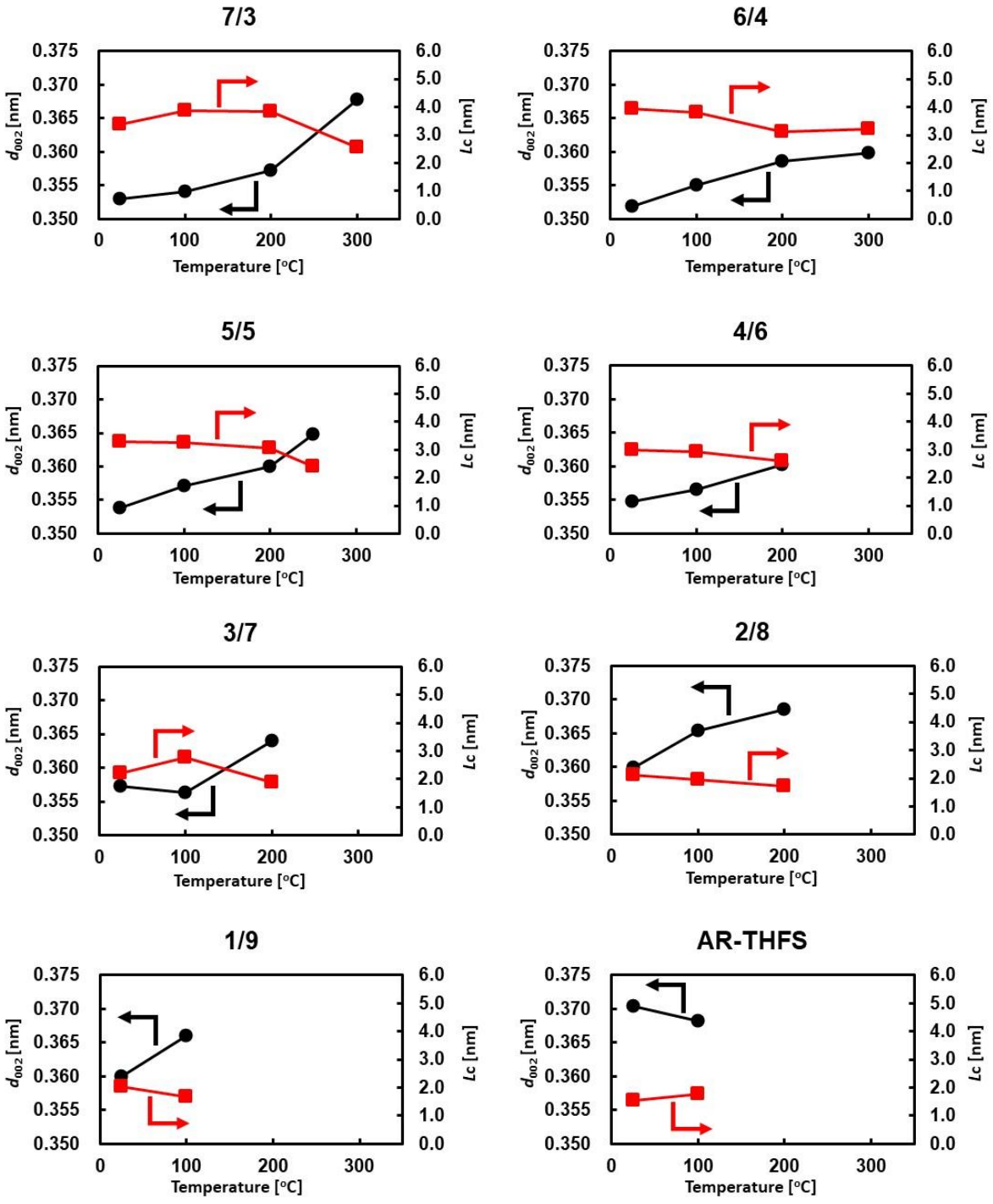

Fig. 4-4. The stacking parameters of the pitches derived from AR-THFI/AR-THFS at various weight ratios and temperatures.

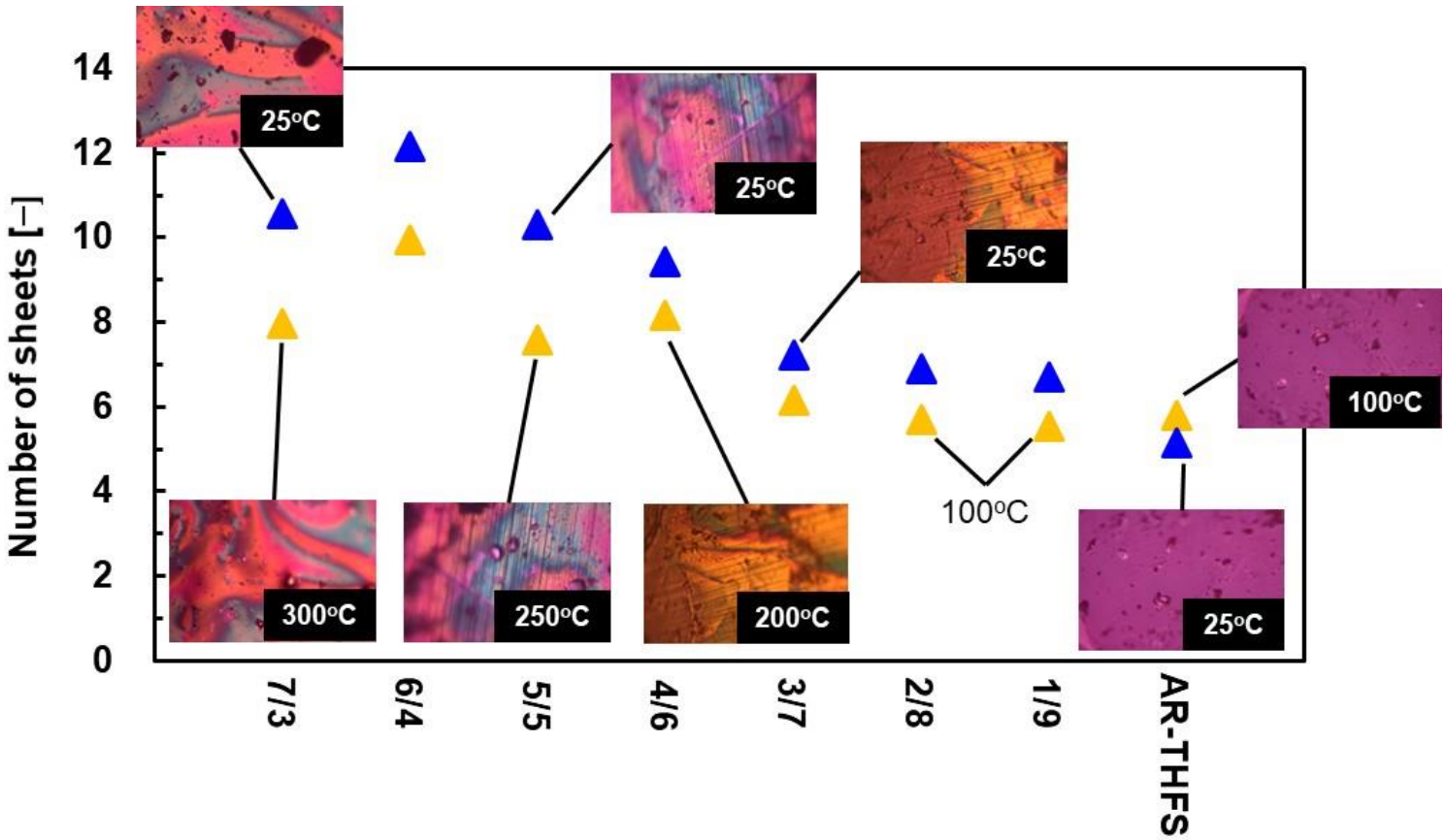

Fig. 4-5. The polarization microscope images and number of stacking sheets of the pitches derived from AR-THFI/AR-THFS at various weight ratios and temperatures.

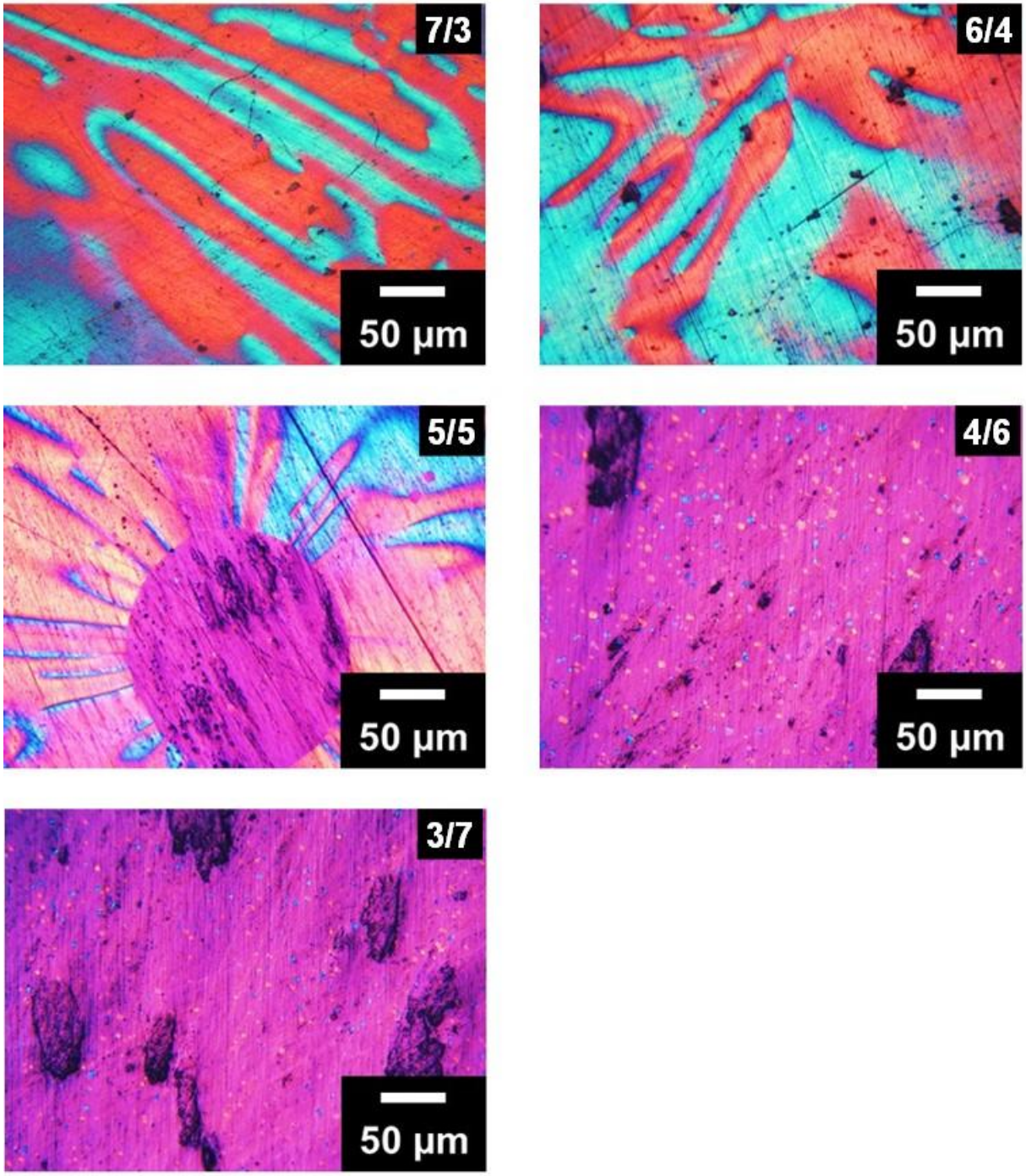

Fig. 4-6. The anisotropic textures of the pitches derived from AR-THFI/CTP140 at various weight ratios.

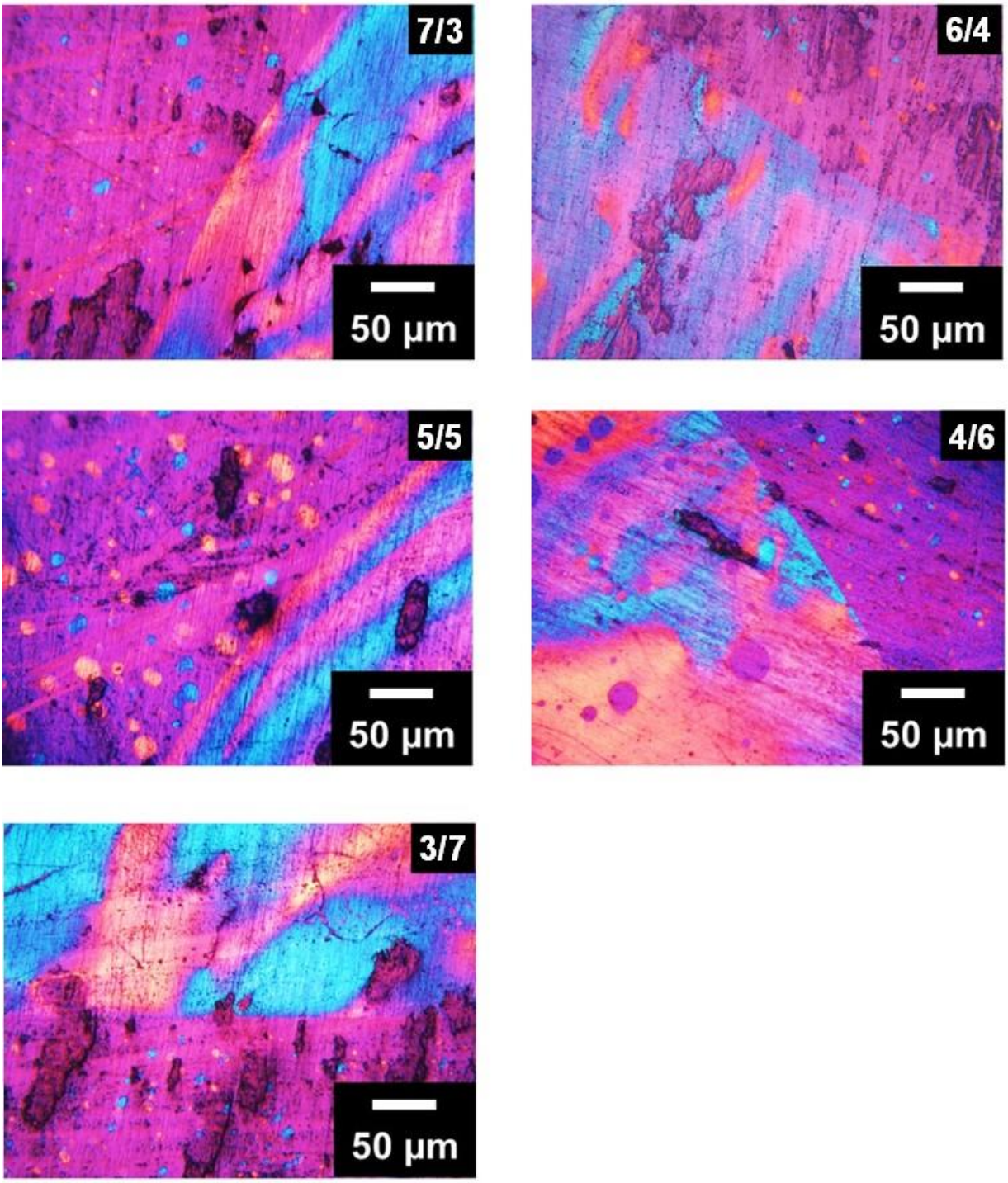

Fig. 4-7. The anisotropic textures of the pitches derived from AR-THFI/SO140 at various weight ratios.

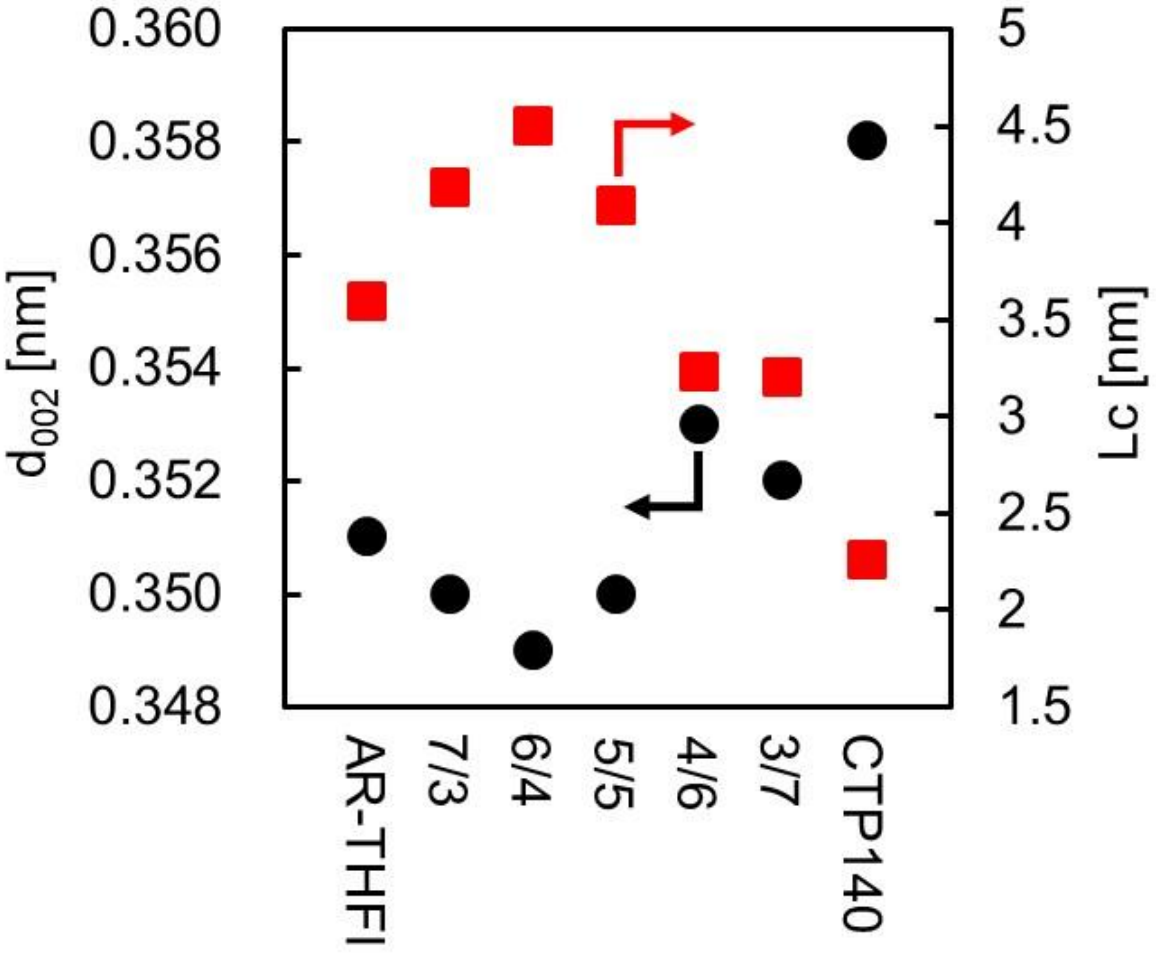

Fig. 4-8. The stacking parameters of the pitches derived from AR-THFI/CTP140 at various weight ratios.

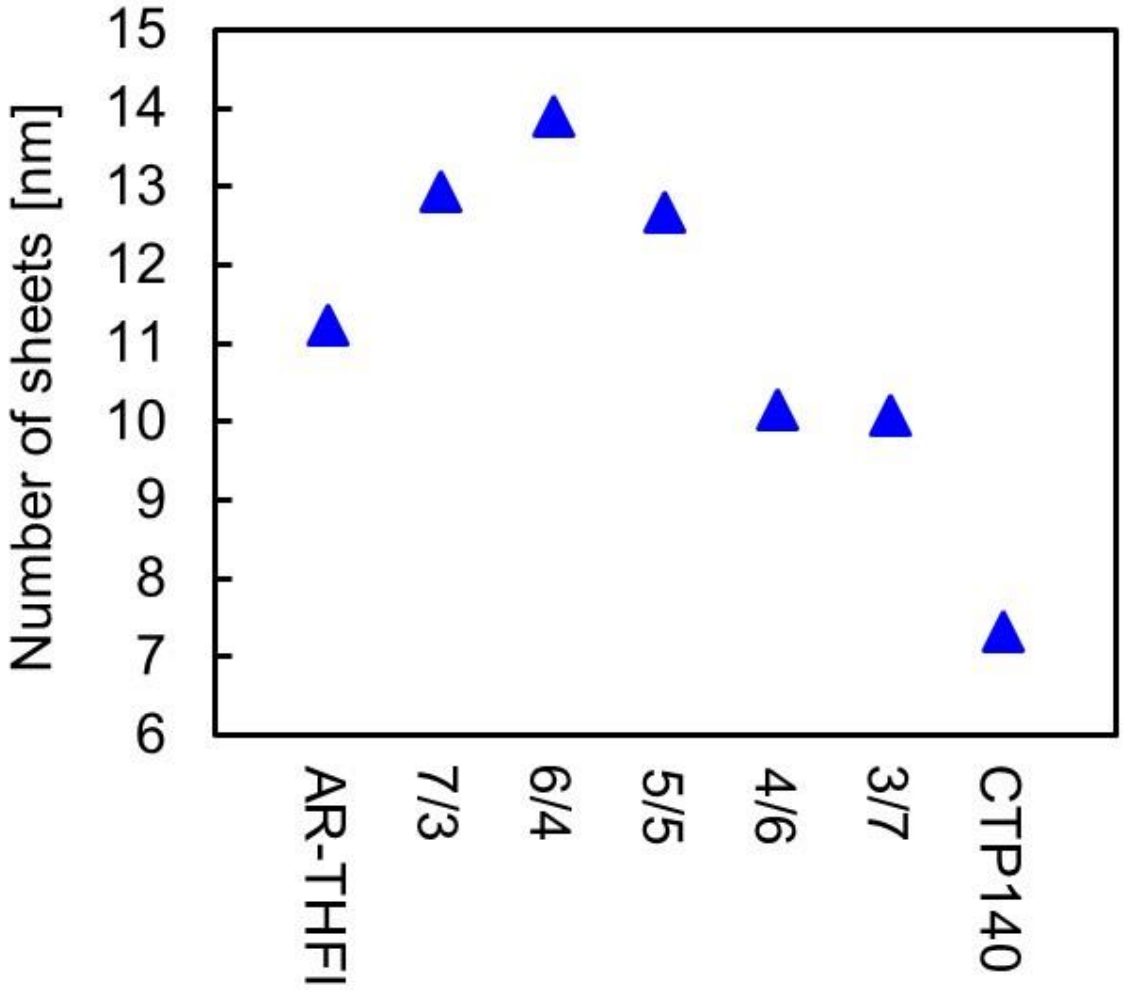

Fig. 4-9. The number of stacking sheets of the pitches derived from AR-THFI/CTP140 at various weight ratios.

Table 4-1 The stacking parameters of the pitches derived from AR-THFI/AR-THFS at various weight ratios

	AR-THFI	AR pitch	Weight ratio of AR-THFI/AR-THFS [w/w]							AR-THFS
			7/3	6/4	5/5	4/6	3/7	2/8	1/9	
d_{002} [nm]	0.351	0.353	0.353	0.352	0.354	0.355	0.357	0.360	0.360	0.370
Lc [nm]	3.59	3.59	3.75	3.93	3.30	2.99	2.22	2.13	2.05	1.53

Table 4-2 The SPs of the pitches derived from AR-THFI/CTP140 and AR-THFI/SO140 at various weight ratios

	Weight ratio	[w/w]	7/3	6/4	5/5	4/6	3/7
AR-THFI/CTP140	SP	[^{o}C]	255	235	223	230	234
AR-THFI/SO140			266	253	240	255	256

Table 4-3 The stacking parameters of the pitches derived from AR-THFI/CTP140 at various weight ratios

	Weight ratio	[w/w]	7/3	6/4	5/5	4/6	3/7
AR-THFI/CTP140	d_{002}	[nm]	0.350	0.349	0.350	0.353	0.352
	Lc	[nm]	4.17	4.50	4.09	3.23	3.20

Chapter 5. Shortening the total oxidation-stabilization time on preparation of mesophase pitch-based carbon fiber

5-1. Introduction

Stabilization process is the most time-consuming process in carbon fiber (CF) manufacturing. Such a long time-consuming in stabilization is usually induced from the slow oxidation of the precursor fiber at relatively low temperature because rapid oxidation might be a reason for deteriorating the final mechanical properties of the obtained CF. Due to this reason, it is one of the most important assignments to decrease the consuming time in the stabilization process in CF manufacturing [1]. The cause of a long stabilization time is the slow diffusion rate of oxygen molecules into the center part of pitch fiber. Yang *et al.* have estimated that the average radii of free volumes on various mesophase pitches (MPs) and their fibers were in the ranges of 0.24–0.25 nm and 0.25–0.26 nm, respectively [2]. The average kinetic radii of oxygen and nitrogen are 0.17 and 0.19 nm, respectively, which means that it is very difficult for the effective air diffusion to occur for optimized oxidation reactions in MP fibers in conventional atmospheric stabilization. The fiber stabilized at low temperature for long time has a uniform distribution of the oxygen amount in the cross-section of pitch fiber and the uniform distribution is one of the prior conditions to obtain the high tensile strength (TS) in the CF after the carbonization [3, 4].

In this work, the effect of oxidation-stabilization under high pressure of air was examined to reduce the total stabilization time without causing deterioration of the mechanical performance of MP-based CFs (MPCFs). Cornec *et al.* and Fathollahi *et al.* have reported that the oxidation-stabilization of MP fibers under a moderate oxygen pressure is effective in raising the amounts of oxygen uptake and increasing the stabilization depths significantly even at low temperature [5, 6]. Therefore, the stabilization-oxidation of MPCF under high air pressure can be expected to enhance

the slow diffusion rate of oxygen molecules and enable the homogeneous oxidation for a short time.

5-2. Experimental

5-2-1. *Material and melt-spinning*

AR mesophase pitch (ARMP) was supplied by Mitsubishi Gas Chemical Co., Japan, and used as a model MP precursor in this study without further treatment. ARMP has softening point (SP) at 240°C, carbon aromaticity of 0.84 and the content of the mesophase texture of 100 vol.%. **Table 5-1** summarizes general properties of ARMP [7, 8].

ARMP was melt-spun into as-spun ARMP fiber (ARMP-F) using a single-hole spinneret at 340°C with a laboratory-type mono-hole melt-spinning apparatus, which has a stainless-steel die hole with diameter and length of 0.3 and 0.6 mm (L/D = 2), respectively [9]. **Fig. 5-1** shows a schematic diagram of the self-designed laboratory-type spinning apparatus. The spinning conditions were carefully controlled to diameters of spun MP fibers of just 10.5 ± 1.0 and 14.0 ± 1.0 μm, which were designated as ARMP-F10 and ARMP-F14, respectively. ARMP-F14 was used to examine the effect of pressure on the oxygen diffusivity and the oxidation reactions in stabilization, and ARMP-F10 was used to prepare the carbonized and graphitized fibers (ARMP-CF10 and ARMP-GF10) to evaluate the mechanical performance.

5-2-2. *Oxidation-stabilization of spun fibers*

Oxidation-stabilization of ARMP-Fs was carried out through thermal oxidation under dry air flow of 0.1–1.0 MPa with a flow rate of 100 mL/min. **Fig. 5-2** shows a schematic diagram and an actual image of the custom-designed oxidation-stabilization apparatus using atmospheric and pressurized air flows. Oxidation-stabilization of

ARMP-F14 was carried out at 270°C with a heating rate of 2.0°C/min for 20 min under air flow pressures of 0.1, 0.5 and 1.0 MPa to evaluate the oxygen distribution across the fiber cross-section. Oxidation-stabilization of ARMP-F10 was carried out at various temperatures, heating rates, soaking times, and air flow pressures of 250–270°C, 0.5–3.0°C/min, 0–60 min, and 0.1–1.0 MPa, respectively, to monitor the oxygen uptake and prepare the optimally oxidation-stabilized fibers for evaluating the mechanical performances of carbonized and graphitized fibers under each stabilization condition. The stabilized fibers of ARMP-F10 and ARMP-F14 were designated ARMP-SF10 and ARMP-SF14, respectively.

5-2-3. *Carbonization and graphitization*

After the stabilization of ARMP-Fs under various conditions, ARMP-SF14s were successively heat-treated at 800°C for 5 min with a heating rate of 5.0°C/min in a N_2 atmosphere for carbonization, and further heat-treated at 2400°C for 10 min with a heating rate of 15°C/min under an Ar atmosphere for graphitization. ARMP-SF10s were heat-treated at 1000°C for 30 min with a heating rate of 20°C/min in a vacuum, and some of the carbonized fibers were also further graphitized at 2800°C for 10 min with a heating rate of 15°C/min in an Ar atmosphere to evaluate the mechanical performance. The carbonized and graphitized fibers of ARMP-SF10 and ARMP-SF14 were named as ARMP-CF10 and ARMP-CF14, and ARMP-GF10 and ARMP-GF14, respectively.

5-2-4. *Characterization*

Spun MP fibers were subjected to thermos-gravimetric analysis (TGA) to track the amount of oxygen uptake under atmospheric and air flow pressure conditions using a magnetic suspension balance (MicrotracBEL MSB-TG-1300; MicrotracBEL Co. Ltd.,

Osaka, Japan). **Fig. 5-3** shows a schematic of MSB-TG-1300. TGA was carried out under various heating rates and air flow pressures of 1.0–4.0°C/min and 0.1–1.0 MPa, respectively. An exclusive alumina pan (diameter: 10 mm, height: 10 mm, weight: 6.11 g) was used under the controlled flows of air/oxygen with a flow rate of 100 mL/min. After TGA, the activation energy of the oxidation-stabilization of ARMP-F14s was calculated by Kissinger's method using **Eq. (5-1)** [10]:

$$\ln (q/T_{max}^2) = -Ea/(RT_{max}) \qquad \textbf{(5-1)}$$

where T_{max}, q, and Ea denote peak temperature, heating rate, and activation energy, respectively.

To evaluate the distribution of the amounts of oxygen uptake in the transverse sections of stabilized fibers, ARMP-SF14s were analyzed using a scanning electron microscope equipped with an electron probe micro-analyzer (JSM-6340F; JEOL, Tokyo, Japan) [11]. Images of the structure of the transverse sections of the graphitized fibers were obtained using a scanning electron microscope (JSM-6700F; JEOL). The surface morphology and mean diameter of the resulting CFs were also measured.

Elemental analysis was used to determine the total amount of oxygen uptake of the stabilized fibers for evaluating the mechanical performance of the obtained carbonized and graphitized fibers. The mechanical properties of the carbonized and graphitized fibers were measured using a universal tensile tester (TENSILON/UTM-II-20; ORIENTEC, Tokyo, Japan), in accordance with the JIS R 7606:2000 method (A method of single filament test) [12]. 25 filaments were tested for obtaining the averaged mechanical properties. The averaged diameters of carbonized and graphitized fibers were checked using a scanning electron microscope (SEM, JSM6700, JEOL, Japan) at 5 kV of acceleration voltage.

5-3. Results and discussion

5-3-1. *Stabilization of MP fibers under atmospheric and pressurised conditions*

Fig. 5-4 shows the TGA profiles of oxygen uptakes of ARMP-F14 and ARMP-F10 in oxidation stabilization with a heating rate of 2.0°C/min under atmospheric and pressurized air flow conditions. ARMP-F10 and ARMP-F14 had very similar profiles of oxygen uptake, which means that they experienced almost the same oxidation reactions under the same applied pressure. **Fig. 5-5** shows TGA profiles of the oxygen uptakes of ARMP-F14 under the various heating rates and air flow pressures. The results clearly revealed two interesting distinctions in the temperatures of the starting and the maximum oxidations, and the amounts of oxygen uptake. First, the oxidation reaction for oxygen uptake occurred earlier in the stabilized fibers under air flow pressures of 0.5 and 1.0 MPa than for the stabilized one under atmospheric pressure. The start of oxygen uptake of ARMP-F14 mainly occurred at over 150°C under atmospheric pressure regardless of the heating rate, whereas the pressurized stabilization under 0.5 and 1.0 MPa allowed this to occur at around 125°C. During the manufacture of MPCFs, the reactions that typically occur during the stabilization process are oxidation, dehydration, condensation, oxidation crosslinking, elimination of volatile matter and oxidative decomposition [13]. Such complexity in oxidation-stabilization reactions makes it difficult to obtain a comprehensive understanding of the stabilization of MP materials. However, Yoon *et al.* have successfully optimized the stabilization process by performing a simple monitoring of oxygen uptake using TGA with several heating rates [1]. For TGA, it allowed only two reactions of the oxidation and oxidative decomposition of alkyl and aromatic molecules as main reactions and proved that the oxidative decomposition of alkyl groups always occurred before that of condensed aromatic ones. Based on this analysis, they explained that oxygen uptake occurred at a lower temperature and higher rate with a decrease of the

heating rate in oxidation stabilization. They also proved that a higher heating rate, which inevitably required a higher temperature to complete the optimal stabilization, easily incurred excess oxidation in the outer section of MP fibers, and such excess oxidation could trigger decomposition of the alkyl groups of pitch molecules with the dissipation of decomposed gases such as CO and CO_2 before the main decomposition of aromatic molecules of MP fibers. In these results, the temperature at which the maximum oxygen uptake in oxidation-stabilization occurred was shifted to a lower position with increasing air pressure. This proved that the main oxygen uptake could start at a lower temperature under pressurized air flow conditions than under atmospheric conditions, and the application of pressure in oxidation stabilization is expected to have a similar effect to decrease the heating rate. The observed earlier start of oxidation and higher amounts of oxygen uptake were well matched with the previous reports [5, 6].

Table 5-2 summarizes the activation energy, Ea, of the oxidation reactions in various stabilized conditions from the calculation based on **Eq. (5-1)** using the Arrhenius plots shown in **Fig. 5-6**. The activation energies at 0.5 MPa and 1.0 MPa were 230 kJ/mol and 271 kJ/mol, respectively, which was less than almost half the value of 535 kJ/mol at atmospheric pressure.

Regarding the maximum amount of oxygen uptake in the oxidation stabilization with applied pressure, different effects of decreasing the heating rate were observed. Specifically, the stabilized fiber of ARMP-SF14 at 0.5 MPa had a higher amount of oxygen uptake at its maximum point of oxygen uptake than the stabilized fiber under atmospheric conditions. However, the maximum amount of oxygen uptake at 1.0 MPa was slightly lower compared with those under atmospheric pressure conditions. As is clearly shown in **Figs. 5-4** and **5-5**, the oxidation rate under the pressure conditions of 1.0 MPa was reliably higher than that under atmospheric conditions. To understand

these results, we must consider the oxygen diffusivity and oxidation reaction in combination.

Fig. 5-7 shows the SEM-EPMA results of ARMP-SF14s stabilized under air flow pressures of 0.1, 0.5 and 1.0 MPa with a heating rate of 2.0°C/min. The distribution of the amounts of oxygen uptake appeared relatively homogeneous in ARMP-SF14 stabilized at an air pressure of 0.5 MPa, with the amounts of oxygen uptake ranging from 8.7–11.4 wt%. The distribution of oxygen uptakes shifted to a higher level and became more homogeneous with increasing the applied pressure of air flow, with the oxygen distribution in ARMP-SF under pressure of 1.0 MPa ranging from 12.1–14.8 wt%. Compared with the distribution of the amounts of oxygen uptake of ARMP-SF14 stabilized under pressurized air flow conditions, that of ARMP-SF14 stabilized under atmospheric conditions was very heterogeneous, with the amounts of oxygen uptake of 3.4–11.2 wt%. From these results, we can see that the oxygen diffusion from the outer surface to the center part of the pitch fiber became more rapid with increasing applied air flow pressure; coincidently, the oxidation reaction was also more rapid because the oxygen density was higher under the pressure conditions. That is, in the more rapid and homogeneous oxidation reactions that occurred at a pressure of 1.0 MPa, oxidation was able to occur easily, but an excess oxidation reaction might also occur, which would be a clear reason for the weight loss associated with attaining the maximum oxygen uptake position of the MP fibers.

In **Fig. 5-8**, SEM images of the transverse sections of graphitized fibers stabilized under air pressures of 0.1, 0.5, and 1.0 MPa are shown. ARMP-GF14 in **Fig. 5-8(a)** showed the typical skin-core structure of MP-based graphitized fibers [14, 15], but there was not the case for ARMP-GF14s in **Fig. 5-8(b)** and **Fig. 5-8(c)**. Mochida *et al.* have reported that a high heating rate and low final temperature in stabilization were responsible for the formation of a distinct skin-core structure, which was one of the

main factors lowering the TS of the obtained graphitized fibers [4]. Here, the rapid heating and low final temperature in the stabilization conditions resulted in stabilized fibers with a deficient oxygen reaction in their center. Such a deficiency of the amounts of oxygen uptake in the thermal oxidation stabilization was the main reason for the formation of the skin-core structure. Our results shown in **Figs. 5-7** and **5-8** confirm the fact that oxygen uptake at least more than 7.0 wt% in stabilized MP fibers was necessary under the present stabilization conditions to obtain carbonized and graphitized fibers that do not have the skin-core structure. The upper limit of the optimized oxygen uptake was still difficult to determine. The stabilized fibers that allow the highest yields after carbonization and graphitization and the highest mechanical performance, especially the highest TS, should have the most optimized oxidation state. The upper limit of oxygen uptake must be determined with such optimized stabilized fibers. From the above oxygen uptake criteria, ARMP-SF stabilized under air pressure of 0.5 MPa may approach the most stabilized state, whereas ARMP-SFs stabilized under air pressures of the atmospheric level and 1.0 MPa have excess and deficient oxygen uptake in the outer and center parts of pitch fibers, respectively.

5-3-2. *Oxidation-stabilization of MP fiber using laboratory stabilization apparatus*

Table 5-3 shows the results of the oxidation stabilization of ARMP-F10s under various pressurized air flows. In the oxidation stabilization using laboratory-type stabilization apparatus, the maximum stabilization temperature was limited to 270°C to achieve oxidation reactions that were as excessive as possible, which should exhibit some differences in the oxidation state of stabilized fibers in the TGA analyses.

In the oxidation-stabilization under atmospheric conditions, the amounts of oxygen uptakes of the stabilized fibers with a soaking time of 0 min at temperatures of 250,

260 and 270°C with a heating rate of 2.0°C/min were evaluated as being 5.2, 6.2 and 8.5 wt%, respectively. The amounts of oxygen uptakes with a heating rate of 3.0°C/min after soaking for 0, 30 and 60 min at 270°C were 6.5, 7.8 and 8.5 wt%, respectively. The increase of the amounts of oxygen uptake for soaking times between 30 and 60 min was very small because the ARMP-F10 almost reached a fully oxidized state under atmospheric air flow pressure with a soaking time of 60 min at 270°C and a heating rate of 3.0°C/min. Compared with this, the amounts of oxygen uptake with a heating rate of 0.5°C/min after soaking for 0 min at 270°C were higher with 11.7 wt%. This higher amount of oxygen uptake at 0.5°C/min demonstrates that a more stabilized state of ARMP-F10 could be obtained with a decreased heating rate of 0.5°C/min in oxidation stabilization under atmospheric air flow pressure.

In the oxidation stabilization under air flow pressure of 0.5 MPa, the amounts of oxygen uptake of the stabilized fibers with a soaking time of 0 min at temperatures of 250, 260, and 270°C and a heating rate of 2.0°C/min were 6.3, 11.4, and 11.9 wt%, respectively. The amounts of oxygen uptake after soaking for 15 min at 260°C with a heating rate of 3.0°C/min was 11.1 wt% and those with soaking times of 0 and 10 min at 270°C with the same heating rate were 10.8 and 11.8 wt%, respectively. The increase of oxygen uptake between 260 and 270°C with 0 min of soaking was very small and the oxygen uptake after soaking for 10 min at 270°C with a heating rate of 3.0°C/min was also 11.8 wt%, which indicates that ARMP-F10 was almost fully stabilized upon soaking for 10 min at 270°C with a heating rate of 3.0°C/min under air flow pressure of 0.5 MPa.

In the oxidation stabilization under air flow pressure of 1.0 MPa, the amounts of oxygen uptakes of the stabilized fibers at soaking temperatures of 250, 260 and 270°C with a heating rate of 2.0°C/min were 7.0, 11.5 and 11.2 wt%, respectively. The amounts of oxygen uptake after soaking for 0 min at 260°C with a heating rate of

3.0°C/min was 11.5 wt% and those after soaking for 0 and 5 min at 270°C with the same heating rate were 11.2 and 11.1 wt%, respectively. The amounts of oxygen uptakes of the stabilized fiber soaked at 270°C were slightly lower than that of the stabilized fiber at 260°C, which indicated that the oxidation decomposition occurred at 270°C with a heating rate of 2.0°C/min through excess oxidation reactions of mainly the exterior of the stabilized fiber. The decrease in oxygen uptakes with soaking times of 0 and 5 min at 270°C with a heating rate of 3.0°C/min was also the result of oxidation decomposition. The amount of oxygen uptake after soaking for 0 min at 270°C with a heating rate of 3.0°C/min was 11.2 wt%. From these results, ARMP-SF10 was fully or excessively stabilized with soaking for 0 min at 270°C with a heating rate of 3.0°C/min under air flow pressure of 1.0 MPa.

5-3-3. *Yields of carbonization and graphitization of the stabilized fibers and the mechanical performances of the carbonized and graphitized fibers*

Table 5-3 also lists the yields of carbonization and graphitization of the oxidation-stabilized fibers and the mechanical performances of carbonized and graphitized fibers. The yields of carbonization and graphitization were evaluated by the weight ratios (percentages) of the carbonized and graphitized fibers relative to the MP fibers.

The carbonization yields of ARMP-CFs stabilized with soaking for 0 min at 250, 260 and 270°C with a heating rate of 2.0°C/min under atmospheric pressure were 81.0, 85.2 and 83.2 wt%, respectively. Moreover, the yields of ARMP-CFs stabilized with soaking for 0, 30 and 60 min at 270°C with a heating rate of 3.0°C/min under atmospheric pressure were 83.2, 85.6 and 87.0 wt%, respectively. The carbonization yield of ARMP-CF stabilized with soaking for 0 min at 270°C with a heating rate of 0.5°C/min under atmospheric pressure was 88.3 wt%. Furthermore, the carbonization yields of ARMP-CFs stabilized with soaking for 0 min at 250, 260 and 270°C with a

heating rate of 2.0°C/min under air flow pressure of 0.5 MPa were 90.0, 90.9 and 89.1 wt%, respectively. The yields of ARMP-CFs stabilized with soaking for 15 min at 260°C and soaking for 0 and 10 min at 270°C with a heating rate of 3.0°C/min under air flow pressure of 0.5 MPa were 88.8, 89.0 and 89.5 wt%, respectively. The analyses also revealed that the carbonization yields of ARMP-CFs stabilized with soaking for 0 min at 250, 260 and 270°C with a heating rate of 2.0°C/min under air flow pressure of 1.0 MPa were 85.3, 85.4 and 85.3 wt%, respectively. The yields of ARMP-CFs stabilized with soaking for 0 min at 260°C and soaking for 0 and 5 min at 270°C with a heating rate of 3.0°C/min under air flow pressure of 1.0 MPa were 89.6, 85.2 and 84.3 wt%, respectively. From these results, the carbonized fibers stabilized under air flow pressure of 0.5 MPa had higher carbonization yields than those stabilized under air flow pressures at the atmospheric level and 1.0 MPa. Generally, the stabilized fibers with oxygen uptakes of less than 7.0 wt% and more than 13.0 wt% had lower carbonization yields than the stabilized fibers with oxygen uptakes of around 11.0–12.0 wt%. These results suggest that oxygen uptakes of 11.0–12.0 wt% might be close to the optimal oxidation state for the oxidation-stabilization of ARMP-F10. The deficiency of oxygen uptake in the fibers stabilized at 270°C with heating rates of 2.0 and 3.0°C/min under the atmospheric air flow pressure was ascribed to the insufficient delivery of oxygen into the center of the pitch fibers under these conditions, conferring excess volatility of light aromatic molecules in the carbonization. In contrast, excessive oxygen uptake in the stabilized fibers usually occurred under an air flow pressure of 1.0 MPa in our study, indicating that the excess oxidation mainly occurred in the exterior of pitch fibers, which might be the principal reason for the oxidation decomposition of pitch and stabilized fibers in the stabilization and carbonization processes.

The graphitization yields revealed a trend very similar to those of carbonization. The average weight loss in the graphitization from the carbonization was estimated to be approximately 1.0–2.0 wt%. The graphitized fibers stabilized under air flow pressure of 0.5 MPa had higher graphitization yields than those stabilized under air flow pressure conditions of the atmospheric level and 1.0 MPa.

With regards to the mechanical performance of the carbonized and graphitized fibers stabilized with soaking for 0 min at 270°C with a heating rate of 2.0°C/min under atmospheric pressure, they had TS of 2.4 and 3.5 GPa, elongation ratios of 1.5% and 0.6%, and YM of 159 and 508 GPa, respectively. The carbonized and graphitized fibers stabilized with soaking for 0 min at 270°C with a heating rate of 0.5°C/min under atmospheric pressure had markedly improved values of TS of 2.9 and 4.0 GPa, elongation ratios of 1.7% and 0.6%, and YM of 171 and 663 GPa, respectively. The carbonized and graphitized fibers stabilized with soaking for 0 min at 260°C with a heating rate of 2.0°C/min under air flow pressure of 0.5 MPa had the best mechanical performance of TS of 3.4 and 4.6 GPa, elongation ratios of 1.7% and 0.6%, and YM of 177 and 765 GPa, respectively. These results indicate that TS, elongation ratio and YM of the carbonized fibers of higher than 1.7 GPa, 1.7% and 170 GPa, respectively, after carbonization at 1000°C for 30 min were successfully obtained within a total stabilization time of less than 60 min.

Fig. 5-9 schematically shows the oxidation and oxidation decomposition in the oxidation stabilization at 270°C for soaking for 0 min with a heating rate of 2.0°C/min under air flow pressures at the atmospheric level, 0.5, and 1.0 MPa. From the model images, we can assume that oxidation-stabilization occurs *via* the following mechanism, as summarized in **Table 5-4**. Specifically, appropriate oxidation reactions can be achieved for the optimization of pitch fibers through oxidation-stabilization

under a mild air flow pressure of 0.5 MPa with a relatively short total stabilization time.

5-4. Conclusion

Oxidation-stabilization under mild air flow pressures of 0.5 and 1.0 MPa can successfully shorten the total stabilization time to less than 60 min to obtain MP-based carbonized and graphitized fibers without deteriorating the mechanical performance than mesophase phase pitch-based carbonized and graphitized ones stabilized for 300 min under atmospheric air flow conditions. Notably, carbonized fibers with high TS and YM of over 3.0 GPa and 170 GPa, respectively, which had only been heat-treated at 1000°C for 30 min, were successfully obtained with a total stabilization time of less than 60 min through oxidation stabilization under air flow pressures of 0.5 MPa.

Activation energies for oxidation reactions in stabilization under air flow pressure were much lower than those of oxidation reactions under atmospheric air flow pressure because of the higher diffusivity of oxygen into the center and a more rapid oxidation reaction on the molecules of MP fibers under mild air flow pressures of 0.5 and 1.0 MPa. The higher oxygen diffusivities resulted in a more homogeneous distribution of oxygen uptake across the transverse section of MP fibers and allowed higher yields of carbonization and graphitization, which were directly related to the improvement of the mechanical properties. Additionally, excess oxidation can bring about the oxidation decomposition of pitch molecules with oxidation stabilization under air flow pressures of 0.1 and 1.0 MPa, which decreased the carbonization yield and TS of the obtained CFs.

Reference

1. Yoon SH, Korai Y, Mochida I. Assessment and optimization of the stabilization process of mesophase pitch fibers by thermal analyses. Carbon 1994;32:281−7.
2. Yang H, Yoon SH, Korai Y, Mochida I, Kato O. Microvoids present in anisotropic mesophase pitch, their as-spun and annealed fibers. Chem Lett 2003;32:168−9.
3. Matsumoto T, Mochida I. Oxygen distribution in oxidatively stabilized mesophase pitch fiber. Carbon 1993;31:143−7.
4. Mochida I, Toshima H, Korai Y, Hino T. Oxygen distribution in the mesophase pitch fibre after oxidative stabilization. J Mater Sci 1989;24:389−94.
5. Fathollahi B, Jones B, Chau PC, White JL. Injection and stabilization of mesophase pitch in the fabrication of carbon–carbon composites. Part III: Mesophase stabilization at low temperatures and elevated oxidation pressures. Carbon 2005;43:143−51.
6. Cornec LP, Rogers DK, Fain CC, Edie DD. A novel stabilization technique and its influence upon carbonization yield. Extended Abstracts, CARBON'92, Deutsche Keramische Gesellschaft, Essen, Germany 1992;710–2.
7. Lee S, Eom Y, Kim BJ, Mochida I, Yoon SH, Kim BC. The thermotropic liquid crystalline behavior of mesophase pitches with different chemical structures. Carbon 2015;81:694−701.
8. Mochida I, Shimizu K, Korai Y, Otsuka H, Sakai Y, Fujiyama S. Preparation of mesophase pitch from aromatic hydrocarbons by the aid of HF/BF_3. Carbon 1990;28:311−9.
9. Korai Y, Ishida S, Watanabe F, Yoon SH, Wang YG, Mochida I, Kato I, Nakamura T, Sakai Y, Komatsu M. Preparation of carbon fiber from isotropic pitch containing mesophase spheres. Carbon 1997;35:1733−7.
10. Régnier N, Fontaine S. Determination of the thermal degradation kinetic parameters of carbon fibre reinforced epoxy using TG. J Therm Anal Calorim 2001;64:789−99.
11. Blanco C, Lu S, Appleyard SP, Rand B. The stabilisation of carbon fibres studied by micro-

thermal analysis. Carbon 2003;41:165−71.

12. Japanese Industrial Standards. Carbon Fiber−Determination of the tensile properties of the single-filament specimens. JIS R 7606:2000.
13. Drbohlav J, Stevenson WTK. The oxidative stabilization and carbonization of a synthetic mesophase pitch, part I: The oxidative stabilization process. Carbon 1995;33:693−711.
14. Mochida I, Zeng SM, Korai Y, Toshima H. The introduction of a skin-core structure in mesophase pitch fibers by oxidative stabilization. Carbon 1990;28:193−8.
15. Mochida I, Zeng SM, Korai Y, Hino T, Toshima H. Structure and properties of mesophase pitch carbon fibre with a skin-core structure carbonized under strain. J Mater Sci 1992;27:1960−8.

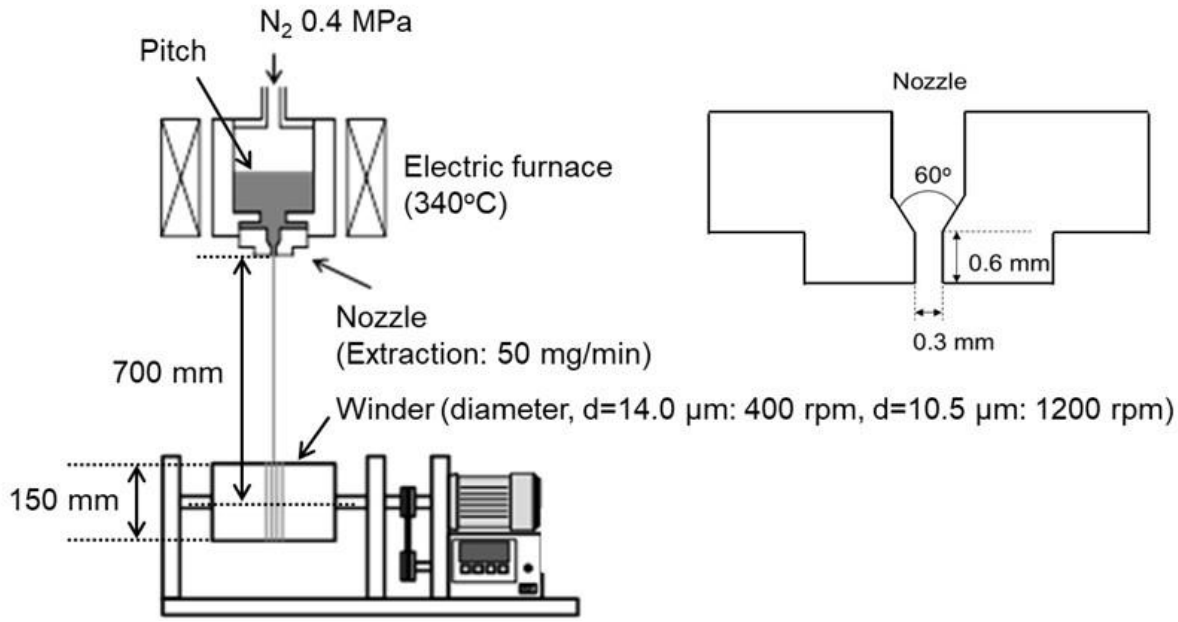

Fig. 5-1. Schematic picture of self-designed laboratory-type mono-hole melt-spinning apparatus.

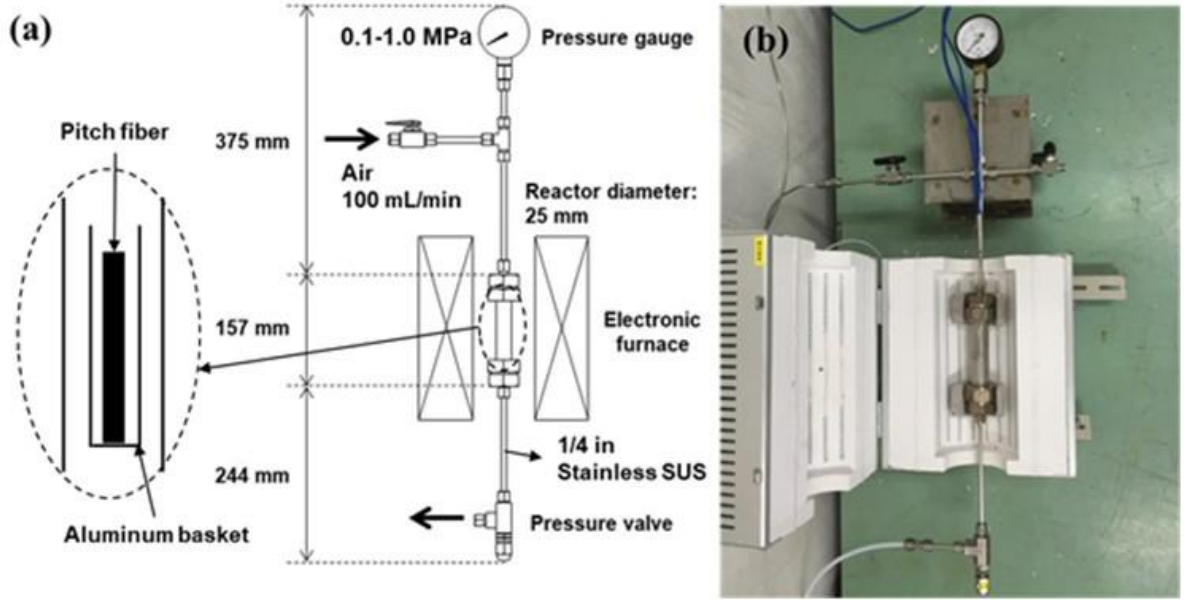

Fig. 5-2. The schematic and real pictures of self-designed laboratory-type oxidative stabilization apparatus: (a) Schematic picture of self-designed laboratory-type oxidative stabilization apparatus, (b) Real picture of self-designed laboratory-type oxidative stabilization apparatus.

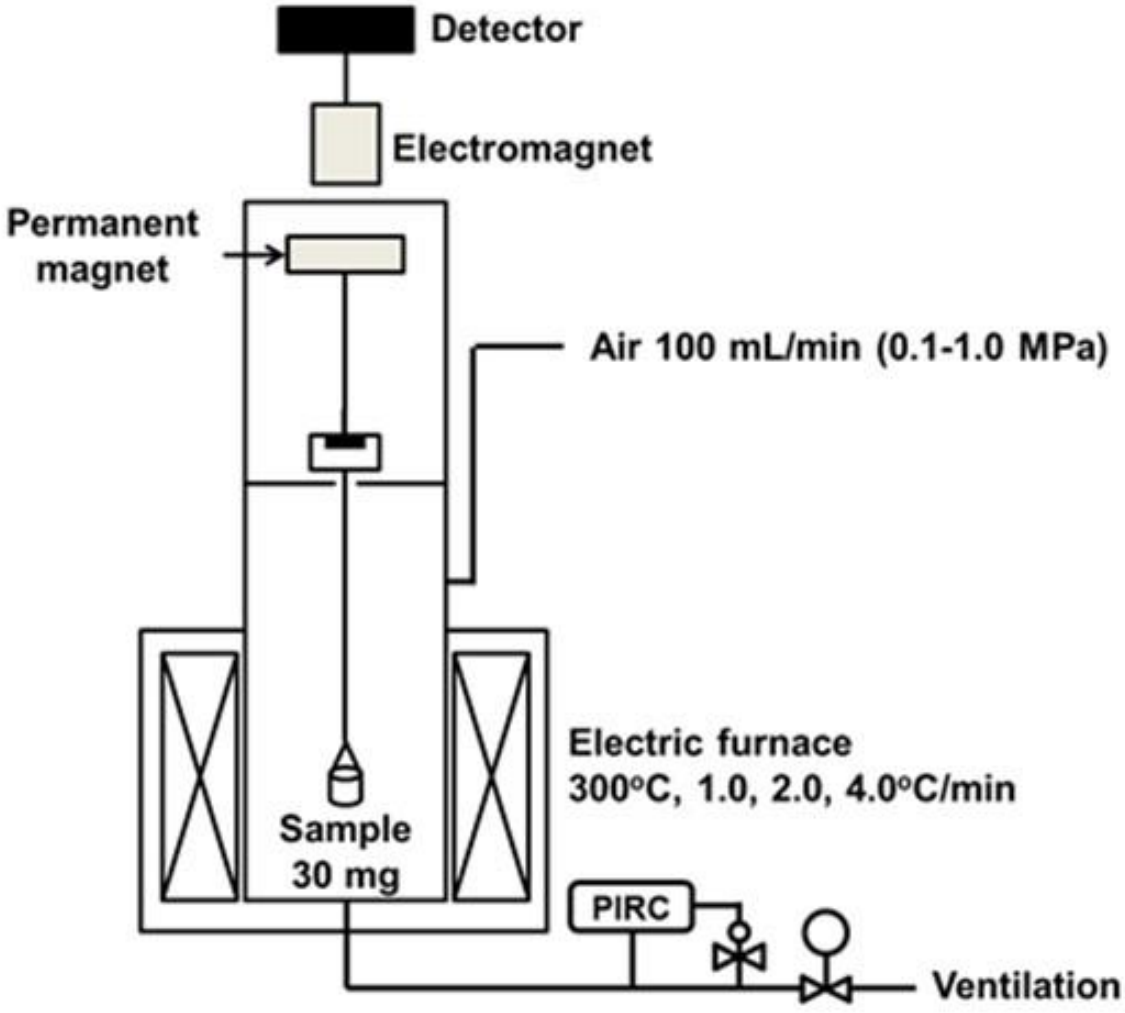

Fig. 5-3. The schematic picture of MSB-TG analyzer for the oxidation stabilization under atmospheric and pressurized conditions.

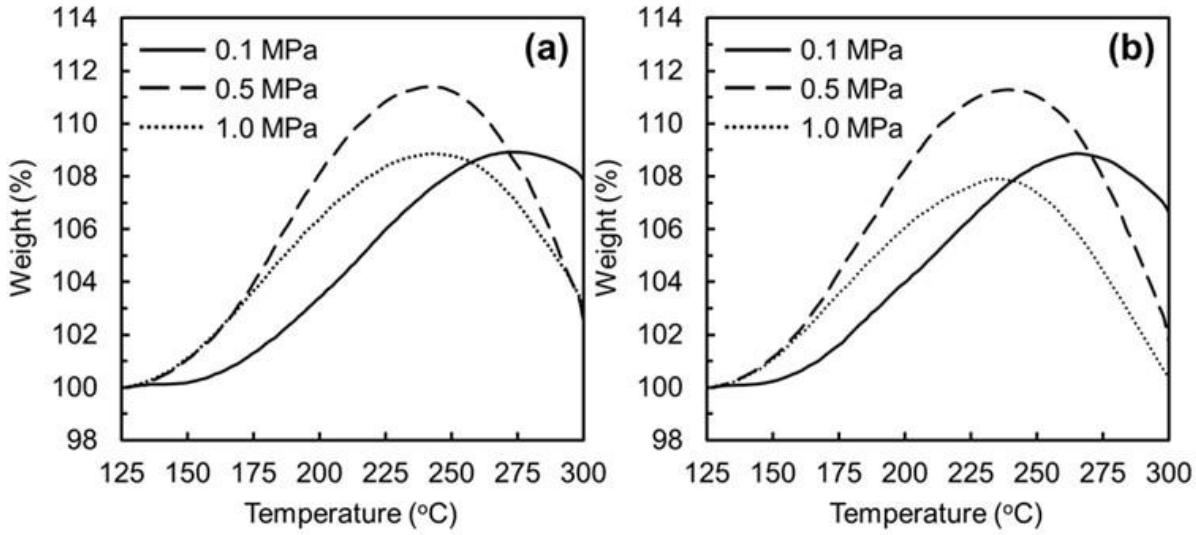

Fig. 5-4. TGA profiles of the oxidation stabilization of mesophase pitch fibers with different applied pressures: (a) ARMP-F14, (b) ARMP-F10.

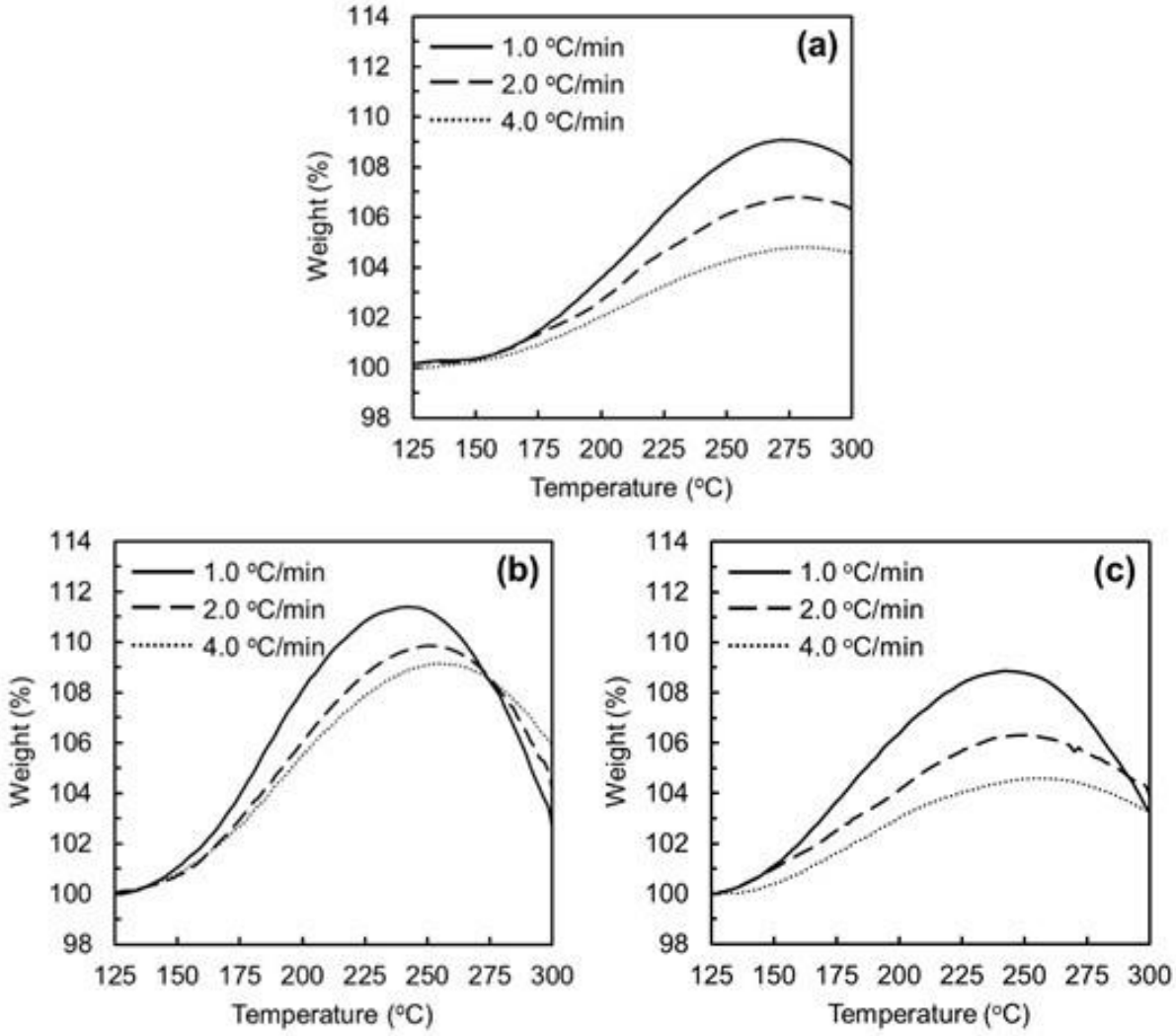

Fig. 5-5. TGA profiles of oxygen uptakes in the oxidation stabilizations of ARMP-F14 with different heating rates: (a) 0.1 MPa, (b) 0.5 MPa, (c) 1.0 MPa.

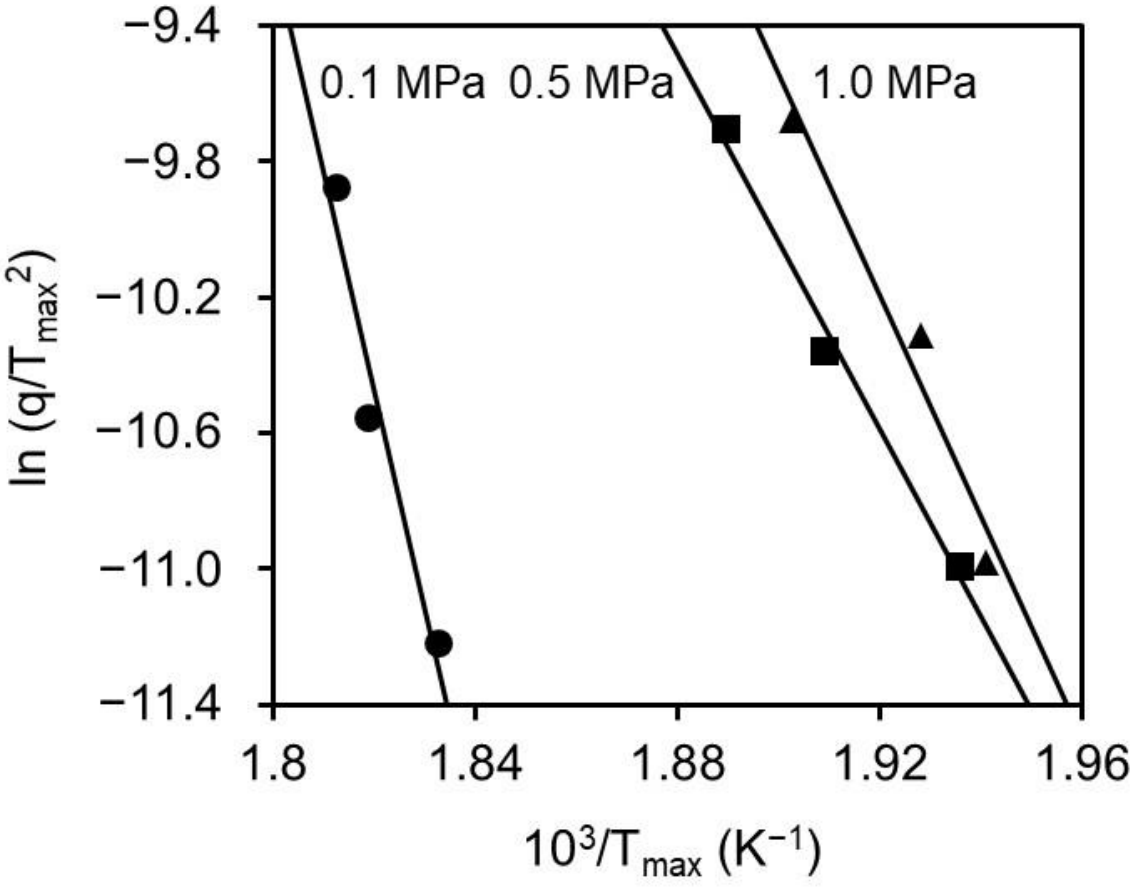

Fig. 5-6. Arrhenius plots of the oxidation stabilization of ARMP-F14 with different applied pressure.

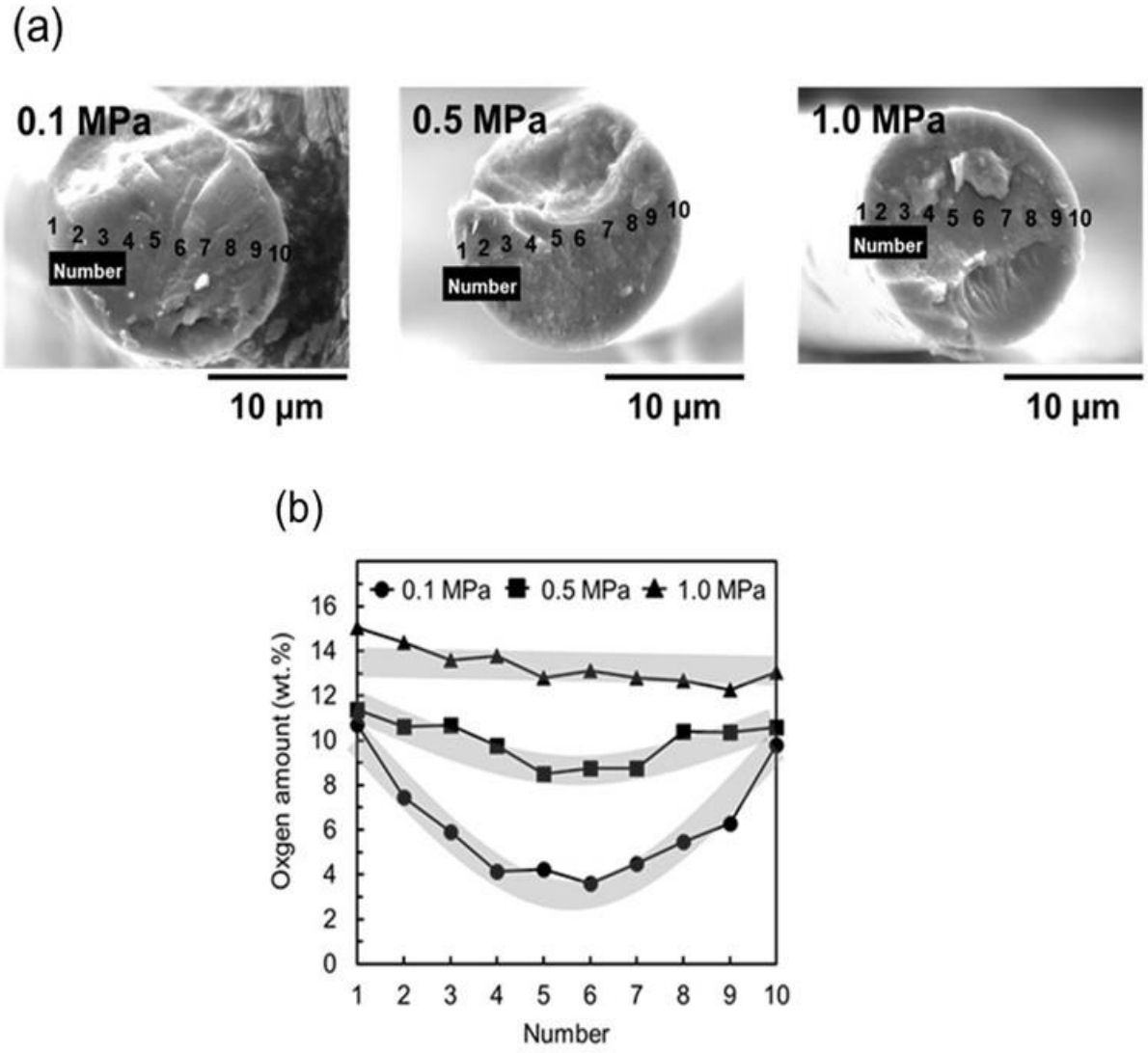

Fig. 5-7. Distributions of the amounts of oxygen uptakes in the transversal sections of ARMP-SF14s using SEM-EPMA: (a) Measuring points of the amounts of oxygen uptakes in ARMP-SF14s, (b) Distributions of the amounts of oxygen uptakes in the transversal sections of ARMP-SF14s

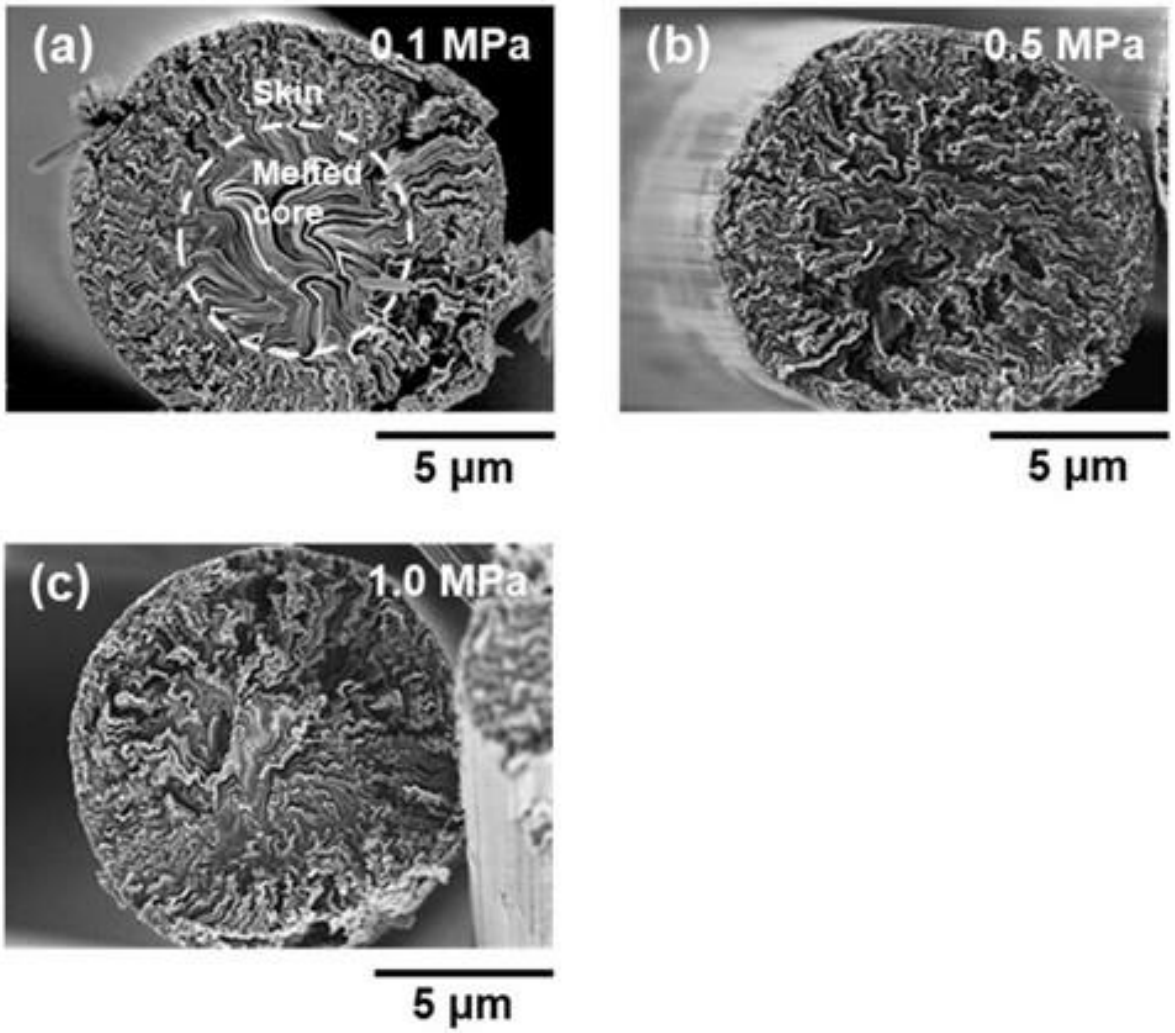

Fig. 5-8. SEM images of the transverse sections of graphitized fibers stabilized under various air flow pressures: (a) 0.1 MPa and (b) 0.5 MPa and 1.0 MPa.

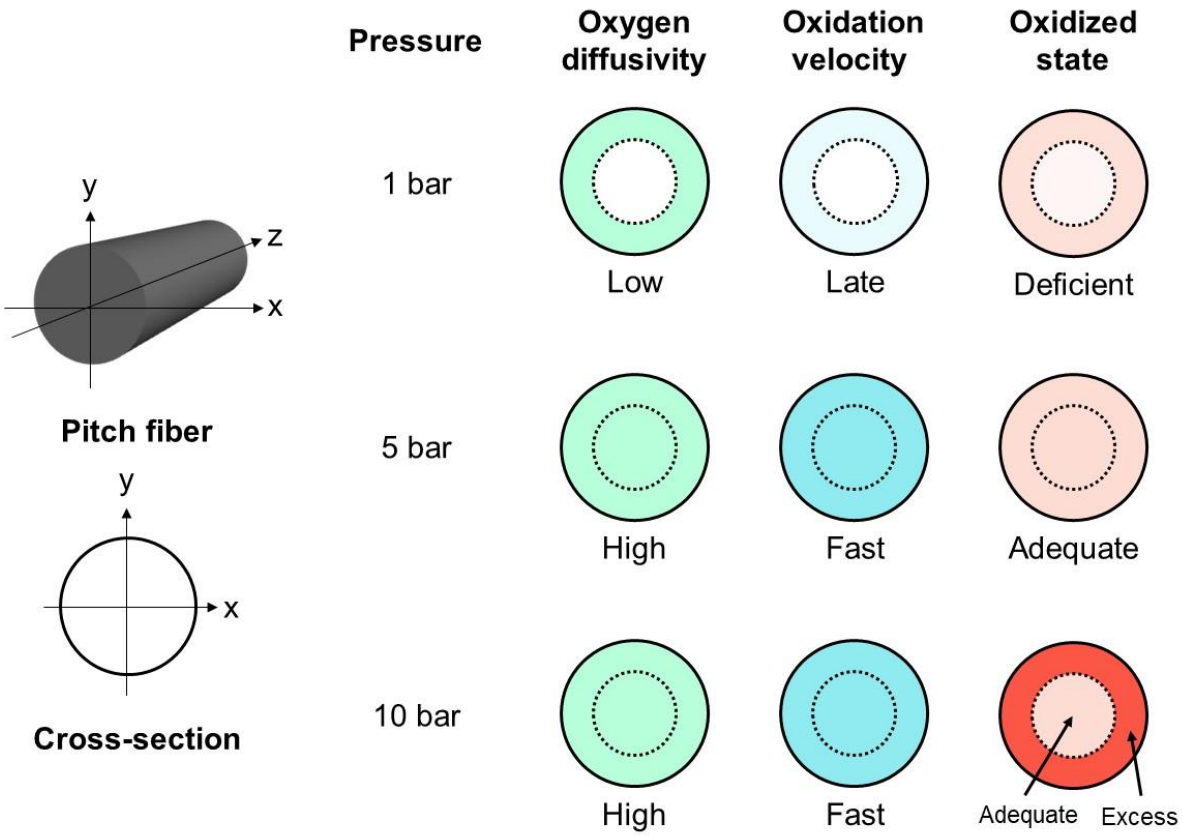

Fig. 5-9. Schematic model pictures of the oxidation and oxidation decomposition in the oxidation stabilization at 270°C for soaking for 0 min with a heating rate of 2.0°C/min under air flow pressures at (a) the atmospheric level (0.1 MPa), (b) 0.5 MPa, (c) 1.0 MPa.

Table 5-1 General properties of ARMP

Pitch	Softening Point[*1] (°C)	Elemental analysis				^{13}C-NMR	Raman spectroscopy	XRD[*3]	
		C	H	N	$O_{diff.}$	fa	I_d/I_g[*2]	d_{002} (Å)	Lc (002) (nm)
		(wt%)							
ARMP	240	94.60	4.89	0.25	0.26	0.84	0.65	3.57	5.23

*1: Softening point determined by thermomechanical analysis (TMA)

*2: Id/Ig determined by the intensity ratio of Intensities at 1350 cm-1 and 1580 cm-1, respectively

*3: Interlayer space (d002) and Stacking height (Lc (002)) determined by wide angel X-ray diffractometry

Table 5-2 Activation energies on the oxidation reactions of ARMP-F14 under various applied pressures

Applied pressure (MPa)	0.1	0.5	1.0
Activation Energy (kJ/mol)	535	230	271

Condition of oxidation reactions of mesophase pitch under various applied pressure Heating rates: 1.0, 2.0, 4.0°C/min, Applied pressure; 0.1, 0.5, 1.0 MPa with pressurized air flow of 100 mL/min

Table 5-3 The results of the stabilization under atmospheric and pressurized conditions using laboratory stabilization apparatus, yields and mechanical properties of carbonized and graphitized fibers

Stabilization condition of mesophase pitch fiber (ARMP-F10)						Yield and mechanical properties of carbonized fiber (ARMP-CF10)*3					Yield and mechanical properties of graphitized fiber (ARMP-GF10)*4				
Applied pressure (MPa)	Heating rate (°C/min)	Soaking temperature (°C)	Soaking time (min)	Oxygen uptake*1 (wt.%)	Total time*2 (min)	Yield (wt.%)	Diameter (μm)	Tensile strength (GPa)	Elongation ratio (%)	Young's modulus (GPa)	Yield (wt.%)	Diameter (μm)	Tensile strength (GPa)	Elongation ratio (%)	Young's modulus (GPa)
0.1	2.0	250	0	5.2	50	81.0	7.6 ±0.4	1.0 ± 0.6	0.9	105 ± 71	-	-	-	-	-
		260	0	6.2	55	85.2	7.8 ±0.2	2.4 ± 0.3	1.0	105 ± 32	83.0	7.6 ±0.1	3.1 ± 0.2	0.5	617 ±44
		270	0	8.5	60	83.2	7.8 ±0.2	2.4 ± 0.3	1.5	159 ± 27	82.4	7.7 ±0.1	3.5 ± 0.3	0.6	508 ±30
	3.0	270	0	6.5	40	83.2	7.7 ±0.1	2.4 ± 0.3	1.5	160 ± 30	82.7	7.5 ±0.1	3.4 ± 0.3	0.5	599 ±31
		270	30	7.8	90	85.6	7.6 ±0.2	2.1 ± 0.3	1.6	141 ± 41	84.7	7.4 ±0.1	3.7 ± 0.3	0.6	612 ±24
		270	60	8.5	100	87.0	7.7 ±0.2	2.4 ± 0.4	1.5	142 ± 34	85.2	7.5 ±0.1	3.3 ± 0.3	0.5	666 ±50
	0.5	270	0	11.7	300	88.3	7.7 ±0.1	2.9 ± 0.4	1.7	171 ± 29	87.1	7.4 ±0.1	4.0 ± 0.3	0.6	663 ±47
0.5	2.0	250	0	6.3	50	90.0	7.6 ±0.1	3.0 ± 0.3	1.6	180 ± 26	87.1	7.5 ±0.1	4.1 ± 0.2	0.6	671 ±39
		260	0	11.4	55	90.9	7.7 ±0.1	3.4 ± 0.2	1.7	177 ± 21	87.3	7.5 ±0.1	4.6 ± 0.2	0.6	765 ±42
		270	0	11.9	60	89.1	7.7 ±0.2	2.8 ± 0.3	1.8	186 ± 28	86.8	7.6 ±0.2	4.6 ± 0.3	0.6	767 ±39
	3.0	260	15	11.1	48	88.8	7.6 ±0.2	2.8 ± 0.5	1.7	166 ± 30	87.0	7.4 ±0.2	4.2 ± 0.4	0.6	699 ±55
		270	0	10.8	40	89.0	7.7 ±0.1	3.3 ± 0.3	1.8	154 ± 54	87.0	7.5 ±0.1	4.5 ± 0.3	0.6	765 ±42
		270	10	11.8	50	89.5	7.8 ±0.1	2.4 ± 0.3	1.7	191 ± 31	86.2	7.6 ±0.1	4.4 ± 0.3	0.6	740 ±43
1.0	2.0	250	0	7.0	50	85.3	7.8 ±0.2	2.3 ± 0.3	1.4	169 ± 22	84.9	7.5 ±0.1	3.3 ± 0.4	0.5	660 ±49-
		260	0	11.5	55	85.4	7.7 ±0.2	2.4 ± 0.3	1.4	165 ± 40	82.8	7.6 ±0.1	3.1 ± 0.4	0.5	615 ±90
		270	0	11.2	60	85.3	7.5 ±0.1	3.2 ± 0.32	1.5	161 ± 48	83.0	7.4 ±0.1	3.5 ± 0.2	0.5	725 ±41
	3.0	260	0	11.5	33	89.6	7.7 ±0.2	2.3 ± 0.4	1.7	185 ± 20	87.1	7.5 ±0.1	3.4 ± 0.2	0.6	733 ±24
		270	0	11.2	40	85.2	7.7 ±0.2	2.6 ± 0.5	1.5	154 ± 55	83.0	7.5 ±0.1	3.5 ± 0.4	0.5	702 ±51
		270	5	11.1	45	84.3	7.5 ±0.3	2.6 ± 0.5	1.6	159 ± 39	82.9	7.3±0.1	3.9 ± 0.5	0.6	667 ±55

*1. Oxygen up-take was determined by elemental analysis.

*2. Total time was determined by the summing of heating time from 150°C to soaking temperature and soaking time at soaking temperature.

*3 Carbonization was carried out at 1000°C for 30 min with the heating rate of 15°C/min under vacuum.

*4 Graphitization was carried out at 2800°C for 10 min with the heating rate of 20°C under Ar atmosphere.

*3 & *4 Mechanical properties were estimated according to JIS R 7606:2000.

Table 5-4 Estimated oxidation state of the stabilized fiber under various air flow pressures based on the model mechanisms of oxidation diffusion and reaction

Stabilization conditions				Oxygen diffusivity from outer surface to center part of pitch fiber	Oxidation reaction and oxidized state on molecules of mesophase pitch fiber	
Applied pressure (MPa)	Heating rate (^{o}C/min)	Soaking temperature (^{o}C)	Soaking time (min)		Outer part of fiber	Center part of fiber
0.1	2.0	270	0	Low	Late, deficient	Late, deficient
	3.0		60	Low	Late, excess	Late, deficient
0.5	2.0		0	High	Fast, adequate	Fast, adequate
	3.0		10	High	Fast, adequate	Fast, adequate
1.0	2.0		0	High	Fast, excess	Fast, adequate
	3.0		5	High	Fast, excess	Fast, excess

*Amount of Air flow: 100 mL/min

Chapter 6. Conclusions

The main purpose of this study is the reduction of the production cost on preparation of mesophase pitch-based carbon fibers (MPCFs). Therefore, we tried to improve the pitch yield and spinnability of spinnable mesophase pitch (SMP) and shorten the total oxidation-stabilization time. SMP with high yield was successfully prepared by selecting and hybridizing raw materials such as a coal direct extracted fraction, ethylene bottom oil and coal tar pitch. On the other hand, the softening point of commercialized mesophase pitch (MP) was able to control by adding isotropic pitch as solvent molecules into mesogen molecules and adjusting their balance. Furthermore, oxidation-stabilization under pressure can reduce the stabilization time of less than 1 h without deteriorating mechanical properties. The conclusions relating to a study of the reduction of the production cost on preparation of high performance MPCFs are summarized as follows;

Chapter 2. Improvement of spinnable mesophase pitch yield using a coal direct extracted fraction

Hyper-coal (HPC) derived SMP with high preparation yield was successfully prepared through the three-step manufacturing process of hydrogenation, N_2 blowing heat treatment, and short thin-layer evaporation (TLE).

The hydrogenation of HPC decreased the amount of methylene chains and heavy molecular components with high polynuclear aromatic compounds. The N_2 blowing heat treatment was necessary to reveal the mesophase texture but not to increase the molecular weight and mesogens, including aromatic carbons. The short TLE treatment was very effective to obtain the spinnable bulk texture of MP through the slight removal of non-mesogen light molecular components.

HPC-derived MPCFs showed high tensile strengths of 1.8 and 3.0 GPa and moduli of 140 and 450 GPa after carbonization and graphitization, respectively.

Chapter 3. Preparation of spinnable mesophase pitch by hybridization of raw materials

SMP with high yield was successfully prepared through pressurized heat treatment of ethylene bottom oil (EBO), bromination-dehydrobromination, N_2 blowing heat treatment, and short TLE using EBO and coal tar pitch (CTP) as cheap raw materials without hydrogenation.

CTP has high molecular stacking property due to polycyclic aromatic hydrocarbons. Therefore, adding CTP into pressurized-heat-treated EBO (EBOp), the components of CTP played a role of mesogen molecules. On the other hand, EBOp has low molecular stacking property due to aromatic hydrocarbons which includes low membered rings and long-chain aliphatic groups. Thus, the components of EBOp played a role of solvent molecules among EBOp/CTP derived MP.

Chapter 4. Elucidation of Lyotropic liquid crystalline characteristics of mesophase pitch and modifying its property and yield

In order to develop an optically anisotropic structure, a certain number of laminated sheets is required. The pitch that shows an optically anisotropic at high temperatures can maintain stacking even at high temperatures.

The softening point decreased less than that of AR pitch by the addition of CTP derived isotropic pitch with low softening point into THF insoluble fraction of AR pitch (AR-THFI) as mesogen molecules. Thus, we may enhance the spinnability of MP by controlling the balance of mesogen molecules and solvent molecules and reduce the production cost of MP by using isotropic pitch with high yield as solvent molecules.

Chapter 5. Shortening the total oxidation-stabilization time on preparation of mesophase pitch-based carbon fiber

Oxidation-stabilization under air high pressures can successfully shorten the total stabilization time to less than 60 min to obtain MP-based carbonized and graphitized fibers without deteriorating the mechanical performance than those stabilized for 300 min under atmospheric air flow conditions.

Activation energies for oxidation reactions in stabilization under air flow pressure were much lower than those of oxidation reactions under atmospheric air flow pressure because of the higher diffusivity of oxygen into the center and a more rapid oxidation reaction on the molecules of MP fibers under air flow pressures of 0.5 and 1.0 MPa. The higher oxygen diffusivities resulted in homogeneous oxidation and allowed higher yields of carbonization and graphitization, which are directly related to the improvement of the mechanical properties.

List of abbreviation

^{13}C-NMR: 13C solid-state nuclear magnetic resonance spectroscopy

AMW: Average molecular weight

ARMP-F: AR mesophase pitch fiber

ARMP-SF: AR mesophase pitch-based stabilized fiber

ARMP-CF: AR mesophase pitch-based carbonized fiber

ARMP-GF: AR mesophase pitch-based graphitized fiber

AR-THFI: Tetrahydrofuran insoluble fraction of AR pitch

AR-THFS: Tetrahydrofuran soluble fraction of AR pitch

CF: Carbon fiber

CFRP: Carbon fiber reinforced plastic

CMC: Critical micelle concentration

CTP: Coal tar pitch

CTP140: Coal tar pitch derived isotropic pitch with softening point of 140°C

d_{002}: The interlayer spacing of the graphitic crystal of (002) plane

DMF: Dimethylformamide

DMSO: Dimethylsulfoxide

EBO: Ethylene bottom oil

EBOp: ethylene bottom oil heat-treated at 370°C for 3 h under an autogenous pressure

EPMA: Electron probe micro-analyzer

EV: Electric vehicle

f_a: Carbon aromaticity

HPC: Hyper-coal

IP: Isotropic pitch

IPCF: Isotropic pitch-based carbon fiber

Lc: The crystal thickness of the graphitic crystal of (002) plane

MAS: Magic-angle spinning

MP: Mesophase pitch

MPCF: mesophase pitch-based carbon fiber

MSB-TG: Thermal gravimetric analysis using a magnetic suspension balance

PAN: Polyacrylonitrile

PANCF: Polyacrylonitrile-based carbon fiber

POM: Polarization microscope

QI free CTP: Quinoline insoluble free coal tar pitch

SEM: Scanning electron microscope

SMP: Spinnable mesophase pitch

SO: Slurry oil

SO140: slurry oil derived isotropic pitch with softening point of 140°C

SP: Softening point

Tetralin: 1, 2, 3, 4-tetrahydronaphthalene

THF: Tetrahydrofuran

TLE: Thin layer evaporation

TMA: Thermal mechanical analysis

TOF-MS: Time-off-flight mass spectrometry

TS: Tensile strength

XRD: X-ray diffractometer

YM: Young's modulus

List of figures

List of tables

Abstract in Japanese

論　文　内　容　の　要　旨

メソフェーズピッチ系高性能炭素繊維（Mesophase pitch based high performance carbon fiber: MPCF）は高い比強度と比弾性率を有し、自動車車体、風車および建築用複合材の構造素材としてその利用が期待されている。しかし、前駆体である紡糸用メソフェーズピッチ（Spinnable mesophase pitch: SMP）の高価格や酸化不融化などの工程が MPCF 製造コスト高騰を招き、現在その利用分野が宇宙、軍事およびスポーツ用として限られている。

前駆体 SMP は、石炭由来のコールタールピッチ（Coal tar pitch: CTP）や石油系重質油（Petroleum heavy oil: PHO）等の化石燃料の副産物を原料として用い、その原料を精製、水素化、液相炭化および揮発分除去といった複雑な精製・改質処理を施すことで得られる。水素化は、多環芳香族分子にナフテン構造を誘導し流動性を高めて紡糸性を向上するために必須であるが、同時に低分子化を招き、SMP 収率を大きく低下させる。これが、高価格化の大きな一因となっている。一方、SMP を紡糸したピッチ繊維の酸化不融化は、炭素化・黒鉛化時に繊維状を保つために必要な工程である。ピッチ繊維の内外部を均一かつ適量に酸化させるため、酸化剤の低い拡散性を補うため長時間かけて行う。そのため、炭素繊維の製造工程において最も時間がかかりエネルギー消費が大きい工程であり、MPCF の高価格化のもう一つの主要因である。

本研究は、これらの問題点を解決し、MPCF の$12 /kg という低価格化製造を果たすため、SMP の高収率（30wt%以上）製造および短時間（1 時間以下）酸化不融化手法の開発を目標とした。これらの目標設定において、SMP の既存の紡糸性や不融化性を維持することと、酸化不融化による製造した MPCF の機械的物性が損なわれないことを前提とする。

本学位論文の構成内容および主たる成果は、以下のとおりである。

第 1 章では、炭素繊維の概略、製造における問題点を紹介した後、本研究目的と研究手法等を説明した。

第 2 章では、石炭直接液化抽出物であるハイパーコール（Hyper coal: HPC）を原

料に選択し、最適の水素化、窒素吹き込み熱処理および比較的低温・短時間減圧蒸留の 3 工程を効果的に組み合わせることで、原料対比 50 wt%以上の高収率で SMP を調製した結果をまとめた。本研究で達成した 54 wt%の SMP 収率は、一般工程による SMP 製造において世界最高収率である。調製した SMP は優れた紡糸性と不融化性を示し、その炭素繊維の引張強度は、1000℃の炭素化処理だけで目標値 1700 MPa よりも高い 1800 MPa を示した。

第 3 章では、SMP 製造工程における高価格化の主な原因である水素化をなくすため、選択した原料の混合、臭素化・脱臭化水素化処理および窒素吹き込み熱処理により、低軟化点 SMP の調製を試みた。安価な原料として CTP、石油系残渣油のエチレンボトムオイル（Ethylene bottom oil: EBO）やスラリーオイル（Slurry oil: SO）を選択し、加圧処理したエチレンボトムオイル（Pressurized heat treated EBO: EBOp）に CTP や SO を適量混合し、さらに適切に臭素化・脱臭化水素化および窒素吹き込み熱処理することで、SMP 製造における CTP や SO の異方性形成（メソゲン化）の特徴を調べた。その結果、EBOp に 30 wt%の CTP を混合した原料を用いて 5%の臭素化-脱臭素化および窒素吹き処理することで、水素化処理なしで、軟化点 285℃、収率 23%および異方性 80 vol%の SMP の製造に成功した。製造した SMP は優れた紡糸性を示した。これらの結果から、異方性形成能が高い CTP と異方性形成性は低いが溶融状態で比較的高い流動性を示す EBOp とを最適混合することによって、水素化なしで SMP の高収率調製が可能であることが示された。

第 4 章では、既商品化された合成 SMP の AR ピッチを標準試料と用いて、SMP の油方的液晶性（Lyotropic liquid crystalline characteristics）を証明すると共に、その油方的液晶性を有効に生かし、SMP の紡糸性や収率向上への適用可能性を調べた。特に、常温と溶融状態で常に 100 vol%の異方性を示す AR ピッチをテトラヒドロフラン（Tetrahydrofuran: THF）で溶媒分離し、その不溶分（AR-THFI）をメソゲン成分、可溶分（AR-THFS）を溶媒成分とした後、AR-THFI/AR-THFS を様々な重量比で混合し製造したピッチの異方性含有量と分子積層の相関性が一致することを確認することで、SMP 油方性液晶性を明らかにした。さらに、溶媒成分の AR-THFS を CTP と SO から調製した等方性ピッチ（CTO140 および SO140）と代替して混合することで、AR ピッチと同様に全面異方性を示しながら、製造した SMP の低軟化点化や高収率化が同時に可能なことを確認した。

第 5 章では、SMP のピッチ繊維の均一かつ適量の酸化不融化に長時間が必要な主な原因である酸化剤空気の液晶ピッチ内部への低拡散性を改善するため、加圧空気による SMP ピッチ繊維の酸化不融化を試みた。酸化剤である空気の加圧により、酸化不融化にかかる時間を大幅に短縮することができ、炭素化や黒鉛化処理後製造した MPCF の機械的物性を向上しながら、不融化時間を 1 時間以内に短縮することに成功した。

第 6 章では、上記の結果をまとめた。

Acknowledgements

I would like to give heartful thanks to Prof. Seong-Ho Yoon, my supervisor, for his guidance and valuable suggestions to accomplish the present study. Without his support, this thesis would not have been possible.

I sincerely thank to Prof. Jin Miyawaki and Prof. Hisahiro Einaga for valuable and critical advice.

I am also in debt to Prof. Jin Miyawaki and Prof. Koji Nakabayashi whose opinions and information have helped me very much throughout this study.

Besides the great teachers, I would like to thank Dr. Osamu Kato, Prof. Takaaki Shimohara, Ms. Keiko Ideta, and Ms. Satoko Gondo for their great support to the experiment.my experiments. And I cannot forget the kindness of Ms. Miho Nakano.

I owe my deepest gratitude to Kobe Steel Co. Ltd. and Mitsubishi Gas Chemical Co. for supplying Hyper-coal and AR mesophase pitch.

This study was supported by the Technology Innovation Program (Project No. 10082582, Development of petroleum-based high quality mesophase pitch and high yield mesophase pitch for premium carbon materials) and Korea Research Institute of Chemical Technology (KRICT).

Finally, I would also like to express my gratitude to my family for their moral support and warm encouragements.

February, 2020

Hiroki Shimanoe